Validation and Verification of an Analytical Method to Identify and Quantify Selected Amphetamine-Related Drugs in Whole Blood

by

Ahmad Alamir

A thesis submitted in partial fulfillment of the requirements for the degree of
Master of Science (MSc) in Chemical Sciences

The Faculty of Graduate Studies
Laurentian University
Sudbury, Ontario, Canada

THESIS DEFENCE COMMITTEE/COMITÉ DE SOUTENANCE DE THÈSE
Laurentian Université/Université Laurentienne
Faculty of Graduate Studies/Faculté des études supérieures

Title of Thesis Titre de la thèse	Validation and Verification of an Analytical Method to Identify and QuantifySelected Amphetamine-Related Drugs in Whole Blood
Name of Candidate Nom du candidat	Alamir, Ahmad
Degree Diplôme	Master of Science
Department/Program Département/Programme	Chemical Sciences
Date of Defence Date de la soutenance	February 5, 2018

APPROVED/APPROUVÉ

Thesis Examiners/Examinateurs de thèse:

Dr. James Watterson
(Supervisor/Directeur de thèse)

Dr. Thomas Merritt
(Committee member/Membre du comité)

Dr. Nelson Belzile
(Committee member/Membre du comité)

Dr. Vivienne Luk
(External Examiner/Examinateur externe)

Approved for the Faculty of Graduate Studies
Approuvé pour la Faculté des études supérieures
Dr. David Lesbarrères
Monsieur David Lesbarrères
Dean, Faculty of Graduate Studies
Doyen, Faculté des études supérieures

ACCESSIBILITY CLAUSE AND PERMISSION TO USE

I, **Ahmad Alamir**, hereby grant to Laurentian University and/or its agents the non-exclusive license to archive and make accessible my thesis, dissertation, or project report in whole or in part in all forms of media, now or for the duration of my copyright ownership. I retain all other ownership rights to the copyright of the thesis, dissertation or project report. I also reserve the right to use in future works (such as articles or books) all or part of this thesis, dissertation, or project report. I further agree that permission for copying of this thesis in any manner, in whole or in part, for scholarly purposes may be granted by the professor or professors who supervised my thesis work or, in their absence, by the Head of the Department in which my thesis work was done. It is understood that any copying or publication or use of this thesis or parts thereof for financial gain shall not be allowed without my written permission. It is also understood that this copy is being made available in this form by the authority of the copyright owner solely for the purpose of private study and research and may not be copied or reproduced except as permitted by the copyright laws without written authority from the copyright owner.

Abstract

The abuse of amphetamine-related drugs (ARDs) is an epidemiological phenomenon in Saudi Arabia. This drug abuse is found to play an important role in early mortality due to traffic accidents, violence, and overdose. Therefore, control ARDs abuse is crucial. In forensic toxicology, ARDs analysis is carried out to identify human actions, such as driving under the influence of drugs, clarify the manner and cause of death, and elucidate drug use. This study has yielded practical analytical assay to using whole blood (WB) as a biological matrix in ARDs analysis by using ultra performance liquid chromatography in coupling with quadrupole time of flight mass spectrometry (UPLC-qTOF-MS). Here, two different types of solid phase extraction (SPE) were evaluated. Molecularly imprinted polymers (MIP-SPE) was found to deliver a highly clean extract, however, ephedrine (EPH) interference was proved to leach from the polymer matrix of the sorbent materials. Mixed mode cation exchange (MMSPE) was found ideal to extract ARDs from WB matrices. The analytical method was developed and validated according to the Scientific Working Group for Forensic Toxicology (SWGTOX) Standard Practices. The validated method was found capable of quantitative analysis of β–methylphenethylamine (BMP) and detection of one of its metabolites in WBs of rats exposed to BMP by peritoneal injections.

Keywords

Forensic Toxicology, ARDs, WB, UPLC-qTOF-MS, MIP-SPE, EPH, MMSPE, SWGTOX, BMP.

Co-Authorship Statement

Chapter 1 of this thesis reviews the chemical, technological, pharmacokinetic, and pharmacodynamic concepts, which are relevant to this project. I am the sole author of this chapter. Dr. James Watterson contributed with structural guidance through this thesis.

Chapter 2 is containing the optimized analytical methods with details regarding the chemicals and materials, pre-treatment and extraction steps, the liquid chromatograph conditions, the mass spectrometer settings, and the data processing software.

Chapter 3 is a manuscript that was presented at the 21st Triennial Meeting of the International Association of Forensic Sciences (Toronto, ON, 2017). The abstract of the study was published in *Forensic Science International*, Volume 277, Supplement 1, p. 230. The published abstract and poster are provided in appendix A. I am the first author on this manuscript, Heather Cornthwaite is the second author and James Watterson is the third author.

Chapter 4 discusses the validation of the analytical method, using criteria based upon those expressed by the Scientific Working Group for Forensic Toxicology (SWGTOX) [176]. This chapter has not yet been published.

Chapter 5 discusses the verification of the validated analytical method, through application of the validated method to analysis of blood of rats exposed to (±) β-methylphenethylamine.

Acknowledgments

First of all, I would like to thank my supervisor, Dr. James Watterson, who has made this thesis possible, without whom I would certainly not have reached this stage. Thank you for all your encouragement, guidance, patience and advice. The knowledge you provided me with, the time you spent resolving various issues of my project and your unlimited support are really appreciated and will not be forgotten. Thank you for accepting and providing me with the opportunity to pursue my education.

I would like to say a huge thank you to the committee members Dr. Nelson Belzile and Dr. Thomas Merritt. Thank you for providing me with advice and feedback at the annual committee meetings. Thank you for all your encouragement and support that positively impacted my project. My appreciation extends to my academic supervisor in Saudi Cultural Bureau in Ottawa, Mrs. Nancy Jad, for her professionality in managing my academic file. Thank you to Saudi Health and Education Ministries for financial support.

Last, but by no means least; I would like to thank my family. My mom, and my dad's soul, my wife and daughters, and my brothers and sister. A huge thank you for being there and believing in me. I could not have completed this without you.

Table of Contents

List of Tables

List of Figures

List of Abbreviations

Abbreviation	Definition
1-AMINO	1-amino-2-phenylpropano-2-ol
4-HYDROXY	4-hydroxy-β-methylphenethylamine
%CV	Coefficient of Variation
˚C	Degrees Celsius
ACN	Acetonitrile
ADHD	Attention deficit hyperactivity disorder
Ae (%)	Amount excreted in urine within 24 h expressed as % of ingested dose
AMPs	Amphetamines
APCI	Atmospheric pressure chemical ionization
ARDs	Amphetamine-related drugs
AUC_{0-24}	Area under the plasma concentration-time curve from 0 to 24 h after administration
BMP	β-methylphenethylamine
CAT	Cathine
CI	Chemical ionization
CNS	Central nervous system
CO2	Carbon dioxide
CP_{max}	Maximum plasma concentration
CU_{max}	Maximum urinary concentration
DAD	Photodiode array detector
EI	Electron impact ionization
EIC	Extracted ion chromatogram
EPH	Ephedrine
ESI	Electrospray ionization
et al.	*et alia*
etc.	*et cetera*
F_B	Plasma protein binding

FL	Fluorescence
FPTE	Filtration Pass Through Extraction
g	Gram
GC	Gas chromatography
GC-MS	Gas chromatography-mass spectrometry
GC-MS/MS	Gas chromatography-tandem mass spectrometry
GHz	Gigahertz
h	Hours
HCl	Hydrochloric acid
HE	High collision energy
HPLC	High performance liquid chromatography
i.e.	*id est*
i.p.	intraperitoneally
IS	Internal standard
kg	Kilogram
kPa	Kilopascal
LC	Liquid chromatography
LC-MS	Liquid chromatography-mass spectrometry
LC-MS/MS	Liquid chromatography-tandem mass spectrometry
LE	Low collision energy
LLE	Liquid-liquid extraction
LOD	Limit of Detection
LOQ	Limit of quantification
MAMP	Methamphetamine
MDA	Methylenedioxyamphetamine
mDa	Millidalton
MDEA	Methylenedioxyethylamphetamine
MDMA	Methylenedioxymethamphetamine
MeOH	Methanol
MEs	Matrix effects
min	Minute

MIPs	Molecularly imprinted polymers
MIP-SPE	Molecularly imprinted polymer solid phase extraction
MM	Mixed Mode
mM	Millimolar
MMSPE	Mixed mode cation exchange solid phase extraction
MRM	Monitor reaction mode
MS	Mass spectrometry
NEPH	Norephedrine
NH_4OH	Ammonia
OPA	*o*-phthalaldehyde
PEPH	Pseudoephedrine
PHE	Phentermine
PMR	Post-mortem redistribution
PNS	Peripheral nervous system
s	Second
SPE	Solid phase extraction
SWGTOX	Scientific Working Group for Forensic Toxicology
t	Time
$T_{1/2\beta}$	Terminal elimination half-life
TIC	Total ion chromatogram
tP_{max}	Time to maximum plasma concentration
tU_{max}	Time to maximum urinary concentration
UPLC	Ultra-performance liquid chromatography
UPLC-qTOF-MS	Ultra performance liquid chromatography quadrupole time of flight mass spectrometry
Vd	Volume of distribution
WB	Whole blood
i.p.	Intraperitoneal injection
CO_2	Carbon dioxide
rpm	Revolutions per minute
kPa	Kilopascal

Chapter 1:

1. Introduction

1.1 General Introduction to Forensic Toxicology

Poisons are substances that are harmful to living organisms when absorbed, ingested, or inhaled in sufficient quantities; toxicology is the study of all such poisons [1]. Encompassing both modern analytical chemistry and fundamental toxicology, forensic toxicology is defined as the study of the effects of drugs and poisons on human beings in a medico-legal context [2]. Post-mortem toxicology is the application of forensic toxicology in death investigations.

1.2 Samples Used for Forensic Toxicological Analysis

Although currently forensic toxicological analyses may be performed using a wide range of sample matrices, such as urine, bile, vitreous humor, hair, saliva, sweat, and nails, blood is the most commonly used matrix for quantifying drugs and their pharmacologically active metabolites, and for correlating the findings with the extent of toxicity [3, 4]. Besides the cerebrospinal fluid, blood is the only biological fluid that reflects drug concentrations in the brain [3]. Furthermore, the determination of drug concentrations in the blood facilitates the rapid approximation of the cut-off values for subsequent confirmatory analyses without yielding too many false positives [5].

1.3 Physiological and Chemical Properties of Blood

Understanding the crucial role of blood in forensic toxicological analysis requires extensive knowledge about its composition, properties, and functions. Blood is a fluid connective tissue, which constantly circulates throughout the body to provide nutrients and oxygen to each cell, and to collect waste products from them. It is a complex mixture of solubilized proteins and fats as well as suspended cells and their fragments in a clear aqueous fluid known as plasma [6, 7]. The

three types of suspended cells are red blood cells (erythrocytes), white blood cells (leukocytes), and platelets (thrombocytes). Erythrocytes represent more than 90% of blood cells; they are responsible for the relatively high blood viscosity. These blood cells are normally distributed in the plasma due to the continuous motion of the blood. However, they immediately precipitate in stagnant plasma because of their higher mass densities than that of plasma. Moreover, blood centrifugation produces three layers based on the differences in mass densities as shown in Figure 1 [8, 9]. Therefore, blood samples contain many endogenous (salts, carbohydrates, amines, urea, lipids, peptides, and metabolites) and exogenous components (anticoagulants) [10].

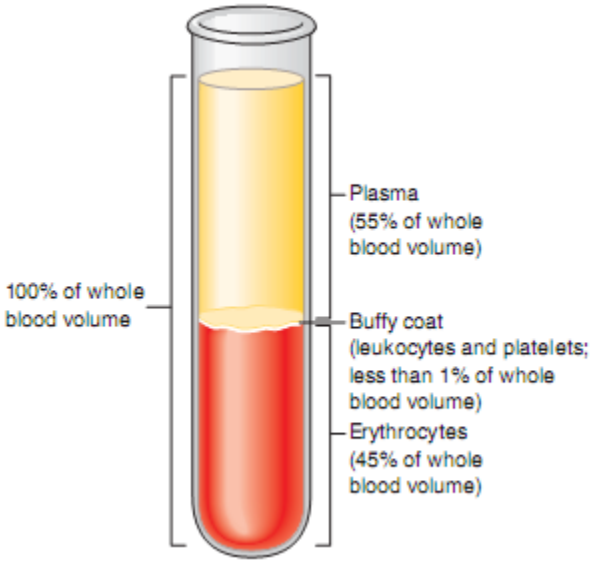

Figure 1: Composition of blood [8]

1.4 Analysis of Drugs in Blood

Blood is primarily responsible for the systemic circulation of a variety of substances, including drugs. An orally administered drug reaches the systemic circulation after absorption from the gastrointestinal tract; this is a relatively slow process. However, an intravenously

administered drug rapidly enters the blood stream directly, not requiring an absorption phase. Once in the blood stream, the drug is distributed to all the tissues; tissue uptake of a drug depends on the properties of both the drug and the tissue in question [13]. Hence, the identification of the physiochemical properties of a drug is required to facilitate its extraction from whole blood (WB) samples. Such specimens must undergo a series of sample pretreatment and extraction steps to remove any endogenous and exogenous substances that may cause analytical interferences; pretreatment is also performed to concentrate drug samples prior to injection into a chromatographic column.

1.5 Pretreatment of Whole Blood Samples and Drug Extraction

Sample pretreatment and extraction prior to chromatographic analysis are critical for the quantification of trace drug concentrations in WB samples [14]. Drugs in WB samples may be bound to proteins; therefore, it is necessary to disrupt drug-protein binding and increase the fraction of free drugs prior to extraction. Commonly used extraction techniques include filtration pass-through extraction (FPTE), liquid-liquid extraction (LLE), solid phase extraction (SPE), supported-liquid extraction, online SPE, and hybrid SPE/protein precipitation extraction [15].

1.5.1 Protein Precipitation

WB is rich in hemoglobin and other plasma proteins that may cause significant interference or damage in instrumental analysis. Therefore, it is vital to release the drug from protein-bound complexes prior to precipitate for accurate analysis. Protein precipitation is carried out in two steps: hemolysis and precipitation.

1.5.1.1 Hemolysis

Hemolysis is a process that releases erythrocyte-bound drugs and metabolites [16–18]. Hemolysis is vital for the accurate and reproducible quantification of drugs and their metabolites

in WB samples. Thus, it is important to lyse erythrocytes to account for any drug taken up by erythrocytes and extracellular fluid. Osmotic breakdown of erythrocytes is commonly used to cause hemolysis. In this process, erythrocytes are lysed by diluting WB with an equal volume of water followed by vortex mixing or sonication [17]. Inorganic denaturation is another way to perform hemolysis and ease drug extraction from WB samples [17, 18]. In this approach, $ZnSO_4$ is used as a protein denaturant and added to WB in a ratio of 1:5. The Zn^{2+} ion forms coordinate bonds with the amino acids of erythrocytic membrane proteins to form insoluble metal-protein complexes that precipitate and lyse the cells. Additionally, protons are displaced from the coordinated amino acids to decrease the pH of the sample. The acidic pH lowers the partition coefficient of the drug and enhances its solubility in acetonitrile (ACN), which is used as a precipitant in the precipitation step.

1.5.1.2 Precipitation

Precipitation can be carried out using water miscible organic solvents, acids, or inorganic salts followed by the addition of an organic solvent. Water miscible organic solvents, such as ACN and methanol (MeOH), precipitate proteins by lowering the dielectric constant of WB, thereby exposing the charges on the proteins and increasing protein-protein electrostatic interactions. Addition of an organic solvent displaces the arrangement of water molecules around hydrophobic regions on protein surfaces, thereby minimizing hydrophobic interactions between proteins. Consequently, electrostatic interactions predominate and lead to protein aggregation [17, 18]. ACN is a more efficient precipitation agent than MeOH because the triple bond in its structure effectively displaces water molecules by forming pi-stacking bonds with cationic and aromatic moieties on protein surfaces [17, 19]. Moreover, it is an aprotic solvent that accepts protons and forms hydrogen bonds with water molecules. Thus, using an acid as a hemolytic

agent prior to precipitation with ACN improves the recovery of analytes [20]. Interestingly, MeOH is a protic solvent that can be used along with ACN to increase the recovery of hydrophobic analytes by improving their solubility. Following hemolysis by osmotic breakdown, a mixture of ACN and MeOH can be added to the sample to precipitate the proteins.

Proteins may also be precipitated by the addition of acids, such as trichloroacetic acid (TCA), $HClO_4$, HCl, and tungstic acid. However, these strong acids can have negative effects on the drug that needs to be extracted; pilot testing may be needed in such cases [21]. After hemolyzing WB samples by osmotic breakdown, 10 %TCA, 1 % HCl, or 6% $HClO_4$ may be added to the sample in a 1:2 ratio [17].

The use of organic salts, such as $ZnSO_4$, for hemolysis followed by the addition of a water-miscible organic solvent is also widely used. In this method, the sample is centrifuged after 5% $ZnSO_4$ is added to the WB sample in a 1:5 ratio, and the resultant pellet is discarded. Further, a water miscible organic solvent, such as ACN, MeOH, or their mixture, is added to the recovered portion of the sample in a 2:1 ratio. Finally, the mixture is centrifuged, and the supernatant is recovered [17].

1.5.2 Analyte Extraction from Pretreated Whole Blood Samples

After denaturing and precipitating the proteins in WB samples, the analytes of interest may be extracted using three different techniques, including FPTE, LLE, and SPE.

1.5.2.1 Filtration Pass Through Extraction

FPTE is a hybrid precipitation/SPE technique that has been increasingly used over the past few years as a method for the selective removal of phospholipids and precipitated proteins [22–26]. This extraction technology incorporates a simple protein precipitation step with a fast and robust SPE method that is designed to remove phospholipids. Each of the distinct types of

commercially available plates, such as Ostro™ (Waters) and Hybrid SPE™ (Sigma Aldrich), relies on different principles of extraction. The Ostro™ plate uses a C18 stationary phase for retaining phospholipids and precipitated proteins [22]. This plate displays high affinity towards phospholipids, and low affinity towards a wide range of basic, neutral, and acidic compounds [27]. This plate has been reported to effectively remove phospholipids and precipitated proteins from WB, serum, and plasma samples [28–30]. Moreover, the Hybrid SPE is designed to retain phospholipids based on Lewis acid-base interactions that occur between zirconia ions bonded to the stationary phase and the phosphate group of phospholipids. Compared to conventional protein precipitation techniques, FPTE has been found to significantly lower phospholipid content in the samples [23].

1.5.2.2 Liquid-Liquid Extraction

LLE is a separation technique in which the analytes of interest are transferred from one phase to another when immiscible or partially miscible liquids are in contact with each other [31]. By adding organic and aqueous solvents with appropriate pH control, the analytes of interest can be extracted from the WB matrix. This method of extraction relies on the pH of the added solvent mixture. Hence, at acidic pH, organic acids are more soluble in organic solvents than in aqueous solvents. Thus, acidic analytes must be ionized to facilitate their extraction. Hence, to extract them from an organic solvent to an aqueous solvent, acidic analytes must be ionized by shifting the pH range to alkaline. Similarly, organic bases are more soluble in organic solvents than in aqueous solvents at alkaline pH. Thus, they may be extracted by changing the pH to the acidic range. Typically, the pH of the solvent mixture must be between the pK_a of the analytes of interest and $pK_a + 2$ (for acidic analytes) or $pK_a - 2$ (for basic analytes) [16, 22, 32]. The advantages and disadvantages of LLE are listed in Table 1 (page 9).

1.5.2.3 Solid Phase Extraction

SPE is a separation technique in which the analytes of interest are selectively transferred from a liquid phase to a solid sorbent. Based on the structure, size, and charge of the analytes, separation is achieved through the difference in their affinities for the two phases. SPE can be carried out by four different mechanisms—reversed phase, normal phase, ion exchange, and through "molecular recognition" using molecularly imprinted polymers (MIPs).

In reversed phase SPE (hydrophobic phase SPE), the sorbent stationary phase is non-polar, and is composed of a silica or polymer backbone modified with an alkyl or aryl group [22, 33]. Reversed phase SPE is usually used to extract relatively non-polar, charge-neutral compounds from complex matrices. Retention occurs due to hydrophobic (non-polar) interactions between the C–H bonds of the analytes and the C–H bonds of the modified sorbent [33]. Due to its selectivity, C18 is the most widely used sorbent.

In normal phase SPE (hydrophilic phase SPE), the sorbent stationary phase is polar, and is composed of a silica backbone bonded with carbon chains containing polar functional groups [22]. Normal phase SPE is usually utilized for extracting analytes with polar groups, such as amines, hydroxyls, and carbonyls [22, 33]. The retention of these polar compounds occurs due to hydrophilic (polar) interactions, including hydrogen bonding, pi-pi, or dipole-dipole interactions, between the functional groups of the analytes and those of the modified sorbent [22, 33].

In ion-exchange SPE, sorbents are composed of a silica backbone bonded with carbon chains terminated by positively or negatively charged functional groups. Thus, ion-exchange SPE may be cation, anion, or copolymeric mixed-mode (MM) ion-exchange.

In cation-exchange SPE, sorbents are composed of a silica backbone bonded to a carbon chain terminated by negatively charged functional groups, such as benzenesulfonic acid (strong), propylsulfonic acid (strong), and carboxylic acid (weak). In this separation technique, analytes

are manipulated to carry a positive charge by adjusting the pH of the aqueous solution to completely ionize the analytes [22]. Thus, the negatively charged functional groups of sorbents interact with the positively charged functional groups of analytes. Generally, these extracted analytes are amine-containing compounds or positively charged metal ions [22, 33].

In anion-exchange SPE, positively charged functional groups, such as primary and secondary amine (weak), aminopropyl (weak), diethylamino (weak), and quaternary amine (strong), are present on carbon chains bonded to the silica backbone of the sorbent. In this technique, the analytes are manipulated to carry a negative charge, which then form strong bonds with the positively charged functional groups of sorbents [22]. This may be done by changing the pH of the solution to completely ionize the analytes. Typically, analytes containing phosphate, carboxylic acid, and sulfonic acid groups are separated by this method [22, 33].

In copolymeric MM ion-exchange SPE, sorbents interact with analytes by forming both hydrophobic and ionic bonds. These sorbents are composed of a silica or polymeric backbone bonded to alkyl functional groups (hydrophobic interaction), and amine or acid functionalities (ionic interaction). This technique is widely used to analyze drugs of abuse because of its ability to extract a wide range of components simultaneously; acidic, neutral, and basic polar compounds can be separated on the same column. Analyte-selective aqueous washing solvents and appropriately selected eluting solvents yield clean extracted samples.

MIPs contain highly selective binding sites for analytes with specific structural features [34]. Accordingly, MIPs have been recommended for the extraction of target analytes and to minimize Matrix effects (MEs) while providing desirable reagent pH stability. Sorbents in this method are synthesized by combining a template molecule solution of monomer and a cross-linking agent, which induces the formation of a rigid polymer around the template. After removing the

template, the polymer with analyte-selective cavities or imprints is obtained. Due to the complementary shape of the polymer and other physicochemical properties, such as hydrogen bonding or ionic and hydrophobic interactions, analytes of interest are retained on these sorbents. However, a key limitation of MIPs is the detection of residual template molecules from the polymerized sorbent matrix by a highly sensitive instrument.

Analyte extraction by SPE includes five steps—conditioning, equilibration, loading, washing, and elution. Conditioning is performed to wet the porous surfaces of the stationary phase and to facilitate the adsorption of analytes on the sorbent. This step is carried out by using organic solvents, such as MeOH [33]. Equilibration is performed to displace MeOH in the pores by using aqueous buffer solvent to allow the analytes of interest to interact with the sorbent [22, 33]. A pretreated sample in the same buffer solvent used in the equilibration step, is then loaded onto the sorbent and allowed to flow under gravity [22]. In the washing step, matrix constituents and impurities that may interfere with the analysis are removed by a series of washing solvents owing to their poor retention affinity towards the sorbent [22]. The sorbent is then dried by vacuum to remove any residual solvent or water after washing [22]. Elution is performed using a strong solvent to break the interaction between the analyte and the sorbent [22]. Table 2 shows the advantages and disadvantages of SPE.

Table 1: Advantages and disadvantages of liquid-liquid extraction (LLE)

Advantages	Disadvantages
- Easy to remove inorganic salts - Rapid method development - Low cost	- Labor-intensive work - Requires large volumes of solvents - Difficult to be automated - Formation of emulsion

Table 2: Advantages and disadvantages of solid phase extraction (SPE)

Advantages	Disadvantages
- Highly selective - Highly effective with complex matrices - High recovery - High reproducibility - Conducive to automation	- Greater complexity - Time-consuming method development - Costly

1.6 Instrumental Analysis of Drugs in Forensic Toxicology

Drug analyses in forensic toxicology are performed to identify the use of drugs of forensic relevance or whether the subject was under the influence of certain drugs during a particular period [36]. Results of these analyses must be accurate and reliable to avoid any false positive or false negative results that could lead to severe consequences. Therefore, the utilization of highly sensitive and selective hyphenated analytical techniques, such as gas chromatography-mass spectrometry (GC-MS) and liquid chromatography-mass spectrometry (LC-MS), is necessary to qualitatively and quantitatively analyze drugs in WB samples [37].

1.6.1 Gas Chromatography-Mass Spectrometry (GC-MS)

GC-MS is an advanced analytical technique that couples the separation capability of GC with the detection properties of MS to identify unknown compounds in a sample [38]. Volatile and thermally stable analytes are separated by GC; MS relies on the ionization and fragmentation of samples compounds to identify their chemical compositions based on the pattern of fragment mass-to-charge ratios (m/z). The addition of another mass analyzer to GC-MS increases its detection sensitivity and selectivity, leading to the superior configuration known as gas chromatography-tandem mass spectrometry (GC-MS/MS) [38].

Separation by GC is initiated by volatilizing the sample by rapid exposure to a high temperature zone (200–300°C) and mixing with a stream of carrier gases, such as Ar, He, N_2, or H_2 (mobile phase). The resulting gas mixture reaches the chromatographic column (separation zone), which is composed of a fused-silica tubular capillary coated internally with a thin polymer film (stationary phase) [39, 40]. Analyte molecules are partitioned between the stationary phase and the mobile phase during their movement through the column, and the degree of partition of the analytes depends on their chemical structures [40]. At the end of the separation zone, the sample is pumped through the sample inlet of a mass spectrometer.

The mass spectrometer is usually composed of the following four components: a sample inlet, an ion source, a mass analyzer, and a detector. The sample inlet is the entry port through which the sample is introduced into the instrument. In GC-MS, the sample inlet of the mass spectrometer is interfaced with the GC, where a gaseous sample is fed into the instrument to reach the ion source [39]. In the ion source, analytes are ionized either by electron ionization (EI) or chemical ionization (CI), and are directed to the mass analyzer. By adjusting the electric field, only a particular ion with a particular m/z is allowed to reach the detector where the mass spectrum is recorded [39, 40].

GC-MS is considered the “gold standard” in the analysis of volatile and heat-stable compounds in modern forensic toxicology because of the availability of extensive libraries for spectral matching-based identification [38-41]. The need for chemical derivatization of non-volatile, polar, and thermally labile analytes to make them sufficiently volatile for GC-MS is labor-intensive and costly, thereby limiting the utility of this technique [39, 41–44].

1.6.2 Liquid Chromatography Mass Spectrometry (LC-MS)

LC-MS is the most advanced analytical technique utilized in contemporary forensic toxicology to identify the presence of drugs in biological samples. It overcomes most of the limitations of GC-MS, and improves the practicality and reproducibility of highly complicated MS analyses [15]. This hyphenated technique exists with single stage MS, (i.e., LC-MS) or with tandem MS processes (LC-MS/MS). In LC-MS, low-resolution molecular-mass-selective detecting devices, such as a single quadrupole or an ion trap, are coupled with LC. These single stage LC-MS platforms have been found to offer limited selectivity for quantifying target analytes in complex biological matrices, such as WB [15]. Although time-of-flight mass analyzers in single-stage LC-MS offer high selectivity due to their high mass resolution, which is a prerequisite for most quantitative assays, they display limited linearity [15, 45, 46]. Interestingly, the introduction of MS/MS, which includes two mass filters coupled to a collision cell, overcomes this limitation of LC-MS because the analytes of interest can be monitored in multiple reaction monitoring (MRM) and their fragmented ions are directly used for analyte quantification [15, 45, 46].

Analytes are separated by LC as the mobile phase is passed under high pressure through a column packed with sorbent materials (stationary phase) having particular physiochemical properties; analytes are separated due to differences in their affinities towards the stationary phase. The following two separation techniques exist: high-performance LC (HPLC) and ultra-performance LC (UPLC). In HPLC, the mobile phase is pumped at high pressures up to 5,800 psi (400 bar) through a column packed with particles having diameters of 3–5 µm with porous shells of 0.25–0.5 µm in thickness [47–49]. In UPLC, the mobile phase is continuously pumped at high pressures up to 15,000 psi (1,034 bar) with low dispersion through a column packed with particles having diameters less than 2 µm [49]. UPLC has a higher separation power than HPLC,

and facilitates the separation of multiple analytes in a short runtime [50]. Eichhorst *et al*. separated 42 compounds within a run time of 5.2 min [51]. This separation power is a result of the reduction in stationary phase particle diameter. The Van Deemter equation is an empirical equation used to mathematically depict the relationship between linear velocity (flow rate) and height equivalent to theoretical plate.

$$H = A + \left(\frac{B}{\mu}\right) + C \times \mu \qquad \textbf{(1)}$$

H, height of a theoretical plate
μ, average linear velocity of the mobile phase
A, eddy diffusion term
B, longitudinal diffusion term
C, mass transfer term

Hence, chromatographic column performance can be evaluated by the Van Deemter curve (see Figure 2) because particle size influences the mass transfer term in the equation [52, 53]. Therefore, particle sizes less than 2 μm would not only significantly increase the separation efficiency, but also allow stable separation at increased flow rates or linear velocities.

Certain applications may call for extended runtimes in UPLC. The separation of structurally isomeric analytes requires an extended runtime to ensure full baseline resolution of the analytes, especially when they yield the same fragment ions. In such an analytical assay, mobile phase composition is maintained isocratic (constant mobile phase composition) or "pseudo-isocratic", where the mobile-phase composition gradient is extremely shallow [54,55]. Chołbiński *et al*. reported an isocratic method to resolve amphetamine (AMP) from its structural isomer, beta-methylphenethylamine (BMP), using UPLC-MS/MS with a runtime of 9.5 min [56].

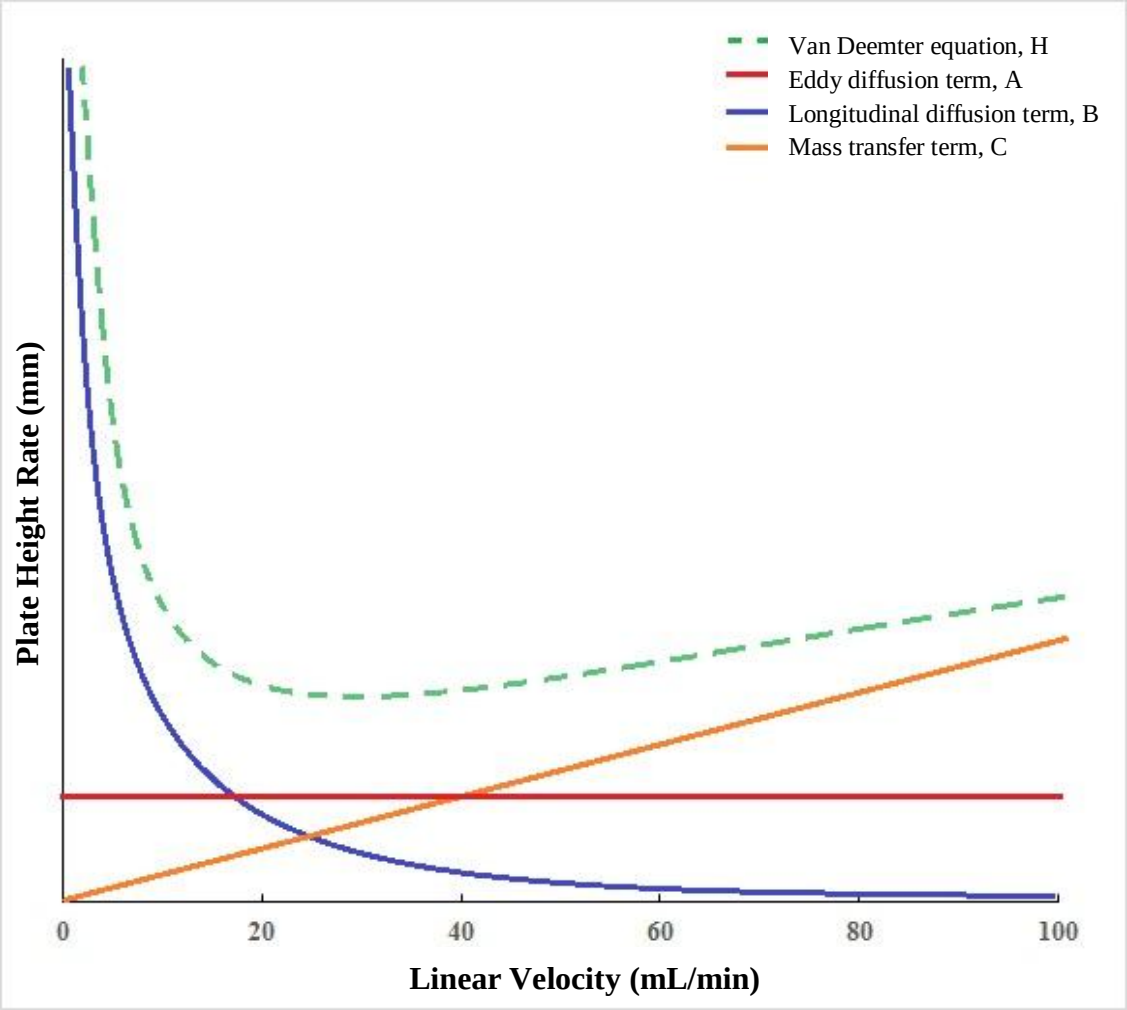

Figure 2: Van Deemter curve

Analyte separation in UPLC starts when the sample is introduced through an injector into the continuously flowing stream of mobile phase that delivers the sample to the UPLC column; the column is packed with the stationary phase [57]. By partitioning between the stationary phase and the mobile phase, analyte molecules are separated from each other as they move through the column based on differences in their partition coefficients between the two phases. [40].

After the analytes are separated by UPLC, they are introduced into the mass spectrometer through the interfaced sample inlet, which carries the separated analytes to the ion source. Ionization is commonly achieved using electrospray ionization (ESI), and can be performed in a

negative or positive mode depending on the chemical properties of the analytes. In ESI, the liquid eluent is pumped through to a heated, charged capillary, which is surrounded by nebulizing inert gas channels that help in forming fine charged droplets [37, 58]. These droplets are evaporated by a desolvation (cone) gas that results in a decrease in droplets size and an increase in charge density [37]. The size of the charged droplets decreases continuously until the charge transfers to the solutes, which then move to the mass analyzer. Mass analyzers sort ions according to mass to charge ratio (m/z), prior to ions reaching the detector, where the mass spectrum is recorded [37]. Figure 3 shows a schematic diagram of the ESI process in the positive ion mode [59].

UPLC-MS differs from UPLC-MS/MS in the number of mass analyzers; UPLC-MS/MS has two mass analyzers, whereas UPLC-MS has only one mass analyzer. Figure 4 shows a schematic diagram of an example of a MS/MS configuration (qTOF) [60].

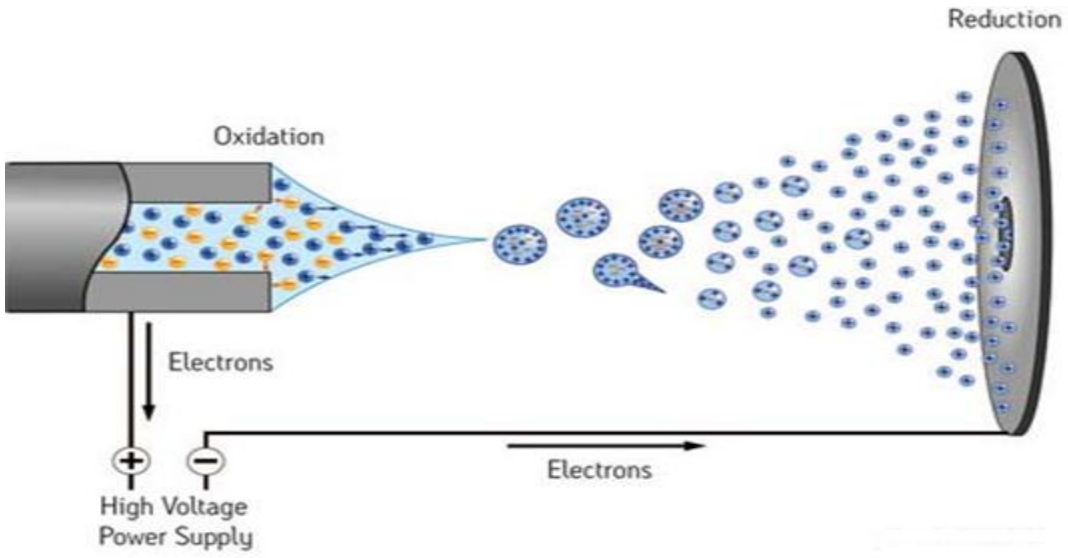

Figure 3: Schematic diagram of electrospray ionization in the positive ion mode [59]

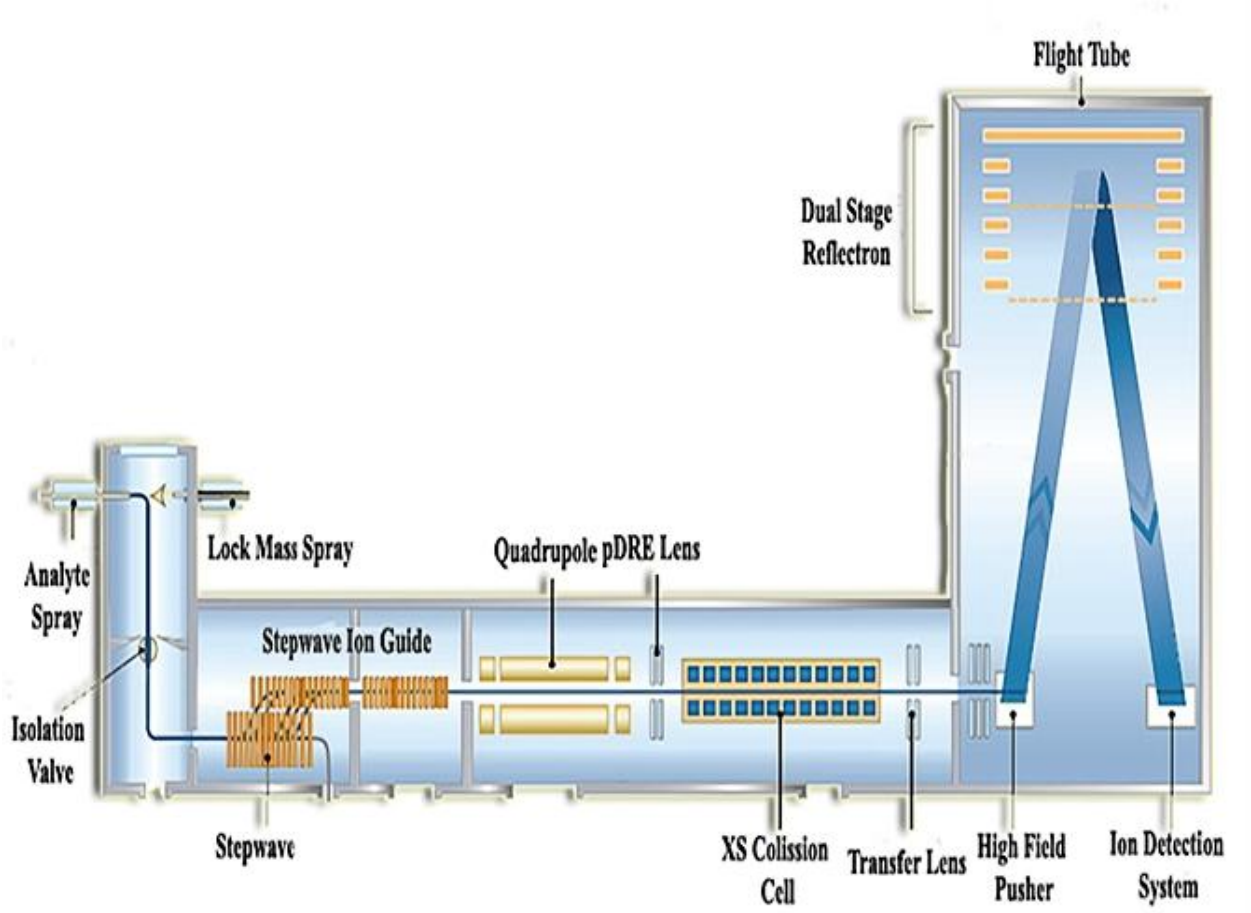

Figure 4: Schematic diagram of tandem mass spectrometry [60]

1.7 Stimulant Drugs in Forensic Toxicology

Forensic toxicological analysis deals with a wide range of therapeutic and abused drugs, many of which are controlled substances that are consumed for their psychoactive effects, and may result in drug addiction or dependence [61]. They may be central nervous system (CNS) depressants or stimulants. Depressants are psychoactive drugs that temporarily slow down activity of the brain and CNS. Opiates, barbiturates, benzodiazepines, and alcohol are examples of CNS depressants [62]. However, CNS stimulants are drugs that have sympathomimetic effects, which temporarily increase the activity of the brain and CNS. These drugs include amphetamines (AMPs) and cocaine [63]. AMPs are stimulant drugs that possess similar structure and functions of endogenous amines, such as dopamine [14]. These sympathomimetic drugs are

composed of a phenyl ring connected to an amine group through a two-carbon side chain bearing a methyl group. Figure 5 shows the chemical structures of endogenous monoaminergic neurotransmitters and the most common ARDs.

ARDs include a wide range of compounds, such as methamphetamine (MAMP), beta-methylphenethylamine (BMP), ephedrine (EPH), pseudoephedrine (PEPH), norephedrine (NEPH), norpseudoephedrine or cathine (CAT), methylenedioxyamphetamine (MDA), methylenedioxymethamphetamine (MDMA), methylenedioxyethylamphetamine (MDEA), and phentermine (PHE). These compounds release catecholamines, such as dopamine, from the presynaptic cleft at both the central and peripheral sites [14]. The abusive potential of these drugs is associated with their psychoactive activity, due to the elevation in dopamine concentrations in the shell region of the nucleus accumbens of the ventral striatum [64].

1.7.1 Properties of Amphetamine-Related Drugs

ARDs are a distinct class of sympathomimetic compounds. Based on their origin, they can be categorized into synthetic (AMP, BMP, MAMP, MDA, MDEA) and naturally-occurring ARDs (EPH, PEPH, NEPH, and CAT) [65]. In this study, a mixture of synthetic and naturally-occurring ARDs, such as AMP, BMP, CAT, EPH, NEPH, and PEPH, has been chosen based on their epidemiological abuse in Saudi Arabia. Structurally, two pairs of these analytes are diastereomers (EPH and PEPH; NEPH and CAT), and one pair represents positional isomerism (AMP and BMP). Pharmacologically, these sympathomimetics induce the release of catecholamines, such as dopamine, serotonin, and noradrenaline [66]. Figure 6 shows the chemical structures of the ARDs selected in this study.

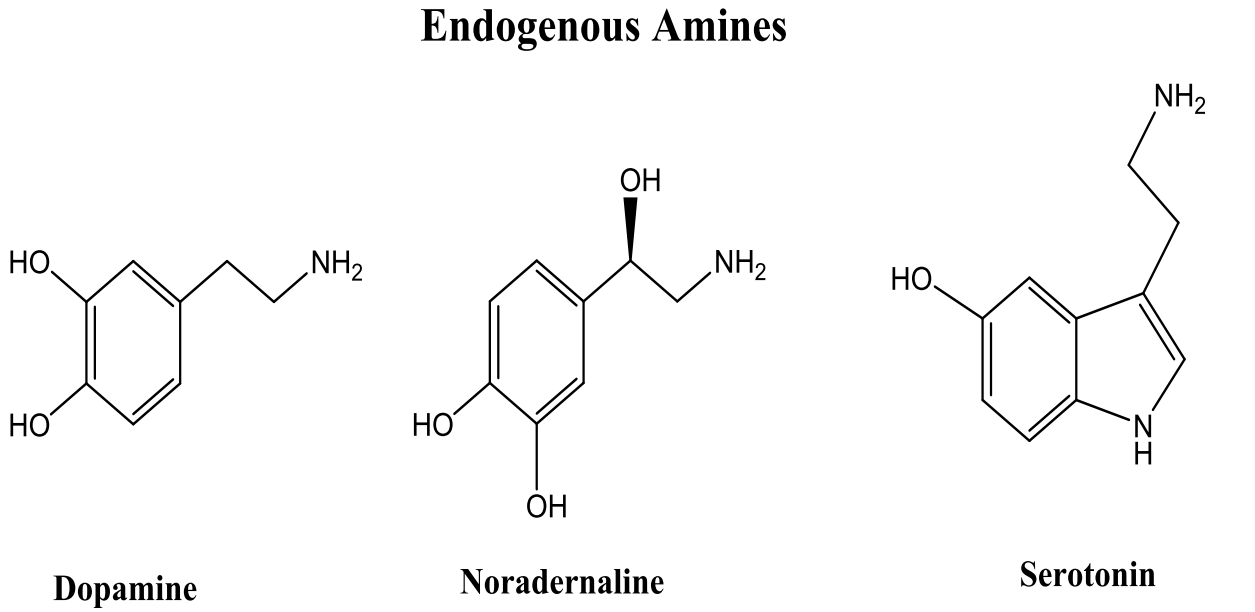

Figure 5: Chemical structures of endogenous monoaminergic neurotransmitters and examples of common amphetamine-related drugs

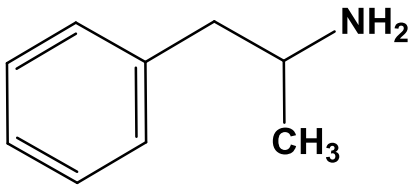

Amphetamine
Nominal Mass: 135 Da

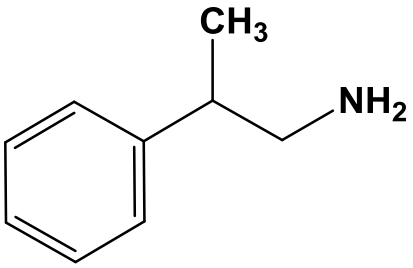

β-methylphenethylamine
Nominal Mass: 135 Da

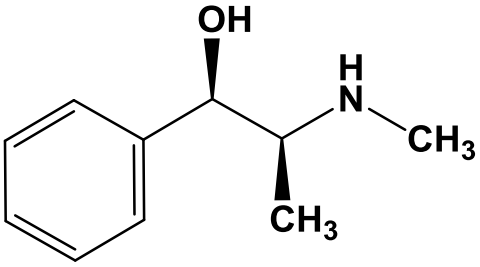

Ephedrine
Nominal Mass: 165 Da

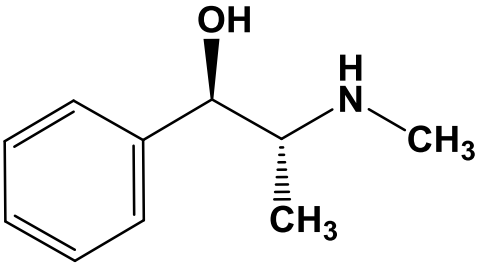

Pseudoephedrine
Nominal Mass: 165 Da

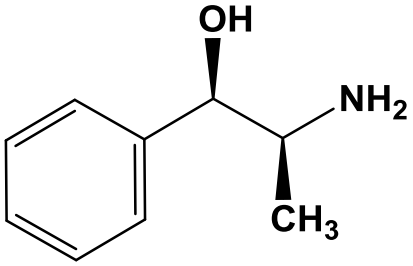

Norephedrine
Nominal Mass: 151Da

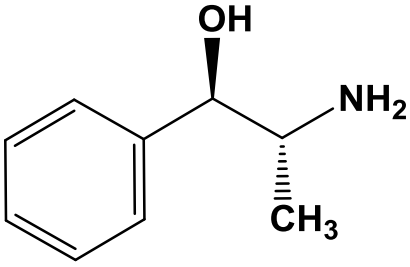

Cathine
Nominal Mass: 151Da

Figure 6: Chemical structures of amphetamine-related stimulants included in this study

1.7.1.1 Amphetamine

AMP was firstly discovered by a Romanian chemist, Lazar Edeleanu, in 1887. It acquired its generic name from the contraction of **a**lpha-**m**ethyl-**ph**en**et**hyl-**amine** [67]. Chemically, it exists as two optically active enantiomers of α-methyl-phenethyl-amine (Figure 7). These two isomers are S-(+)-AMP or dextro-AMP (d-AMP) and R-(-)-AMP or levo-AMP (l-AMP); d-AMP is three to four times more potent than l-AMP with regard to CNS stimulation, whereas l-AMP is more potent than d-AMP with regard to peripheral nervous system (PNS) [66, 67]. Pharmacologically, AMP is one of the most effective sympathomimetic amines that stimulates the CNS [66]. It effectively stimulates the CNS because it is structurally similar to endogenous catecholamine neurotransmitters (noradrenaline and dopamine) as shown in Figure 6 [66]. AMP pharmacokinetics and pharmacodynamics are characterized by its ability to cross the blood-brain barrier to release monoamine neurotransmitters from nerve endings. It is considered as a prototype and reference drug to which the stimulant effects and potencies of other ARDs can be compared [66–69]. AMP is used in the treatment of attention deficit hyperactivity disorder (ADHD), narcolepsy, and obesity due to its unique mechanism of action in which dopamine is released and its reuptake is inhibited [66–69].

1.7.1.1.1 Mechanism of Action

AMP increases the release of dopamine, norepinephrine (noradrenaline), and serotonin. It acts as a potent CNS stimulant by elevating extracellular dopamine levels and prolonging dopamine signaling in the striatum through the following three mechanisms: 1) it competes with dopamine to bind to the dopamine transporter, leading to the inhibition of dopamine reuptake by dopamine transporter; 2) it eases the transport of dopamine from the vesicles to the cytoplasm; 3) it facilitates dopamine transporter-mediated reverse transport of dopamine into the synaptic cleft,

without necessitating action potential generation for inducing its vesicular release [69, 70]. AMP also inhibits monoamine oxidase activity, which is the enzyme responsible for breaking down dopamine in the cytosol. Dberkow *et al*. have demonstrated that both the *in vivo* and *in vitro* acute effects of AMP are related to its dose, and AMP could work as a dopamine reuptake inhibitor at low concentrations, whereas it releases dopamine at high concentrations [71]. Accordingly, AMP is used at low doses for its therapeutic effects and at high doses for its abusive effects.

1.7.1.1.2 Intoxication Symptoms

AMP is clinically used to suppress appetite, treat narcolepsy, and manage ADHD. However, its use is associated with adverse effects, such as insomnia, weight loss, and anorexia. In a study carried out in 2001 by James *et al*, the adverse effects of using d-AMP in the management of ADHD in children included insomnia, nightmares, anxiety, biting of fingernails, poor appetite, and euphoria [72]. Other adverse effects of using AMP for therapeutic purposes include abdominal cramps, nausea, vomiting, hypertension, and tachycardia [72–77].

Abusively high doses of AMP are associated with serious adverse effects, such as paranoia, hallucinations, panic attacks, and violence. These effects gradually increase with the frequency of AMP abuse. In 1996, Hall *et al*. found that the most common adverse effects of AMP were depression (79%), anxiety (76%), paranoia (52%), hallucinations (46%), and violent behavior (44%) among young adults in Sydney, Australia; their intensities and incident frequencies correlated with the route of administration of AMP [79]. The magnitude of the adverse effects depends on various factors, such as dose, route of administration, tolerance, and reactivity of AMP with other drugs.

1.7.1.1.3 Pharmacokinetics of AMP

Typically, AMP has a high oral bioavailability, a moderate volume of distribution (4 L/kg), and exhibits low plasma protein binding (< 20%). It is extensively metabolized in the liver, and eliminated from the liver and kidneys with an elimination half-life of 6–12 h. AMP is a basic drug (pKa 9.9) with a relatively low molecular weight, which allows it to easily cross lipophilic cellular membranes [81].

AMP is commonly administered orally in the form of d-AMP or as a racemic mixture (d, l-amphetamine sulphate). The peak plasma concentration (C_{max}) is generally attained within 4 h of oral ingestion (t_{max}). Area under the plasma concentration-time curve after 24 h of administration ($AUC_{0–24}$) and C_{max} are proportional to the ingested dose, and do not differ for the two isomers of AMP [81–83]. Table 3 shows the pharmacokinetic parameters of AMP in humans after single oral administration [81].

AMP exhibits low protein binding; therefore, most of the AMP available in the plasma can diffuse into the extracellular compartment. Accordingly, amphetamine-dependent individuals, who are tolerant to AMP, exhibit a larger volume of distribution (6.1 L/kg) than drug-naïve individuals (3.2 L/kg). This difference in AMP distribution can be explained by the higher tissue affinity to AMP in those who are tolerant. Tissue affinity to AMP increases because of altered pharmacokinetic tolerance and tissue sequestration. The protein binding and volume of distribution of d- and l-AMP enantiomers are similar (Table 3) [81, 83, 84].

AMP is metabolized by N-deamination and oxidation into benzoic acid derivatives, which further conjugate with glycine to form hippuric acid derivatives. It is also metabolized through aromatic C-4 hydroxylation to 4-hydroxyamphetamine, which is further conjugated with sulphate or glucuronic acid [81–83]. AMP also undergoes hydroxylation to form a reactive intermediate, which can further react with glutathione to form a (glutathione-S-yl)-*p*-

hydroxyamphetamine adduct [81, 85]. The formation of NEPH occurs through a minor metabolic pathway in which the β-carbon of the side chain is oxidized. The aromatic ring of NEPH is further oxidized to form hydroxynorephedrine [81, 86]. These metabolic pathways of AMP appear to be catalyzed by CYP450 isoenzymes; the CYP2C and CYP2D6 subfamilies catalyze the N-deamination and aromatic ring hydroxylation, respectively. Figure 8 shows the metabolic pathway of AMP [81, 86–88].

AMP undergoes extensive excretion by the kidneys. The plasma half-life of AMP is, to a certain extent, dependent on urine pH. Because AMP is a weak base, its renal excretion increases with acidic urine and decreases with alkaline urine [81, 88-94]. Therefore, the elimination half-life of AMP has a wide variability; it has a plasma elimination half-life of 6–12 h. This elimination half-life was found to be longer in AMP-dependent individuals than drug-naïve individuals (21.8 ± 1.4 vs 13.9 ± 3.4 h in alkaline urine) at the same oral dose of 25 mg (Table 3) [81, 82, 84]. The elimination half-life of AMP is found to be independent of its route of administration, and tends to be longer in AMP abusers [81, 85].

d-amphetamine **l-amphetamine**

Figure 7 : Chemical structures of the enantiomers of amphetamine

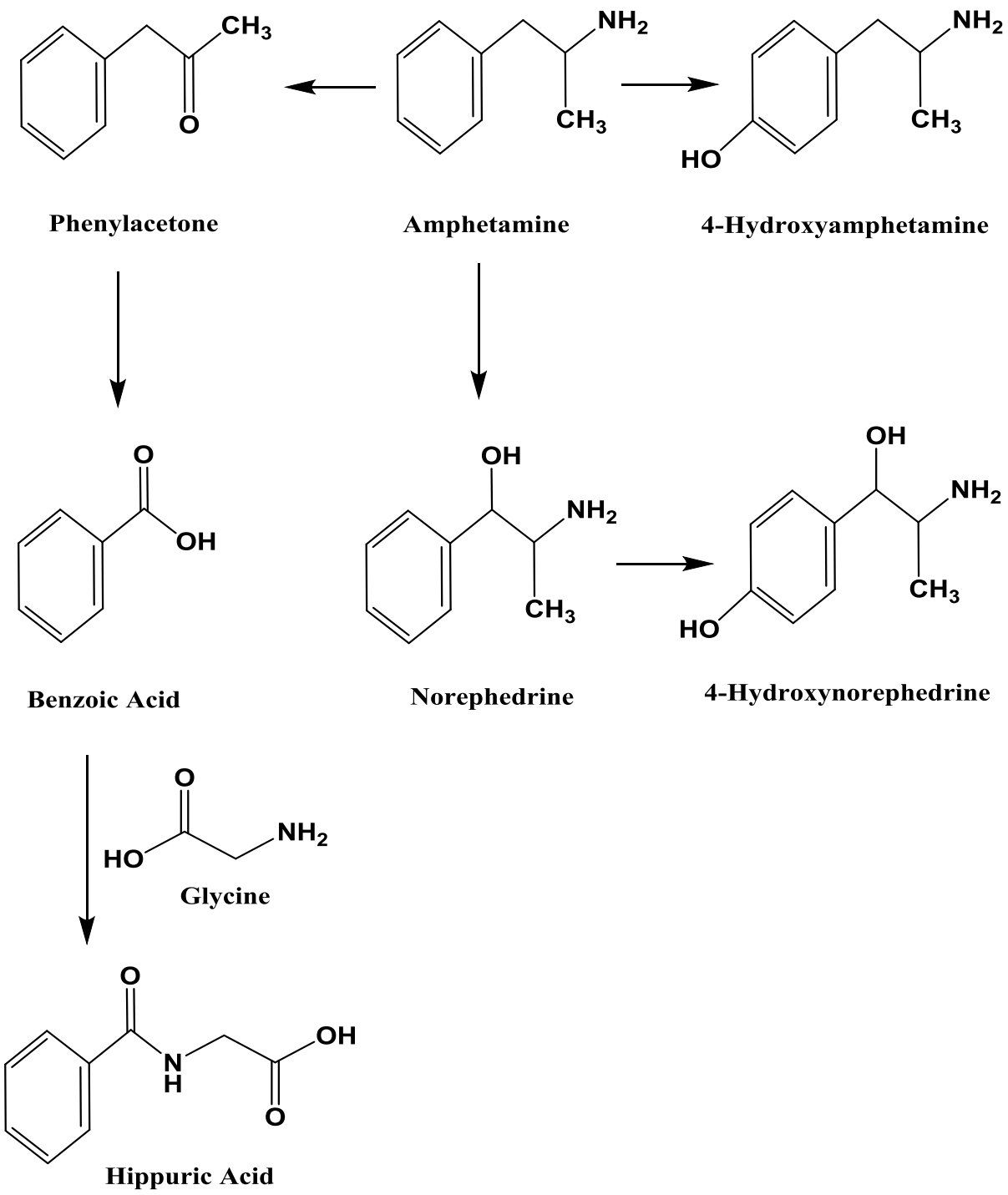

Figure 8: Metabolic pathways of amphetamine

Table 3: Pharmacokinetic parameters of amphetamine in humans after single oral administration

Dose (mg)	n	Isomer	CP_{max} (ng/mL)	CU_{max} (ng/mL)	tP_{max} (h)	tU_{max} (h)	AUC_{0-24} (ng*h/mL)	Vd (L)	$T_{1/2\beta}$ (h)	Ae (%)	Reference
20	2	Racemate	(36.6–38.8)[a]		(3–2)		(482.5–431.6)				68
30	2	Racemate	(57.3–57.8)[a]		(3–2)		(790.2–753.1)				
35	2	Racemate	(63.5–57.5)[a]		(2–2)		(822.9–758.6)				
40	11	Racemate	(69.1–5.7)[b]		2.2 ± 1.0		(945.4 ± 71.8)				
0.25 (mg/kg)	7	S	39.6 ± 2.8[b]		3						89
0. 5 (mg/kg)	8	S	67.3 ± 5.4[b]		4						
0. 06 (mg/kg)	12	S	18.3 ± 1.4[b]		1.9 ± 0.2		49.4 ± 3.4[d]				90
0. 10 (mg/kg)	12	S	21.4 ± 0.7[b]		2.5 ± 0.3		58.3 ± 2.3[d]				
10 (with $NaHCO_3$)	4	Racemate	20[f] (R[e])		4[f]			237.6 ± 26.9	17.0 ± 1.5		91
			20[f] (R[e])		4[f]			243.4 ± 29.0[c]	23.7 ±3.5		
10 (with NH_4Cl)	4	Racemate	18[f] (R[e])		4[f]			210.3 ± 51.3[c]	6.8 ± 1.0		
			17[f] (R[e])		4[f]			248.1 ± 78.3[c]	7.7 ± 1.0		
10 (with $NaHCO_3$)	4	S	40[f] (R[e])		2.5[f]			258.1 ± 32.7[c]	15.6 ± 1.3		
		R	40[f] (R[e])		3[f]			267.4 ± 38.1[c]	25.0 ±2.3		
10 (with NH_4Cl)	7	S		1,635.7±1091.0[b]		4.9 ± 3.0				44.0 ± 6.7	92
10 (with NH_4Cl)	6	S		2,508.3 ± 493.1[b]		5.3 ± 3.9				41.9 ± 4.8	
10 (with NH_4Cl)	7	S		3,308.6±1212.5[b]		9.7 ± 7.1				34.7 ± 5.2	

Adopted from [81, 82, 83]

CP_{max}, maximum plasma concentration; **CU_{max}**, maximum urinary concentration**; tP_{max}**, time to maximum plasma concentration; **tU_{max},** time to maximum urinary concentration; **AUC_{0-24},** area under the plasma concentration-time curve from 0 to 24 h after administration; **Vd,** volume of distribution; **$T_{1/2\beta}$**, terminal elimination half-life; **Ae (%)** amount excreted in urine within 24 h expressed as % of ingested dose.

[a] *n* = 2 (individual values)

[b] *n* = 2 (mean ± SD)

[c] *n* = 2 (mean ± SEM)

[d] AUC from 0 to 4 h after administration

[e] Isomer studied

[f] Approximate value

1.7.1.2 β-methylphenethylamine

BMP is a recreational drug that was synthesized in 1930 as an alternative analog of AMP [95, 96]. BMP is a positional isomer of AMP. Figure 9 shows the chemical structures of AMP and BMP [96]. BMP exists as two optically active enantiomers of β-methylphenethylamine; they are R-(+)-BMP or dextro-BMP (d-BMP) and S-(-)-BMP or levo-BMP (l-BMP). Figure 10 shows the chemical structures of these BMP enantiomers. Pharmacologically, BMP acts as a dopamine receptor agonist, facilitating dopamine release and inhibiting dopamine reuptake from the synaptic cleft; however, several studies carried out on cats and dogs between 1930 and 1940 found that BMP has a lower potency than AMP in terms of anti-hypotensive activity. Nevertheless, BMP was found to be a better bronchodilator than AMP [95-102]. Studies on rats showed that BMP crosses the blood-brain barrier [103]. However, only one animal study has been carried out to investigate the CNS stimulation effects of BMP [104]. Interestingly, studies on its pharmacokinetics, safety, and efficacy in humans and animals are limited [96]. The FDA banned its use in dietary supplements and weight-loss products after it was found in multiple supplemental products labelled as containing extracts of *Acacia rigidula* and *Acacia arabica* [96]. To date, no study on BMP pharmacokinetics has been conducted on humans or animals. Hence, one of the main goals of this project was to investigate the metabolites of BMP in rats.

Amphetamine **β-methylphenethylamine**

Figure 9: Chemical structures of amphetamine and β-methylphenethylamine

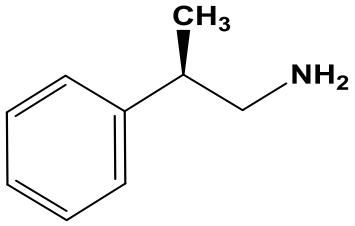

d-β-methylphenethylamine

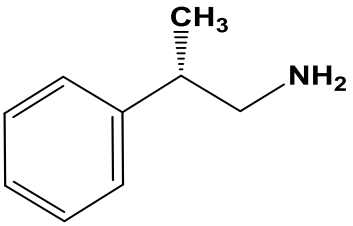

l-β-methylphenethylamine

Figure 10: Chemical structures of beta-methylphenethylamine isomers

1.7.1.3 Ephedrine

EPH is a natural sympathomimetic amine that occurs in many Ephedra plant species [94]. It was first isolated in the late 18th century, and first synthesized in 1920 in Japan [105, 106]. Chemically, EPH exists as two optically active enantiomers of phenylpropanolmethylamine. These isomers are (1S,2R)-(+)-EPH (d-EPH) and (1R,2S)-(-)-EPH (l-EPH) as shown in Figure 11; l-EPH is more potent than d-EPH with regard to its β-adrenergic agonistic action. l-EPH is a naturally occurring compound that was found to have a pronounced peripheral and mild central stimulant effects [94]. Clinically, EPH is used as a medication for asthma, nasal congestion, and obesity [107]. Pharmacologically, EPH induces the release of norepinephrine, from the vesicles of sympathetic neurons, so that they can directly interact with alpha- and beta-adrenergic receptors [108].

1.7.1.3.1 Mechanism of Action

The stimulation effect of EPH is a result of its direct and indirect activation of alpha- and beta-adrenergic receptors [109, 110]. It indirectly activates these receptors by inducing the release of norepinephrine from peripheral sympathetic neurons and inhibiting their neuronal reuptake [109, 110]. l-EPH exerts indirect sympathomimetic effects similar to those caused by

AMP, albeit to a lesser extent. Because of its similarity to AMP, EPH crosses the blood-brain barrier and releases epinephrine and dopamine in the substantia nigra at high doses [111].

1.7.1.3.2 Intoxication Symptoms

The intoxication symptoms of EPH can be categorized into two categories. The first category deals with the therapy-related adverse effects of EPH, including hypertension, headache, palpitation, sweating, weakness, tremors, myocardial infarction, seizures, and stroke [94, 105, 107–110]. The second category focuses on adverse effects associated with EPH overdose; these are similar to those of AMP and include paranoia, delusions, hallucination, and hostile behavior [94, 112, 113].

1.7.1.3.3 Pharmacokinetics of EPH

EPH exhibits high bioavailability. It is a basic drug (pKa 9.6) with relatively low molecular weight; therefore, it easily crosses lipophilic cellular membranes [94, 114]. EPH can be orally, intravenously, or intramuscularly administered in the form of (1R,2S)-(-)-EPH enantiomer (l-EPH) or as a racemic mixture (d,l-ephedrine sulphate or hydrochloride). Plasma C_{max} is generally attained within 2 h (t_{max}) of oral ingestion. EPH exhibits a volume of distribution of 2.4–3.6 L/kg [94, 114–116]. It is mainly metabolized in the liver by N-demethylation to NEPH (catalyzed by CYP450 isoenzymes). It also undergoes *p*-hydroxylation and conjugation [94]. Figure 12 shows the main metabolic pathway of EPH. It is mainly eliminated by renal excretion, and its plasma half-life is, to a certain extent, dependent on urine pH. Being a basic drug, it is rapidly excreted in acidic urine [94,114]. This explains the wide variability in its elimination half-life, which is found to be 4–10 h [94]. Table 4 shows the pharmacokinetic parameters of EPH in humans after single oral administration [114].

Figure 11: Chemical structures of ephedrine isomers

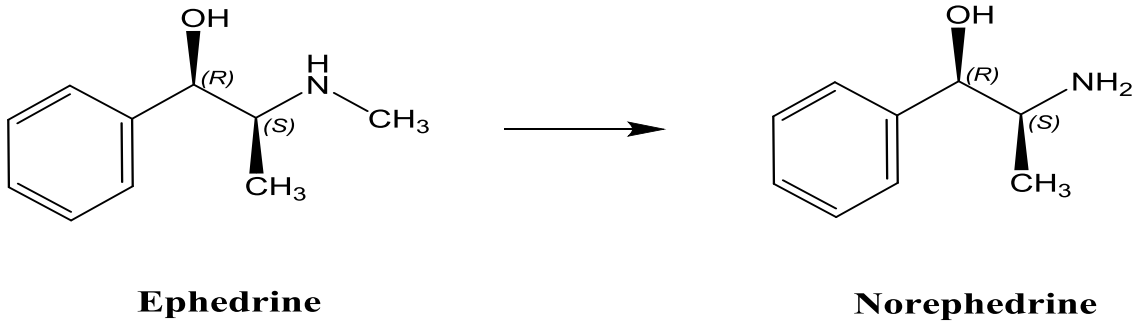

Figure 12: Main metabolism pathway of ephedrine

1.7.1.4 Pseudoephedrine

PEPH is a naturally occurring alkaloid in various Ephedra plant species [94]. PEPH was firstly isolated in 1889 by Ladenburg and Olschlägel [122, 123]. Chemically, PEPH is a diastereomer of EPH, and exists in two optically active enantiomers of phenyl propanolmethylamine; they are (1S,2S)-(+)-PEPH (d-PEPH) and (1R,2R)-(-)-PEPH (l-PEPH) as shown in Figure 13. PEPH is a naturally occurring sympathomimetic amine that has pronounced peripheral and mild central stimulant effects; however, it has lower potency than EPH with regard to its β-adrenergic agonistic action [124]. Clinically, PEPH is used as a nasal decongestant and bronchodilator [94]. Pharmacologically, PEPH induces the release of norepinephrine, which

is stored in the vesicles of sympathetic neurons, so that it can directly interact with alpha- and beta-adrenergic receptors; PEPH interacts with beta-adrenergic receptors to a lesser extent than EPH [124].

*Table 4: Pharmacokinetic parameters of ephedrine in human volunteers**

Subject No.	Body Weight Kg	t_{max} (h)	C_{max} (ng/mL)	$t_{\frac{1}{2}}$ (h)	AUC (ng · h/mL)	CL/F (L/h · kg)	V/F (L/kg)	CL_R (L/h · kg)
1	78.6	2.0	49.5	4.65	537.9	0.41	2.14	0.14
2	68.1	2.0	69.0	7.25	947.9	0.27	2.18	0.20
3	52.0	4.0	63.4	8.18	1000.4	0.33	3.06	0.19
4	76.2	4.0	58.1	5.62	748.7	0.30	1.92	0.12
5	56.8	2.0	77.2	4.90	727.2	0.42	2.31	0.33
6	72.7	2.0	51.6	5.32	517.9	0.46	2.75	0.20
7	54.6	1.5	80.0	5.51	950.3	0.33	2.07	0.25
8	88.9	1.5	59.5	7.0	645.0	0.30	2.38	0.23
Mean	—	2.4	63.5	6.06	759.4	0.35	2.35	0.21
SD	—	1.0	11.2	1.26	189.6	0.07	0.38	0.07

*Dose of 17.3 mg

Adopted from [114]

t_{max}, time after dosing to maximum plasma concentration; **C_{max}**, maximum plasma concentration achieved after a single oral dose; **$t_{1/2}$**, elimination half-life; **AUC**, area under the plasma concentration-time curve; **CL/F**, clearance divided by bioavailability; **V/F**, apparent volume of distribution; **CL_R**, renal clearance.

1.7.1.4.1 Mechanism of Action

The stimulation effect of PEPH is a result of its direct interaction with alpha-adrenergic receptors in the mucosa of the respiratory tract [124]. This direct interaction leads to vasocontraction and decreases nasal congestion. PEPH has lesser effectiveness on beta-adrenergic receptors than EPH because of the differences in their structural configurations; consequently, it exerts lower bronchodilator and pressor effects than EPH [124]. At high doses, the action of PEPH was found to be mediated by the release of dopamine and the activation of dopamine receptors [125].

1.7.1.4.2 Intoxication Symptoms

The symptoms of PEPH intoxication include headache, dizziness, palpitations, tachycardia, restlessness, tremor, anxiety, insomnia, dyspnea, hallucinations, pallor, weakness, convulsions, arrhythmia, hypotension, and cardiovascular collapse [94, 105, 107–110].

1.7.1.4.3 Pharmacokinetics of PEPH

PEPH has high bioavailability and volume of distribution (2–3 L/kg); it hardly exhibits any plasma protein binding (F_B=0.20). It is a basic drug (pKa 9.4) with a low molecular weight; therefore, it easily crosses lipophilic cellular membranes [94, 114]. It is commonly administered orally, and the plasma C_{max} is attained within 2 h (t_{max}) of oral ingestion (Table 5) [94, 114, 126–128]. Although almost 88% of PEPH is eliminated unchanged, less than 1% is metabolized by N-demethylation to norepseudoephrine (catalyzed by CYP450 isoenzymes) [94, 129]. PEPH is mainly eliminated by renal excretion, and its plasma half-life is, to a certain extent, dependent on urine pH; its excretion rate increases with acidic urine [94,114]. This explains the wide variability in its elimination half-life, which is found to be 3–16 h [94]. Table 5 shows the pharmacokinetic parameters of PEPH in humans after single oral administration [114].

d-pseudoephedrine **l-pseudoephedrine**

Figure 13: Chemical structures of pseudoephedrine isomers

*Table 5: Pharmacokinetic parameters of pseudoephedrine in human volunteers**

Subject No.	t_{max} (h)	C_{max} (ng/mL)	$t_{\frac{1}{2}}$ (h)	AUC (ng · h/mL)	CL/F (L/h · kg)	V/F (L/kg)	CL_R (L/h · kg)
1	4.0	19.4	5.87	245.2	0.28	2.33	0.16
2	2.0	24.1	6.88	305.5	0.26	2.53	0.23
3	2.0	23.1	9.83	398.7	0.26	3.62	0.19
4	4.0	22.1	6.43	323.0	0.22	2.00	0.14
5	2.0	29.3	4.55	254.8	0.37	2.40	0.32
6	2.0	22.1	6.00	228.6	0.32	2.76	0.20
7	1.5	29.1	5.38	318.6	0.31	2.37	0.30
8	2.0	23.7	5.15	223.8	0.27	1.98	0.25
Mean	2.4	24.1	6.26	287.3	0.28	2.50	0.22
SD	1.0	3.5	1.62	60.1	0.05	0.52	0.06

*Dose of 5.3 mg

Adopted from [114]

t_{max}, Time after dosing to maximum plasma concentration; **C_{max}**, maximum plasma concentration achieved after a single oral dose; **$t_{1/2}$**, elimination half-life; **AUC**, area under the plasma concentration-time curve; **CL/F**, clearance divided by bioavailability; **V/F**, apparent volume of distribution; **CL_R**, renal clearance.

1.7.1.5 Norephedrine

NEPH is a naturally occurring sympathomimetic amine in Khat (*Catha edulis* Forsk) [134, 135]. Chemically, NEPH exists as two optically active enantiomers of phenylpropanolamine; they are (1S,2R)-(+)-NEPH (d-NEPH) and (1R,2S)-(-)-NEPH (l-NEPH) as shown in Figure 14. NEPH is a sympathomimetic alkaloid that is pharmacologically similar to EPH [94]. Clinically, NEPH is used to treat nasal decongestion without excessively stimulating the CNS [94, 136, 137]. NEPH stimulates the sympathetic nervous system either by directly interacting with adrenergic receptors or by indirect carrier-mediated exchange with norepinephrine [136].

1.7.1.5.1 Mechanism of Action

The stimulation effect of NEPH is a result of its ability to selectively release norepinephrine [135]. Interestingly, NEPH releases dopamine at higher doses [135].

1.7.1.5.2 Intoxication Symptoms

The symptoms of NEPH intoxication include headache, dizziness, palpitations, tachycardia, nervousness, anxiety, arrhythmia, insomnia, agitation, tremors, hallucinations, pallor, weakness, convulsions, hypotension, and cardiovascular collapse [94].

1.7.1.5.3 Pharmacokinetics of NEPH

NEPH has a high bioavailability. It is a basic drug (pKa 9.1) [94]. It is commonly administered orally. The C_{max} is generally attained within 2.8 h (t_{max}) of oral ingestion [94]. Its volume of distribution was found to be 4.5 L/kg (Table 8) [94, 138]. In the first 24 h after dosing, NEPH is excreted unchanged in the urine with a mean recovery of 97% [94]. Heimlich *et al.* in 1961 reported that NEPH forms a *p*-hydroxy metabolite through a minor metabolism pathway (Figure 15) [139]. Its elimination half-life depends on urine pH, and is 3–4.4 h; an acidic urine

enhances the execration rate of NEPH, whereas an alkaline urine decreases it [94, 140, 141]. Table 6 shows pharmacokinetic parameters of NEPH.

Figure 14: Chemical structures of norephedrine isomers

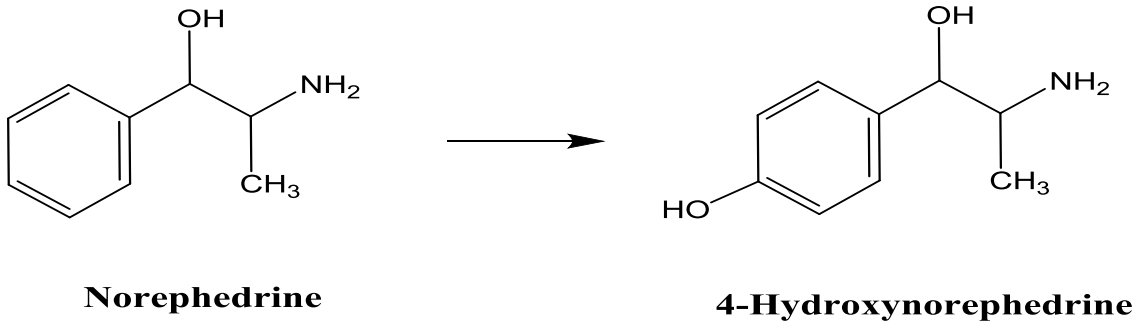

Figure 15: Minor metabolism pathway of norephedrine

Table 6: Pharmacokinetic parameters of norephedrine

Parameters	Participants				Mean ± SD
	1-Male	2-female	3-female	4- male	
Body weight (kg)	95.0	58.0	59.0	74.0	71.5 ± 17.3
Khat chewed (g)	59.2	36.1	36.1	43.6	43.8 ± 10.9
Amount in residue (% of original content)	4.8	5.9	7.2	6.1	6.1 ± 1.0
Ingested dose (mg)	25.0	15.1	14.9	18.2	18.3 ± 4.7
t_{lag1} (h)	0.01	0.20	0.18	0.30	0.17 ± 0.12
t_{lag2} (h)	1.03	1.03	0.99	2.22	1.32 ± 0.60
t_{max} (h)	2.48	2.92	2.56	3.41	2.84 ± 0.42
C_{max} (ng/mL)	76.3	84.2	55.3	72.7	72.0 ± 12.2
AUC (ng · min/mL)	690	942	525	681	710 ± 173

Adopted from [138]

t_{lag}, Lag time until appearance of substance in the central compartment; **C_{max}**, maximal plasma concentration; **t_{max}**, corresponding time to **C_{max}**; **AUC**, area under the concentration-time curve (by curve integration)

1.7.1.6 Cathine

CAT, d-norpseudoephedrine, is one of the naturally occurring sympathomimetic alkaloid amines in Khat [134, 135]. Chemically, CAT is a diastereomer of NEPH. It exists as two optically active enantiomers of phenylpropanolamine; they are (1S,2S)-(+)-CAT (d-CAT) and (1R,2R)-(-)-CAT (l-CAT) as shown in Figure 16. d-CAT is a more potent sympathomimetic agent than l-CAT [146, 147]. It exhibits 7–10 times lower psychostimulant potency than AMP [146].

1.7.1.6.1 Mechanism of Action

CAT is a psychostimulant known for its ability to release norepinephrine (norepinephrine agonist) and dopamine (dopamine agonist). At high doses, CAT induces the release of dopamine from nerve terminals [146, 147].

1.7.1.6.2 Intoxication Symptoms

The symptoms of CAT intoxication include headache, dizziness, palpitations, tachycardia, nervousness, anxiety, arrhythmia, insomnia, agitation, tremors, hallucinations, pallor, weakness, convulsions, palpitations, hypertension, vasoconstriction, ischemia, infarction, pulmonary edema, and cerebral hemorrhage [94, 148]. It also causes spermatorrhea, impotence, changes in libido, and urinary retention [148].

1.7.1.6.3 Pharmacokinetics of CAT

CAT has a high bioavailability and a low volume of distribution (0.74 L/kg). It is a basic compound (pKa 9.37) [138, 149]. It is commonly orally administered. The plasma C_{max} is generally attained within 2.6 h (t_{max}) of oral ingestion. Its elimination half-life (5.22 h) is dependent on urine pH (Table 7) [138]. It is excreted unchanged for almost 24 h [150]. Table 7 shows pharmacokinetic parameters of CAT.

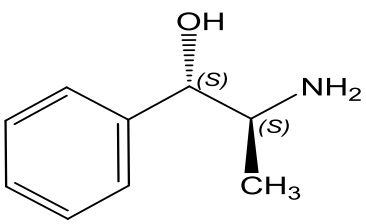

d-cathine

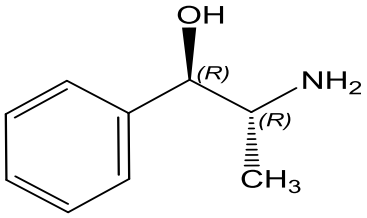

l-cathine

Figure 16*: Chemical structures of cathine isomers*

Table 7: Pharmacokinetic parameters of cathine

Parameters	Participants				Mean ± SD
	1-male	2-female	3-female	4-male	
Body weight (kg)	95.0	58.0	59.0	74.0	71.5 ± 17.3
Khat chewed (g)	59.2	36.1	36.1	43.6	43.8 ± 10.9
Amount in residue (% of original content)	8.0	6.2	17.3	12.3	10.9 ± 5.0
Ingested dose (mg)	45.4	28.1	24.8	31.7	32.4 ± 8.9
t_{lag} 1 (h)	0.13	0.001	0.52	0.20	0.21 ± 0.22
t_{lag} 2 (h)	1.33	1.10	1.07	2.32	1.46 ± 0.59
F_{abs} 1 (%)	84	77	92	84	84 ± 6
F_{abs} 2 (%)	16	23	8	16	16 ± 6
t_{max} (h)	1.65	2.46	2.88	3.49	2.62 ± 0.77
C_{max} (ng/mL)	67.2	87.6	54.6	75.2	71.2 ± 13.9
AUC (ng · min/mL)	598	881	620	753	713 ± 131
CL_{total}/F (mL min^{-1})	1,250	530	672	710	791 ± 316
MRT (h)	7.13	10.70	13.30	9.70	10.21 ± 2.55
Vc/F (L/kg)	1.08	0.67	0.28	0.94	0.74 ± 0.35
$t_{1/2\alpha}$ (h)	0.08	0.37	0.11	0.41	0.24 ± 0.17
$t_{1/2\beta}$ (h)	2.72	4.71	10.10	3.34	5.22 ± 3.36

Adopted from [138]

t_{lag}, Lag time until appearance of substance in the central compartment; **F_{abs}**, absorbed proportion; **C_{max}**, maximal plasma concentration; **t_{max}**, corresponding time to **C_{max}**; **CL_{total}/F**, apparent total body clearance; **MRT**, mean residence time; **AUC**, area under the concentration-time curve (by curve integration); **Vc/F**, apparent volume of the central compartment; **$t_{1/2\alpha}$**, half-life of the distribution phase; **$t_{1/2\beta}$**, terminal elimination half-life

Table 8: Pharmacokinetic parameters of the amphetamine-related drugs

Compound	$t_{1/2}$ (h)	V/F (L/kg)	F_B	pKa	Reference
Amphetamine	7-34	3.2–5.6	0.16	9.90	[94]
B-methylphenethylamine	---	---	---	10.2	[151]
Ephedrine	4–10	2.6–3.1	---	9.6	[94]
Pseudoephedrine	3.0–16	2.0–3.0	0.20	9.4	[94]
Norephedrine	3.0–4.4	4.5	---	9.10	[94]
Cathine	5.22	0.74	---	9.37	[138, 149]

1.8 Detection of Selected ARDs in Whole Blood

In contemporary forensic toxicology, analyses of selected ARDs in the blood are mainly carried out by using GC-MS or LC-MS to prevent doping, detain impaired drivers, stop drug abuse at workplaces, and investigate criminal cases (ante- and post-mortem) where drug abuse is expected.

Prior to GC-MS analysis, WB samples must be pretreated to facilitate the extraction of ARDs from WB. Due to their polarity, ARDs can be directly analyzed by GC-MS without derivatization; however, this direct analytical method is not recommended, particularly for WB samples because the fragment ions of ARDs bear similarity with those of other blood components, especially in post-mortem WB samples [152]. Therefore, the derivatization of

ARDs is recommended. ARDs can be derivatized by different derivatizing agents, such as heptafluorobutyric anhydride, pentafluoropropionic anhydride, trifluoroacetic anhydride, acetic anhydride, N-methyl bis (trifluoroacetamide), and 4-carbethoxyhexafluorobutyryl chloride [152–154]. Derivatization occurs due to the direct interaction of the derivatizing agent with the amine group of ARDs. Each one of these derivatized products yields fragmented ions that can be chosen to represent all parts of the fragmented compound [152–154].

The analytical detection of ARDs in WB by GC-MS was the ideal standard analytical method before the emergence of hyphenated LC-MS. Kudo *et al*. have reported an analytical method for qualifying and quantifying 13 ARDs in WB using GC-MS with an enhanced polymer column after extracting the analytes from WB using SPE and derivatization by acetalization; this study did not focus on resolving isomeric analytes [155]. Table 9 shows the 13 analytes and their limits of detection [155]. Furthermore, Kankaanpää *et al*. developed and validated a rapid GC-MS analytical method for 15 ARDs in human blood by extracting and derivatizing the analytes in a single step [156]. In this study, PEPH was fully resolved from its diastereoisomer, EPH.

The extraction of ARDs from WB samples may be challenging for analysis by GC-MS or LC-MS. If the polarity and volatility of ARDs are not controlled during extraction, they may be lost by evaporation or by adsorptive losses to activated glass present in the glass tubes or liners of the injection ports. Therefore, samples must be evaporated at 40°C or less during extraction, under acidic conditions. Furthermore, all glass apparatus must be deactivated to prevent the reaction of the protonated amine groups of ARDs and the silanol groups of glass. [152–154, 157].

Table 9: Limits of detection of 13 analytes

No.	Compound	LOD (ng/mL)
1	3,4-methylenedioxyamphetamine	7
2	3,4-methylenedioxymethamphetamine	7
3	4-methylthioamphetamine	10
4	amphetamine	7
5	dimethylamphetamine	7
6	ephedrine	50
7	methamphetamine	7
8	methylephedrine	50
9	N-methyl-1-(3,4-methylene dioxyphenyl)-2-butanamine	5
10	phenylpropanolamine	50
11	p-methoxyamphetamine	7
12	p-methoxymethamphetamine	50
13	β-phenethylamine	50

Adopted from [155]

ARDs can be directly determined by using LC-MS without derivatization. Moreover, LC-MS is significantly more sensitive than GC-MS [158]. However, the same analytical challenges encountered during GC-MS analysis, such as sample polarity and volatility, also affect LC-MS analysis. Furthermore, LC-MS analyses require the samples to be extensively pretreated and cleaned up to avoid any MEs that are most likely to interfere with analyses. Although such clean samples may be easily obtained in ante-mortem blood samples, an extensively putrefied post-mortem WB sample can present challenges. Another issue during the analysis of ARDs by LC-MS is the potential for extensive analyte fragmentation within the ion source chamber of the mass spectrometer. These analytical challenges must be overcome to develop and validate an

analytical assay for the identification and quantification of ARDs in WB by LC-MS. Dalsgaard *et al*. developed and validated an analytical method for the identification and quantification of 30 drugs in WB by using SPE and UPLC-qTOF-MS [159]. Practically, it is a challenge to obtain a fully resolved chromatogram of diastereomers by LC. Therefore, it requires the selection of the most suitable type of column, mobile phase, and chromatographic conditions. Accordingly, Sørensen described the analysis of cathinones and related ephedrines in forensic WB samples by simple extraction methods and LC-MS/MS analyses [160]. In this study, two pairs of diastereomers (EPH and PEPH; NEPH and CAT) were studied. These diastereoisomers were not fully resolved because of employing gradient elution (Figure 17) [160]. Apollonio *et al*. reported the use of UPLC/MS in the determination of ARDs and ketamine for forensic and toxicological analysis [161]. In this study, EPH and PEPH were fully resolved by employing an isocratic elution [161]. Table 14 shows LC-MS procedures for the identification and/or quantification of ARDs in WB [160–164].

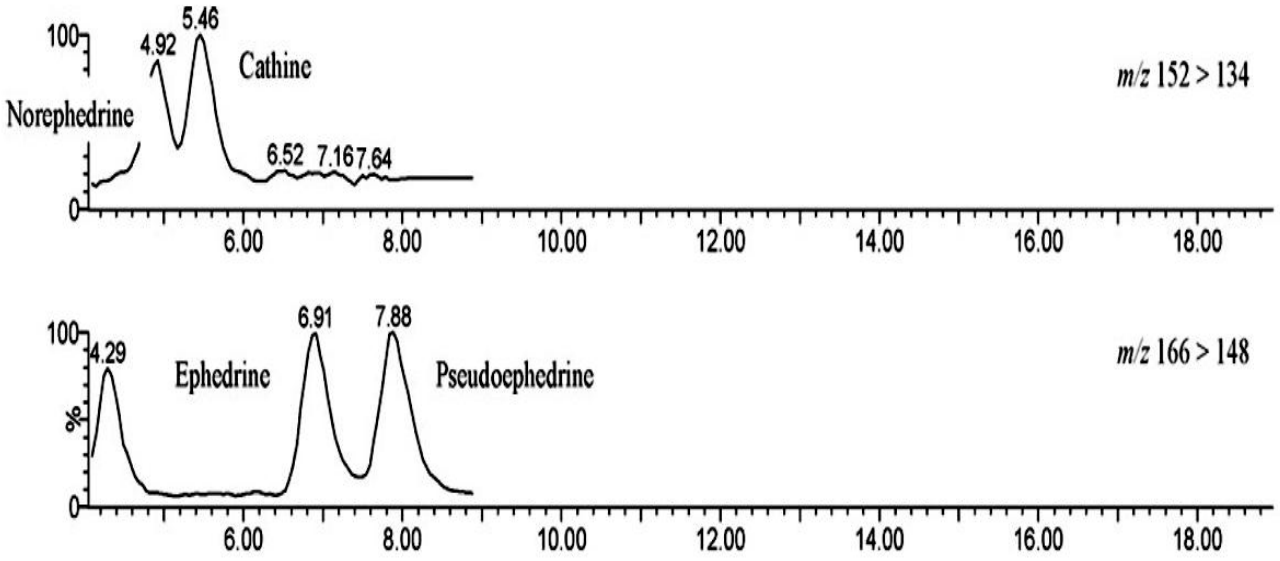

Figure 17: Extracted ion chromatograms of the quantifier ion of norephedrine and cathine (top), and ephedrine and pseudoephedrine (bottom); adopted from [160].

1.9 Interpretive Challenges

The forensic toxicology of ARDs in WB is not only challenging in analytical terms, but also in the toxicological interpretation of the measurements. Interpretations must consider several factors that can enhance or suppress intoxication symptoms in ante-mortem WB, and concentrations in post-mortem cases [165].

1.9.1 Drug Tolerance

Tolerance is a phenomenon in which a drug user is adapted to the effect of that drug. Consequently, a higher dose of the drug is required to induce the same effect as that experienced when the drug was used for the first time [166]. Tolerant abusers of ARDs require high doses that are toxic to naïve individuals.

There are mainly two types of tolerance; pharmacodynamic and pharmacokinetic tolerance. Pharmacodynamic tolerance occurs due to neuroadaptation that reduces the number or sensitivity of dopamine, alpha- and beta-adrenergic, and norepinephrine receptors to induce physiological responses [166]. Pharmacokinetic tolerance occurs because of decreased quantity of ARDs reaching dopamine, alpha- and beta-adrenergic, and norepinephrine receptors. This type of tolerance may be caused by increased in enzyme activities that required to metabolize ARDs (CYP450 enzymes). In such cases, intoxication symptoms are masked. Therefore, tolerance is an unpredictable phenomenon that challenges the interpretability of blood ARD concentrations in relation to behavioral effects, or the prediction of toxicity when the dose, route of administration, and time of last dose are not known [165]. Accordingly, the plasma concentration of AMP was found to be 590 ng/mL after 1 h of intravenous dl-AMP (160 mg) administration in a chronic user [94, 167]. Moreover, the steady-state AMP blood level was 2,000–3,000 ng/mL in a tolerant individual abusing AMP at an oral dose of 1000 mg daily [94, 168]. Serum EPH

concentration in a user addicted to EPH was 23,000 ng/mL after 1.5 h of ingestion of 7,500 mg of EPH [94, 169]. In 10 chronic users of PEPH, the average steady-state plasma concentration was 500–640 ng/mL after ingesting 360 mg of PEPH daily for 14 days [94, 129]. In six volunteers who orally ingested 150 mg of phenylpropanolamine, the serum concentration peaked to 280 ng/mL after 6 h [94, 170].

1.9.2 Post-mortem Redistribution

PMR is one of the major obstacles encountered during the analysis of drug concentrations in post-mortem cases [171]. Theoretically, it is defined as the change in drug concentration after death [172]. In such cases, drugs redistribute from solid organs (liver, lung, and myocardium) into the blood depending on the physiochemical and pharmacokinetic properties of drugs, such as volume of distribution, lipophilicity, and pKa [172]. ARDs exhibit PMR due to their high volumes of distribution and lipophilicities (Table 8). Consequently, it is necessary to consider PMR when interpreting the concentration of ARDs in the post-mortem blood. Failure to account for PMR could result in misleading interpretations of the cause of death [172].

AMP exhibits PMR. Accordingly, AMP concentration ratio in the heart:femoral blood was 1.5 in three cases [93, 94, 179]. In 17 fatal cases solely attributed to AMP, its concentrations in the femoral post-mortem blood were found to be 1,100–7,400 ng/mL [93, 94]. Interestingly, EPH was not found to show PMR, although the number of cases studied was small. Dalpe-Scott *et al.* reported that EPH concentration in the heart was equal to that in the femoral blood in three separate post-mortem cases [119, 121]. In five cases of death related to voluntary overdose of EPH, its concentration in the post-mortem blood was found to be 3,500–21,000 ng/mL [94, 117–119]. In contrast to EPH, PEPH exhibits PMR. Accordingly, Dalpe-Scott *et al.* reported that PEPH concentration ratio in the heart:femoral blood was 1.5 in three post-mortem cases [120]. In

two cases of death in children due to unintentional overdose of PEPH in combination with other agents, PEPH concentration in the post-mortem blood was found to be 6,000–13,000 ng/mL [94, 130, 131]. Reynolds reported a PEPH post-mortem blood level of 66,000 ng/mL in a case of PEPH overdose-related death in a child [132]. NEPH is also exhibited post-mortem redistribution. Accordingly, Dalpe-Scott *et al.* reported that the concentrations of NEPH in the heart:femoral blood were in the ratio of 2.4 in three post-mortem cases [120]. In two cases of death due to NEPH overdose, NEPH concentrations in the post-mortem blood were reported to be 2,000–4,600 ng/mL [94, 142-145]. PMR data for BMP and CAT in fatal cases are not available. Table 11 show the tissue distribution of AMP, EPH, PEPH, and NEPH in fatal cases.

1.10 Goals of This Study

The preliminary goal of this research was to develop and validate a new analytical method for identifying and quantifying ARDs in WB by SPE and LC-MS/MS. In this method, WB was pretreated by using a precipitation agent in form of an organic solvent (ACN) and extracted by MIP-SPE and MMSPE. The extracted samples were analyzed by UPLC-qTOF-MS. Method development and validation steps were based on the standard practices of the Scientific Working Group for Forensic Toxicology (SWGTOX) [176].

The secondary goal of this project was to apply the validated method to analysis of BMP in rats, and to attempt to identify BMP metabolite(s). An experimental study employing four groups (control, low dose, high dose, and high delayed dose) of rats (n_i = 3) was designed. Blood samples obtained from the rats were pretreated, extracted, and analyzed according to the validated analytical method.

Table 10: LC-MS procedures for the identification and/or quantification of ARDs in WB

Compound	Sample	Internal Standard	Extraction	Stationary Phase	Mobile Phase	Detection Mode	Validation Data	Reference
EPH PEPH NOR CAT	Blood	Norephedrine – D3 Cathine – D3 Ephedrine – D3 Pseudoephedrine – D3	LLE	Prodigy Phenyl-3 (150 x 2 mm I.D., 5 µm)	Gradient elution: water and MeOH acidified with 0.1 formic acid	Micromass Quattro Micro API triple-quadrupole	Recovery: 87-100 % LOD:0.5-3 µg/L Linearity: 10-250 µg/L	[160]
AMP	Blood	----	LLE	Aluspher RP-select B (125 x 4 mm I.D., 5 µm)	Gradient elution: 0.0125 M NaOH in MeOH-aqueous mM NaOH	DAD 225–350		[162]
AMP Hydroxyamphetamine	Blood	Tryptamine	LLE, OPA (or microdialysates, MD)	Supelco LC18 (250 x 4.6 mm, I.D., 5 µm)	Gradient elution: Methanol-potassium phosphate buffer pH (5.5)	FL (340/440)	Recovery: 99 % Linearity: 11–460 ng/ml	[163]

LLE, liquid-liquid extraction; **LOD**, limit of detection; **DAD**, photodiode array detector; **OPA**, *o*-phthalaldehyde, **FL**, fluorescence**.**

Table 11: Tissue concentrations of amphetamine-related drugs in fatal cases

Compound		Blood	Brain	Liver	Kidney	Urine	Gastric	Reference
Amphetamine	**Average (ng/mL or ng/kg)**	8,600	2,900	3,000	17,000	237,000	-----	[93, 94, 179]
	Range (ng/mL or ng/kg)	500–4,100	2,800–3,000	4,300–74,000	3,200–52,000	25,000–700,000	-----	
	Number of Samples	11	2	11	6	8	-----	
β-methylphenethyamine	**No Data Available**							
Ephedrine	**Average (ng/mL or ng/kg)**	9,700	8,200	50,000	22,000	262,000	24,000	[94]
	Range (ng/mL or ng/kg)	3,500–21,000	7,400–8,900	10,000–151,000	14,000–28,000	0–545,000	0–60,000	
	Number of Samples	5	5	5	5	5	5	
Pseudoephedrine	**Concentration (ng/mL or ng/kg)**	19,000	22,000	33,000	-----	105,000	102,000	[94, 133]
	Number of Samples	1	1	1	-----	1	1	
Norephedrine	**Concentration (ng/mL or ng/kg)**	48,000	86,000	460,000	-----	-----	20,000	[94, 142]
	Number of Samples	1	1	1	-----	-----	1	
Cathine	**No Data Available**							

CHAPTER 2

2. Methods

2.1 Chemicals and Materials

Standards for (±) amphetamine, (S,S)-(+)-pseudoephedrine, (1S,2R)-(+)-ephedrine-d_3 HCl, and (±)-amphetamine-d_{11} were purchased from Cerilliant (Round Rock, TX, USA) as 1 mg/mL methanolic solutions and diluted as required. (R*,S*)-(±)-ephedrine HCl, DL-norephedrine, and (R)-(+)-β-methylphenethylamine were obtained from Sigma Aldrich (Oakville, Ontario, Canada) as 1 mg/mL methanolic solutions and diluted as required. (+)-Norpseudoephedrine hydrochloride (cathine hydrochloride) was purchased from LGC Standards (Manchester, NH, USA) as a 0.1 mg/mL methanolic solution and diluted as required. ACN, MeOH, and purified water, used in drug extraction and UPLC analysis, were of reagent grade and obtained from EMD Milipore (Billerica, MA, USA). Ammonium acetate was purchased from Mallinckrodt Baker Inc. (Phillipsburg, NJ, USA). Acetic acid and HCl were obtained from BDH (Radnor, PA, USA). Ammonium hydroxide, ammonium formate, and formic acid were purchased from Fisher Chemicals (Bridgewater, NJ, USA). Amphetamines-specific MIP-SPE (25 mg) was purchased from Biotage (Uppsala, Sweden). Mixed-mode SPE (Oasis MCX, 30 mg) and FTPE (HLB Prime, 100 mg) were purchased from Waters (Milford, MA, USA). Aged animal blood was obtained from Ottawa Laboratory (Nepean, Ontario, Canada). Blank human whole blood was obtained from Utak Laboratories Inc. (Valencia, CA, USA).

2.2 Combined Working Solutions (Neat Standard Mix)

Methanolic combined working solutions of the analytes were made at different concentrations levels (20, 40, 200, 500, 800, and 1000 ng/mL) for the spiking of drug-free WB, and the preparation of calibration standards samples. Three internal standard (IS) solutions

containing 20, 500, 1000 ng/mL of the deuterated analogues of ephedrine and amphetamine were also prepared in MeOH for determining MEs

2.3 Molecularly Imprinted Polymer Solid Phase Extraction (MIP-SPE)

2.3.1 Whole Blood Sample Pretreatment

Aliquots (250 μL) of spiked and drug-free WB or aqueous samples were mixed with 1 mL of 10 mM ammonium acetate (pH 7), followed by an addition of 1 mL of ACN. The mixtures were vortexed and centrifuged at 5000 rpm for 15 min at room temperature, and the supernatants were decanted into clean tubes.

2.3.2 Whole Blood Sample Extraction

The MIP-SPE was carried out on an SPE vacuum manifold. The cartridges were conditioned with 1 mL of MeOH and equilibrated with 1 mL of 10 mM ammonium acetate (pH 7). The supernatants obtained from the pre-treatment step were loaded under gravity, and the cartridges were washed twice with 1 mL of water and once with 1 mL of ACN/water (60:40, v/v). The cartridges were then dried for 10 min at -40 kPa, washed with 1 mL of acetic acid/ACN (1:100, v/v), and dried again for 30 s at -10 kPa. The analytes of interest were then eluted with 2 mL of formic acid/MeOH (1:100, v/v). Figure 18 shows a schematic diagram for the extraction process. The eluates were evaporated to dryness under vacuum centrifugation at 30°C, and the residues were reconstituted in 200 μL of mobile phase A (5 mM ammonium formate + 0.1% formic acid in water). The reconstituted residues were subjected to UPLC-qTOF-MS analysis. Figure 20 shows the analytical method used in this study.

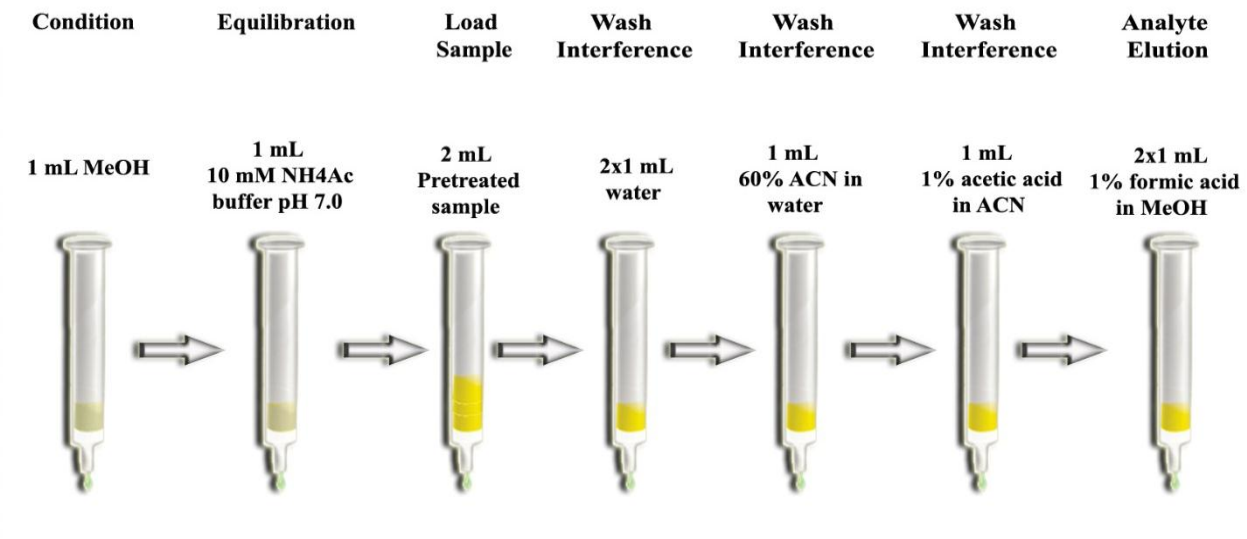

Figure 18: Schematic diagram of MIP-SPE extraction

2.4 Mixed Mode Solid Phase Extraction (MMSPE)

2.4.1 Whole Blood Sample Pretreatment

Spiked and drug-free WB or aqueous samples (250 µL) were mixed sequentially with 1 mL each of 0.1 M HCl and ACN. The mixtures were vortexed and centrifuged at 5000 rpm for 15 min at room temperature, and the supernatants were decanted into clean tubes.

2.4.2 Whole Blood Sample Extraction

MMSPE was carried out by using Oasis MCX 96-well plates. The wells were conditioned with 1 mL of MeOH and equilibrated with 1 mL of water. The supernatants obtained from the pre-treatment step were loaded under gravity, and SPE wells were washed sequentially with 1 mL each of 0.1 M HCl, MeOH, and 5% NH_4OH. The wells were dried under vacuum (-10 kPa) for 10 min, and the analytes were eluted with 1 mL of 5% NH_4OH in MeOH (Figure 19). The eluates were evaporated to dryness under vacuum centrifugation at 30 °C, the residues were

reconstituted in 200 µL of mobile phase A, and then underwent UPLC-qTOF-MS analysis (Figure 20).

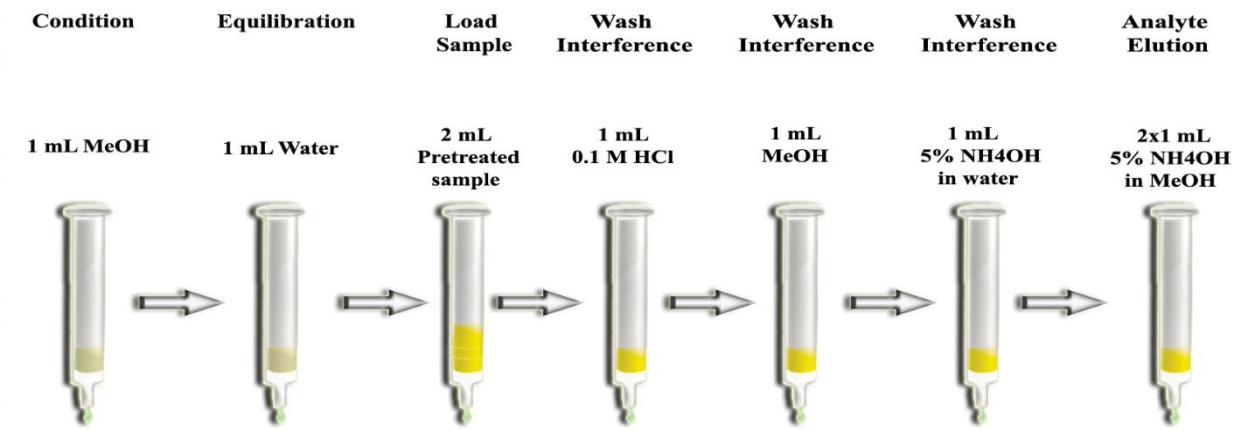

Figure 19: Schematic diagram of MMSPE extraction

2.5 Filtration Pass Through Extraction (FPTE)

2.5.1 Whole Blood Sample Pretreatment

Drug-free WB or aqueous samples (250 µL) were diluted with 1 mL of MeOH. The mixtures were then mixed with 1 mL of ACN. The mixtures were vortexed and centrifuged at 5,000 rpm for 15 min at room temperature, and the supernatants were decanted into clean tubes.

2.5.2 Whole Blood Sample Extraction

FPTE was carried out by using HLB Prime 96-well plates. The supernatants were directly loaded under gravity into the SPE wells. The eluates were collected and evaporated to dryness under vacuum centrifugation at 30°C. The dry residues were reconstituted in 200 µL of mobile phase A, and submitted for UPLC-qTOF-MS analysis (Figure 20).

2.6 UPLC-qTOF-MS Analysis: UPLC Conditions

Chromatographic separations were obtained on an ACQUITY UPLC™ HSS T3 column (100 mm × 2.1 mm, 1.8 µm) maintained at 45°C. Mobile phase A consisted of water, 0.1% formic acid, and 5 mM sodium formate; mobile phase B was composed of ACN and 0.1 % formic acid. The mobile phase composition was controlled as follows: 0–1 min, 0% B; and 1–10 min, 5% B (pseudo-isocratic) for baseline resolution of the isomeric analytes (see Figure 35); 10–11 min, 30% B, 11–12 min, 50% B; 12–13 min, 100% B; and 13–15 min 0% B. The flow rate was 0.5 mL/min, and the injection volume was 5 µL. Table 12 shows the optimized run method conditions.

2.7 UPLC-qTOF-MS: MS Settings

Mass spectrometry was performed on a Waters Acquity UPLC equipped with a Waters Xevo G2-XS-qTOF-MS (Waters, Medford, MA). Data was acquired in sensitivity mode using positive electrospray ionization with a resolution > 20,000 at full width half maximum. The acquisition range was m/z 50–601 using a scan time of 0.1 s. Capillary voltage and cone voltage were 0.8 kV and 20 V, respectively. The source temperature was 140°C, the desolvation gas flow rate was 900 L/h at 250°C, and the cone gas flow rate was 50 L/h. Data acquisition used the MS^E mode, with low collision energy (4 eV) and high-energy ramp (10–40 eV). Mass correction was performed during acquisition using an external reference (lockspray) composed of 2 µg/mL leucine enkephalin (monitoring m/z = 278.1114) solution infused at a flow rate of 5 µL/min. Table 12 shows the optimized method settings.

2.8 Data Processing

The raw data obtained after analysis were processed by two types of software. Analyte identification criteria were manually assessed using Masslynx 4.1 software (Waters, Manchester,

UK); the raw data were also processed automatically using the streamlined workflow of the UNIFI 1.7.0 software (Waters, Manchester, UK) for identification and quantification of the analytes. Compound identification was based on retention time (±0.05 min), mass deviation (± 10 mDa) and appropriate isotope profile.

Figure 20: Schematic diagram of the analytical method used in this study

Table 12: Optimized UPLC-qTOF-MS method parameters

Chromatography	
Liquid chromatography system:	Waters ACQUITY UPLC
Column:	Waters ACQUITY® HSS T3 (2.1 x 100 mm, 1.8 μm)
Column temperature:	45 °C
Injection volume:	5 μL
Solvent A:	5 mM ammonium formate, adjusted to pH 2.9 using formic acid
Solvent B:	Acetonitrile containing 0.1% (v/v) formic acid
Gradient:	0 % solvent B (0-1 min) 5 % solvent B (1-10 min) 5-30 % solvent B (10-11 min) 30-50 % solvent B (11-12min) 50-100 % solvent B (12-13min) 100-0 % solvent B (13-14 min) 0 % solvent B (14-15 min)
Flow rate:	0.5 mL/min

Mass Spectrometry	
Mass spectrometer:	Waters Xevo G2-XS QTof
Ionizations mode:	Electrospray +ve
Capillary voltage:	800 V
Cone voltage:	20 V
Cone gas:	50 L/h
Desolvation temperature:	250°C
Desolvation gas:	900 L/h
Source temperature:	140°C
Data acquisition:	MS^E centroid (data independent acquisition)
Function 1:	4 eV
Function 2:	Ramp 10-40 eV
Mass ange:	50 to 601 Da
Resolution:	> 20,000 @ 278 m/z (resolution mode)
Lock Spray:	leucine enkephalin = 278.1114 m/z
Lock Spray Infused Rate:	5 μl/min

CHAPTER 3

3. Analytical Interference in MIP-SPE / UPLC-qTOF-MS

3.1 Introduction

MIPs provide a medium with highly selective binding sites for analytes with specific structural features [174]. Accordingly, they have been promoted as highly selective SPE media for the extraction of target analytes and to minimize MEs while providing desirable reagent pH stability. However, the bleeding/leaching of residual template molecules from the polymer matrix is problematic with the advent of highly sensitive LC-MS detection schemes [175].

We investigated this issue in the analysis of ARDs in aged blood by UPLC-qTOF-MS. EPH, a toxicologically important analyte, was observed to leach from a commercially available MIP template across numerous extracts of drug-free aged WB blood and aqueous matrices, increasing apparent instrument EPH response by more than 25% at an absolute EPH concentration of 20 ng/mL. During the validation experiments, EPH interference were observed in the analysis of various aged, drug-free WB matrices. The method protocol was thoroughly investigated to identify the source of EPH observed

3.2 MIP-SPE UPLC-qTOF-MS – Validation Experiments

3.2.1 Evaluation of Matrix Effects (MEs)

According to the SWGTOX standard practices for method validation in forensic toxicology, a study on MEs must include an evaluation of the matrix interference and ME (ionization suppression/enhancement) [176].

3.2.1.1 Evaluation of Matrix Interferences (MIs)

MIs were evaluated to demonstrate the absence of common interferences from the WB matrix. Four different types of aged animal drug-free WB samples were pretreated and extracted

in triplicate by following the MIP pretreatment and extraction method explained in section 2.3 (chapter 2). The extracted samples were then analyzed for the presence of any interferences.

3.2.1.2 Evaluation of ME (Ionization Suppression/Enhancement)

ME is analytically defined as the direct or indirect alteration or interference in the instrument response due to the presence of coeluting compounds [176]. Two different types of aged animal drug-free WB samples were pretreated and extracted in triplicate by following the MIP pretreatment and extraction method explained in Section 2.3. After extraction, the extracts were spiked and diluted to 20, 500, and 1000 ng/mL of the combined standard working solutions and IS solutions. Further, the spiked blood samples and the corresponding neat combined working standards were analyzed, and their instrumental responses were used to determine the magnitude of ME for each component by using the following equation:

$$\%\mathbf{ME} = \frac{\text{Response}_{\text{spiked post-extracted sample}}}{\text{Response}_{\text{standard (working) solution}}} \text{ x } 100 \qquad \textit{(2)}$$

where,

ME < 100 indicates ion response suppression,

ME > 100 indicates ion response enhancement.

The acceptable range of ME is 100% ± 25% = 75%–125%

3.2.2 Experimental Evaluation of EPH Interference

WB samples (250 µL) from drug-free aged animal blood matrices, and aqueous samples (250 µL) from drug-free aqueous solutions were extracted in triplicate by MIP-SPE, MMSPE, and FPTE by following the pretreatment and extraction methods described in chapter 2 (sections 2.3,

2.4, and 2.5, respectively). Extracts were then analyzed by the optimized UPLC-qTOF-MS method. Figure 21 shows the experimental design for the evaluation of EPH interference.

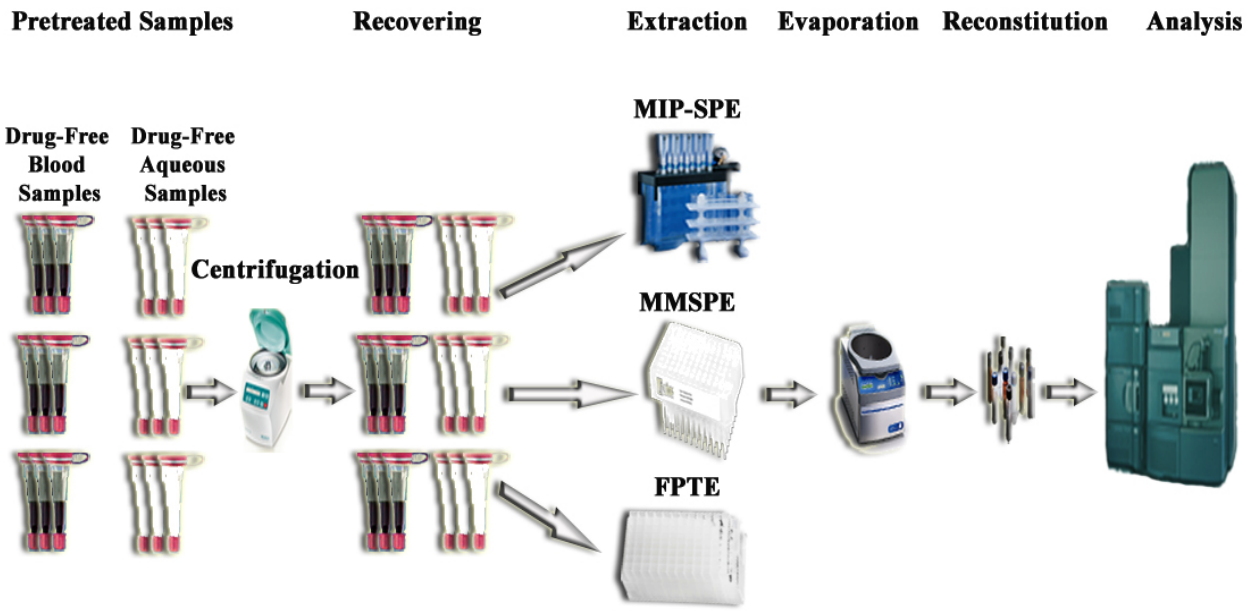

Figure 21: Schematic diagram of the analytical method designed to evaluate ephedrine interference

3.2 Results

Data corresponding to the samples prepared by MIP-SPE and analyzed by the optimized UPLC-qTOF-MS method are summarized in Table 13 and shown in Figure 22. MIs and MEs were assessed as per the SWGTOX guidelines [176].

3.3.1 Matrix interferences

Four different drug-free WB matrices were pretreated and extracted by MIP-SPE. The extracted samples were analyzed by the optimized UPLC-qTOF-MS method and their total ion

chromatograms (TICs) were checked for the presence of any interferences with respect to the retention time of the project analytes. An interferent was seen at the retention time of EPH in the total ion chromatogram (Figure 23). The extracted ion chromatogram (EIC) obtained by using the molecular ion of EPH (m/z 166) showed a peak at the same retention time as that of EPH (Figure 24). The mass spectrum of the interfering compound was obtained and compared with that of EPH (Figure 25). The interferent was identified as EPH after its retention time and mass spectrum profile matched those of EPH.

3.3.2 Matrix Effects (Ionization Suppression/Enhancement)

For EPH, measured ME values exceeded acceptable limits (≤ 25 %). Table 14 shows mean ME values for each analyte at three concentration levels (low, medium, and high) in aged bovine WB. Figure 26 graphically represents the mean ME values of analytes and internal standards at three concentration levels. Error bars represent the standard error of mean, whereas the two red lines represent the acceptable ME limits. EPH at a low concentration displayed an ME of 128% ± 9%, which was above the acceptable limit of enhancement. Table 15 shows that EPH at a low concentration displayed an ME (131% ± 10%) beyond acceptable limits; sheep WB was used in this assay. Figure 27 graphically represents the mean ME values on analytes and internal standards at three concentration levels. The ME value of EPH at the low concentration level was 131% ± 10%, which was above the acceptable limit of enhancement.

3.3.3 Ephedrine (EPH) Interference

3.3.3.1 Analysis of Drug-free Aged Animal Whole Blood

EPH interference was seen in drug-free aged animal WB samples that were extracted by MIP-SPE, but not by MMSPE or FPTE as observed in the TICs (Figure 28) and EIC (Figure 29).

Moreover, the mass spectrum of EPH matched with that of the interfering compound (Figure 30). The interfering compound was identified based on criteria shown in Table 16.

3.3.3.2 Analysis of Drug-Free Aqueous Solution

EPH interference was also seen in drug-free aqueous samples that were extracted by MIP-SPE, but not by MMSPE or FPTE. The EICs showed the presence of EPH interference at the retention time of that of EPH (Figure 31). Moreover, the mass spectrum of EPH matched with that of the interfering compound (Figure 32), and the compound was identified based on criteria as shown in Table 17.

Table 13: Analyte Parameters under Optimized MIP-SPE and UPLC-qTOF-MS Conditions

Drug	Ionization Mode	Molecular Ion (m/z)	Fragmented Ion (m/z) (± 0.01)	Retention Time (min) (± 0.05)
Amphetamine−d_{11}	Positive	147.1938	98.1078* / 130.1653	9.00
Ephedrine−d_3	Positive	169.1568	136.1195 / 151.1433*	7.54
Norephedrine	Positive	152.1180	115.0736 / 117.0736 / 134.0975*	5.36
Cathine	Positive	152.1180	115.0736 / 117.0736 / 134.0975*	6.05
Ephedrine	Positive	166.1378	115.0556 / 148.1208* / 149.1260	7.54
Pseudoephedrine	Positive	166.1378	115.0556 / 148.1208* / 149.1260	8.22
Amphetamine	Positive	136.1219	91.0553 / 119.0868*	9.31
β-methylphenetylamine	Positive	136.1219	91.0553 / 119.0868*	9.86

Quantifier Ions
Selection of the quantifier and qualifier ions was based on transitions from the molecular ion to the most and second-most predominant fragment ions respectively, expect for the amphetamine and β-methylphenethylamine the second most predominant fragmented ion was use as a quantifier ion (m/z 119 above m/z 100) to avoid any common putrefactive amine ion from the aged WB matrix, whereas the most predominant ion (m/z 91) was use as qualifier

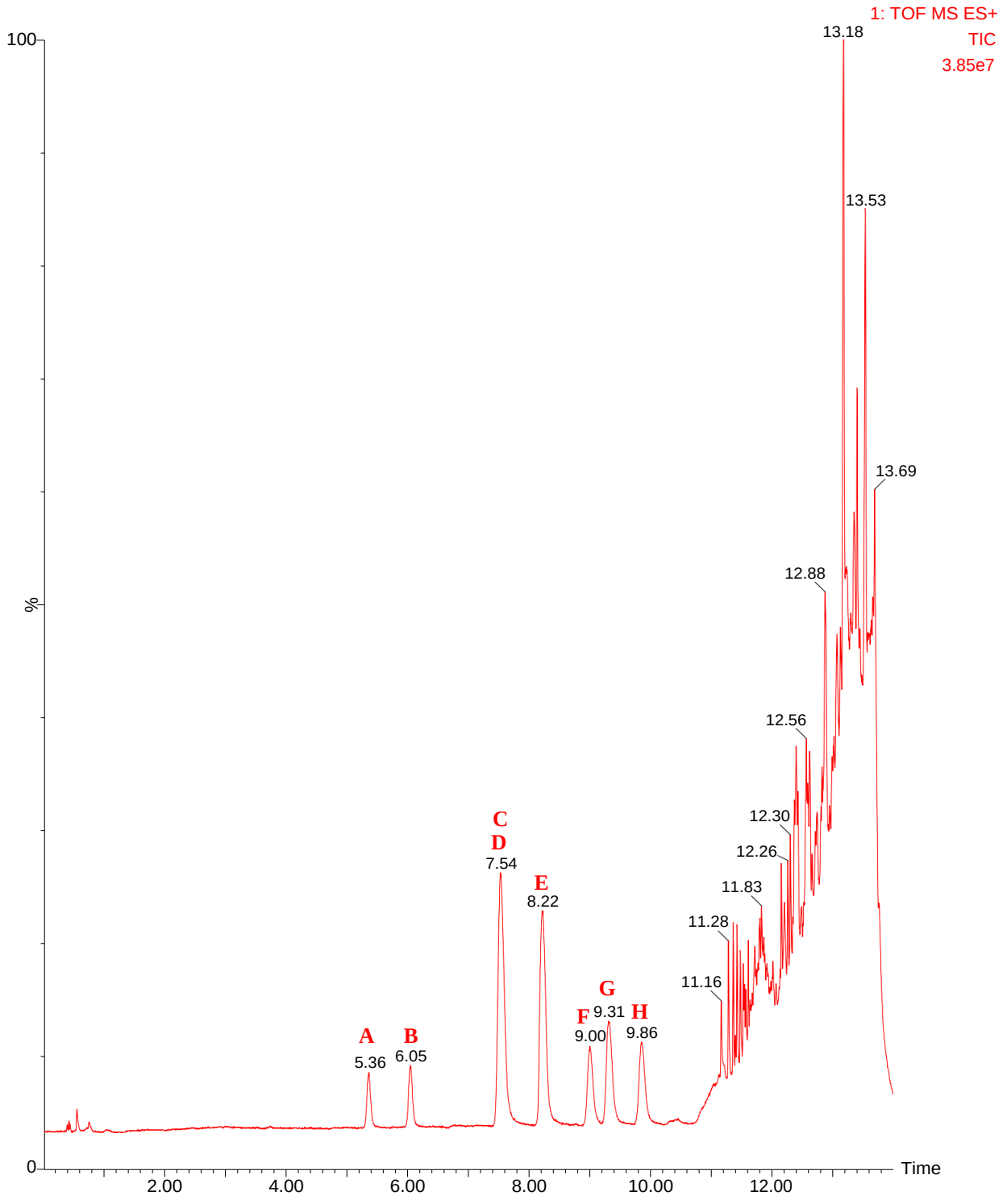

Figure 22: Total ion chromatogram of a neat standard mixture of the amphetamine-related drugs (1000 ng/mL) and deuterated analogues (500 ng/mL). A; norephedrine, B; cathine, C; ephedrine, D; ephedrine-d_3, E; pseudoephedrine, F; amphetamine-d_{11}, G; amphetamine, H;β-methylphenethylamine.

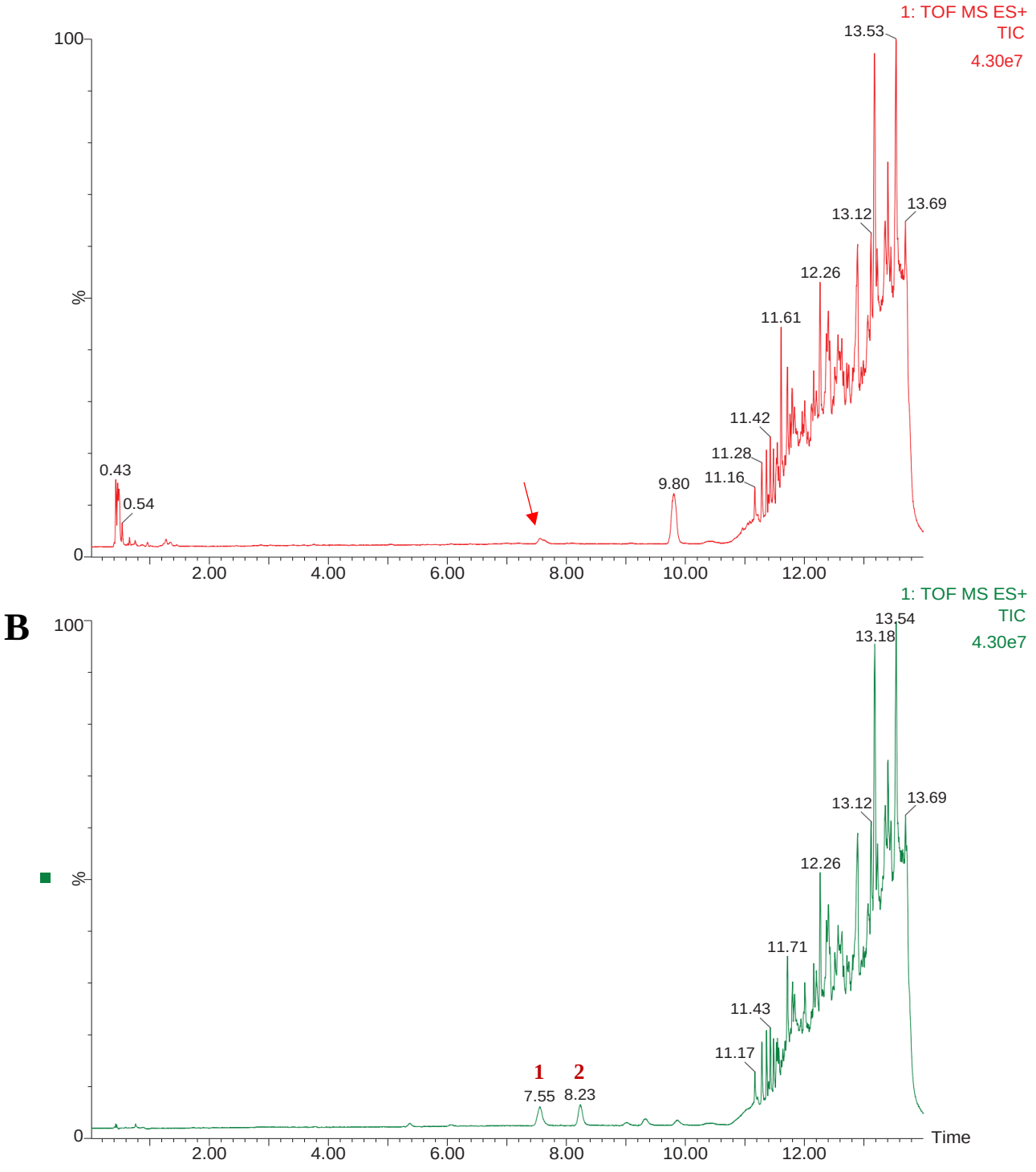

Figure 23: Total ion chromatogram of extract of drug-free bovine whole blood sample, extracted by molecular-imprinted polymer-solid phase extraction (A), and a 1 ng/mL neat standard mixture of ephedrine (1) and pseudoephedrine (2) (B). The red arrow indicates ephedrine interference observed in the total ion chromatograms of the drug-free bovine whole blood sample extracted by molecular imprinted polymer-solid phase extraction

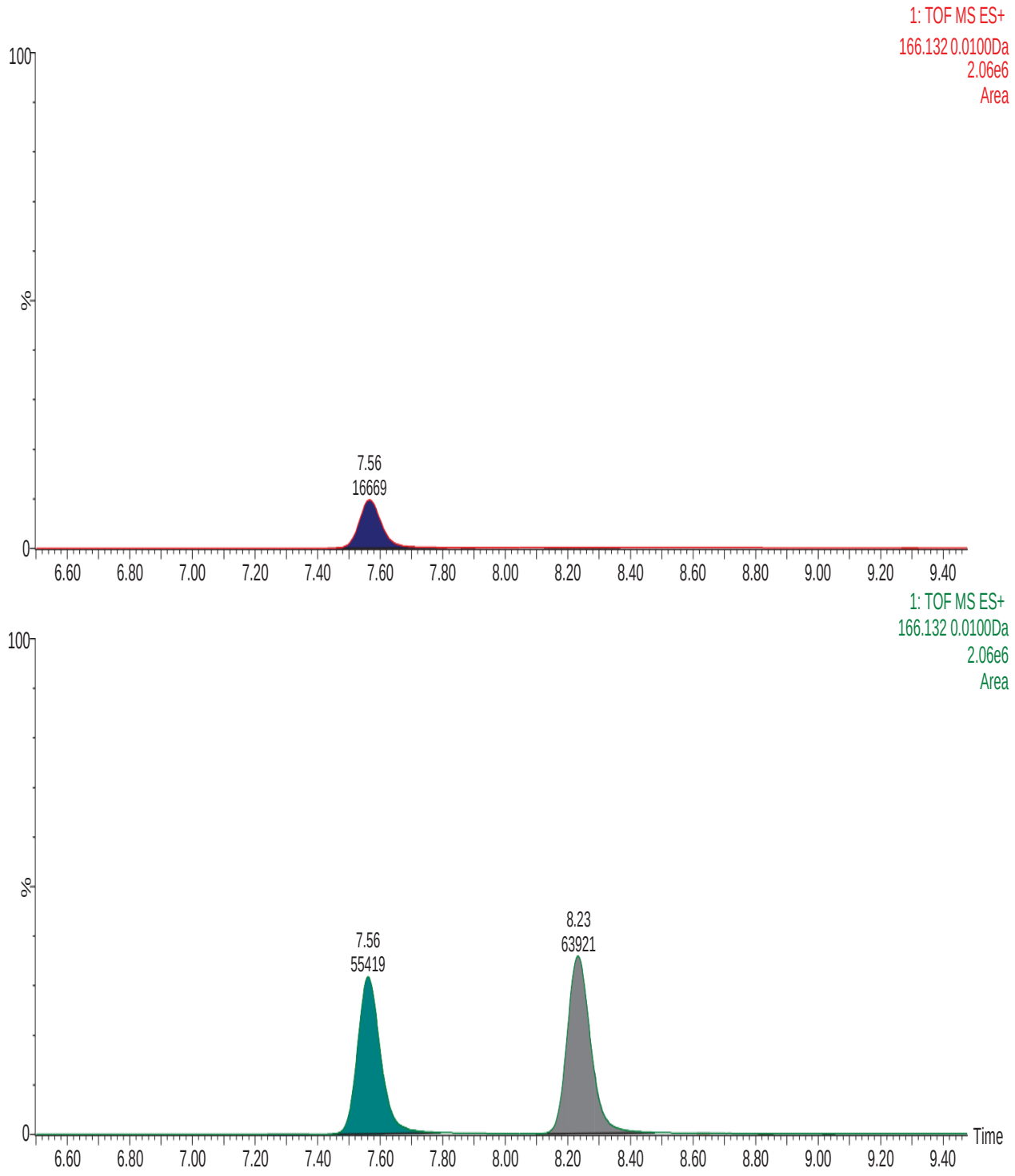

Figure 24: Extracted ion chromatogram of the molecular ion of ephedrine (m/z 166) of a drug-free bovine whole blood sample extracted by molecular imprinted polymer-solid phase extraction (A), and a 1 ng/mL neat standard mixture (B).

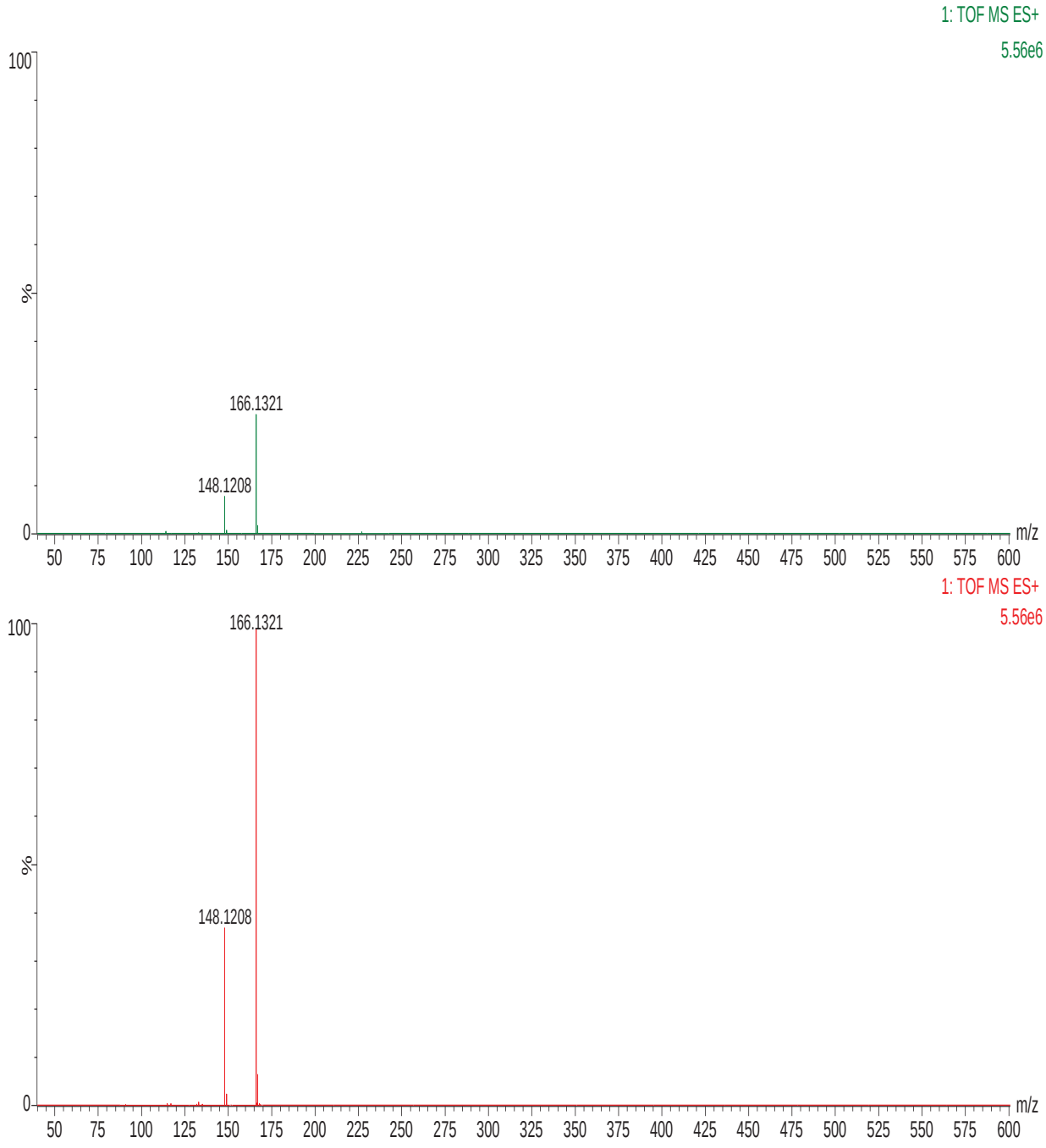

Figure 25: Mass spectrum of ephedrine in a drug-free bovine blood sample extracted by molecular imprinted polymer-solid phase extraction (A), and in a 1 ng/mL neat standard mixture (B).

Table 14: Evaluation of matrix effects (%) of amphetamine-related drugs and deuterated analogues of aged bovine blood

Analyte	Concentration					
	Low 20 ng/mL	% CV	Medium 500 ng/mL	% CV	High 1000 ng/mL	% CV
Amphetamine $-d_{11}$	99 ± 7	7.07	100 ± 6	6.00	109 ± 7	6.42
Ephedrine$-d_3$	102 ± 5	4.90	101 ± 1	0.99	106 ± 1	0.94
Norephedrine	102 ± 1	0.98	96 ± 1	1.04	97 ± 6	6.19
Cathine	103 ± 9	8.74	95 ± 1	1.05	93 ± 1	1.08
Ephedrine	128 ± 9	7.03	110 ± 3	2.73	105 ± 2	1.90
Pseudoephedrine	94 ± 2	2.13	104 ± 3	2.88	97 ± 6	6.19
Amphetamine	95 ± 8	8.42	95 ± 5	5.26	98 ± 3	3.06
β-methylphenethylamine	86 ± 4	4.65	92 ± 3	3.26	93 ± 2	2.15

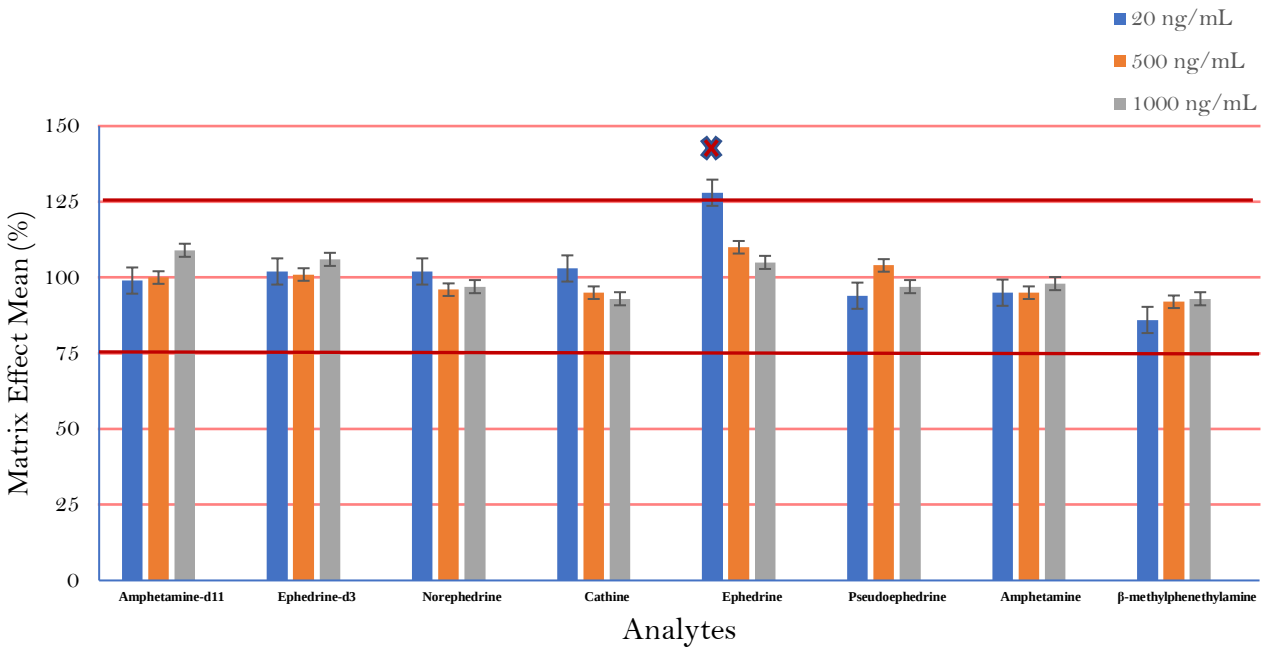

Figure 26: Matrix effects (%) of amphetamine-related stimulants and two deuterated analogues at three different concentrations measured in extracted aged bovine whole blood. The data represent the mean of triplicate measurements; error bars represent the standard error of the mean and red lines represent the acceptable limits of matrix effects

Table 15: Evaluation of matrix effects (%) of amphetamine-related drugs and deuterated analogues of aged sheep blood

Analyte	Concentration					
	Low 20 ng/mL	% CV	Medium 500 ng/mL	% CV	High 1000 ng/mL	% CV
Amphetamine−d_{11}	101 ± 2	1.98	100 ± 3	3.00	105 ± 4	3.81
Ephedrine−d_3	101 ± 1	0.99	104 ± 9	8.65	100 ± 1	1.00
Norephedrine	104 ± 5	4.81	98 ± 4	4.08	97 ± 3	3.09
Cathine	104 ± 6	5.77	98 ± 5	5.10	97 ± 1	1.03
Ephedrine	131 ± 10	7.63	99 ± 4	4.04	98 ± 2	2.04
Pseudoephedrine	103 ± 2	1.94	101 ± 6	5.94	90 ± 6	6.67
Amphetamine	96 ± 1	1.04	99 ± 3	3.03	99 ± 2	2.02
β -methylphenethylamine	90 ± 2	2.22	87 ± 3	3.45	91± 1	1.10

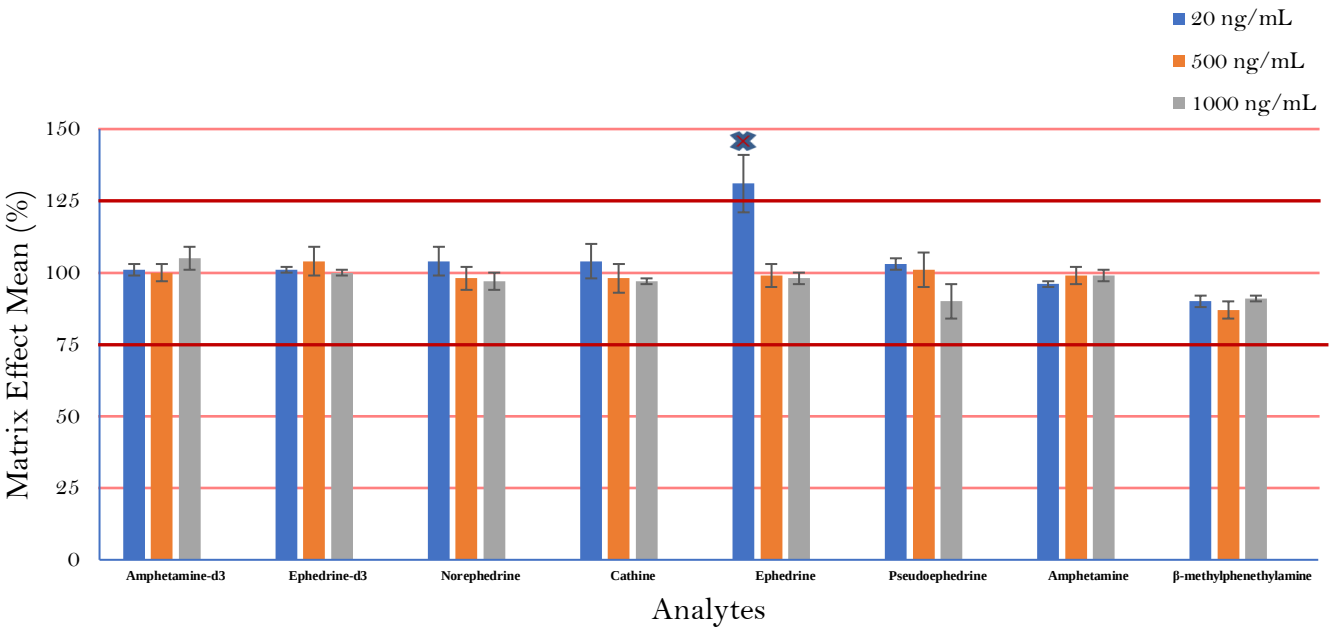

Figure 27: Matrix effects (%) amphetamine-related drugs and two deuterated analogues at three different concentrations measured in extracted aged sheep whole blood. The data represent the mean of triplicate measurements; error bars represent the standard error of the mean and red lines represent the acceptable limits of matrix effects

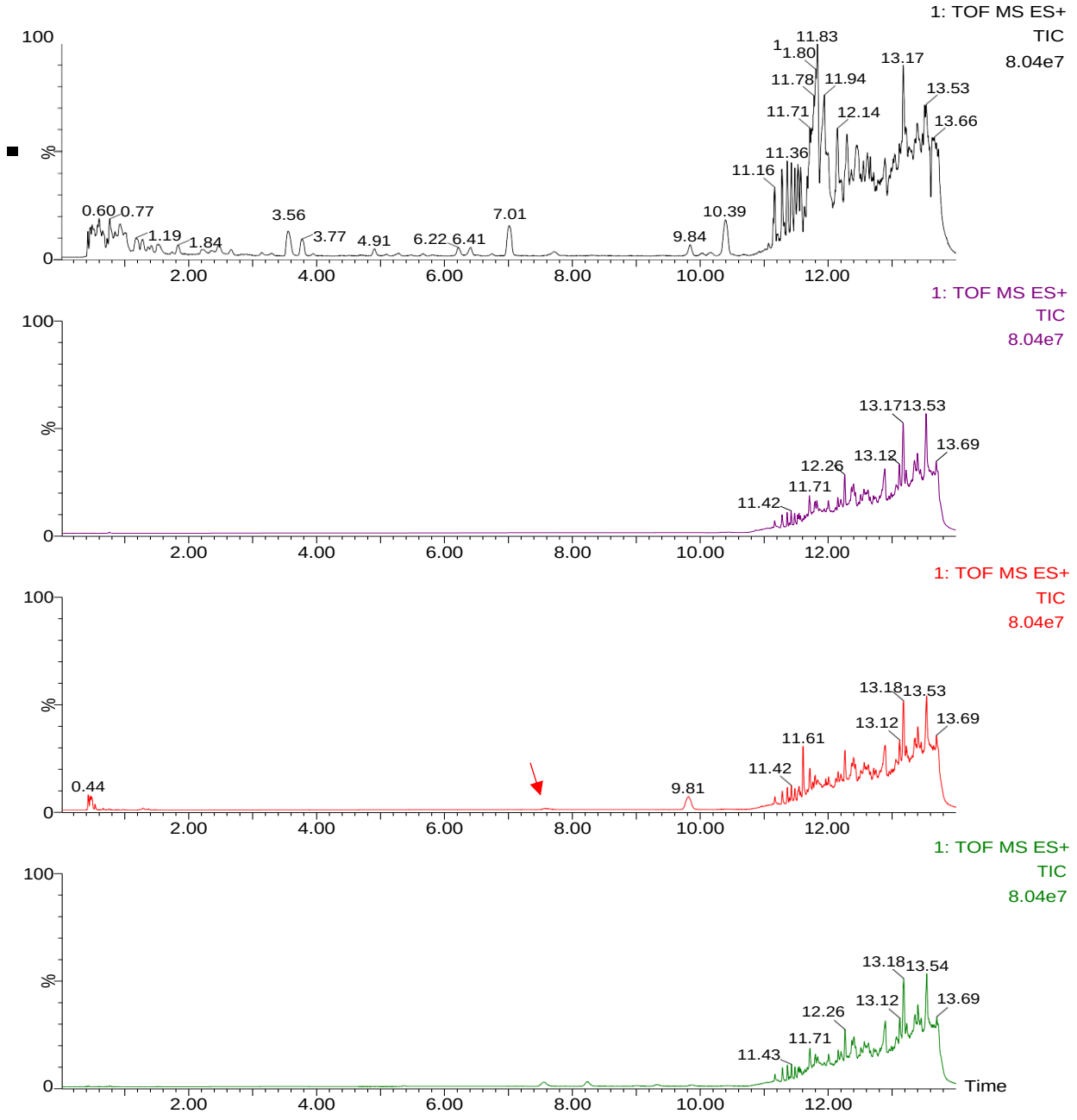

Figure 28: Total ion chromatograms of drug-free bovine whole blood samples extracted by filtration pass-through extraction (A), mixed-mode solid phase extraction (B), molecular imprinted polymer-solid phase extraction (C), and a 1 ng/mL neat standard mixture of ephedrine and pseudoephedrine (D). The red arrow indicates ephedrine interference observed in the total ion chromatograms of the drug-free bovine blood sample extracted by molecular imprinted polymer-solid phase extraction

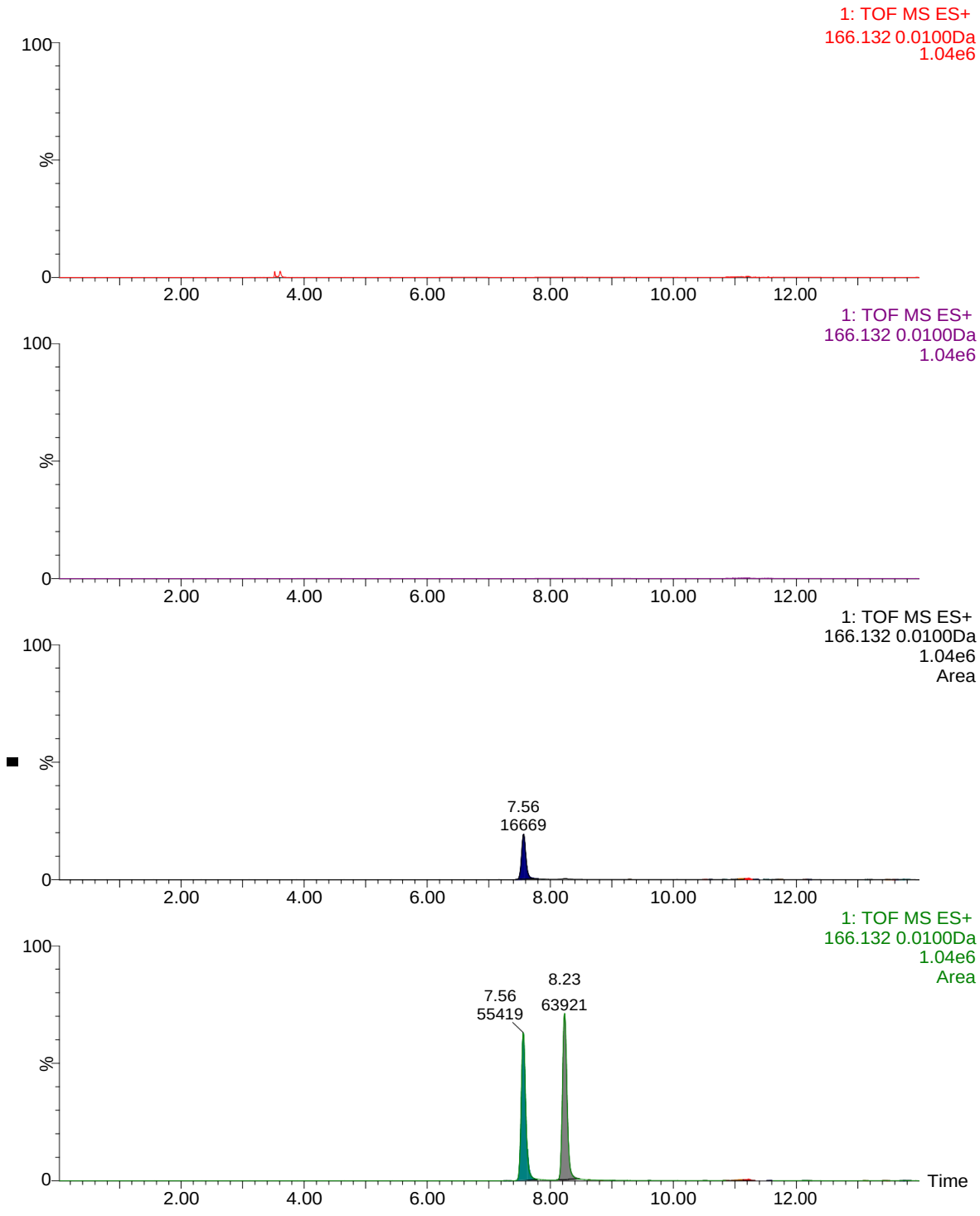

Figure 29: Extracted ion chromatograms of ephedrine by using the molecular ion m/z 166 of drug-free bovine whole blood samples extracted by filtration pass-through extraction (A), mixed-mode solid phase extraction (B), molecular imprinted polymer-solid phase extraction (C), and in a 1 ng/mL neat standard mixture (D)

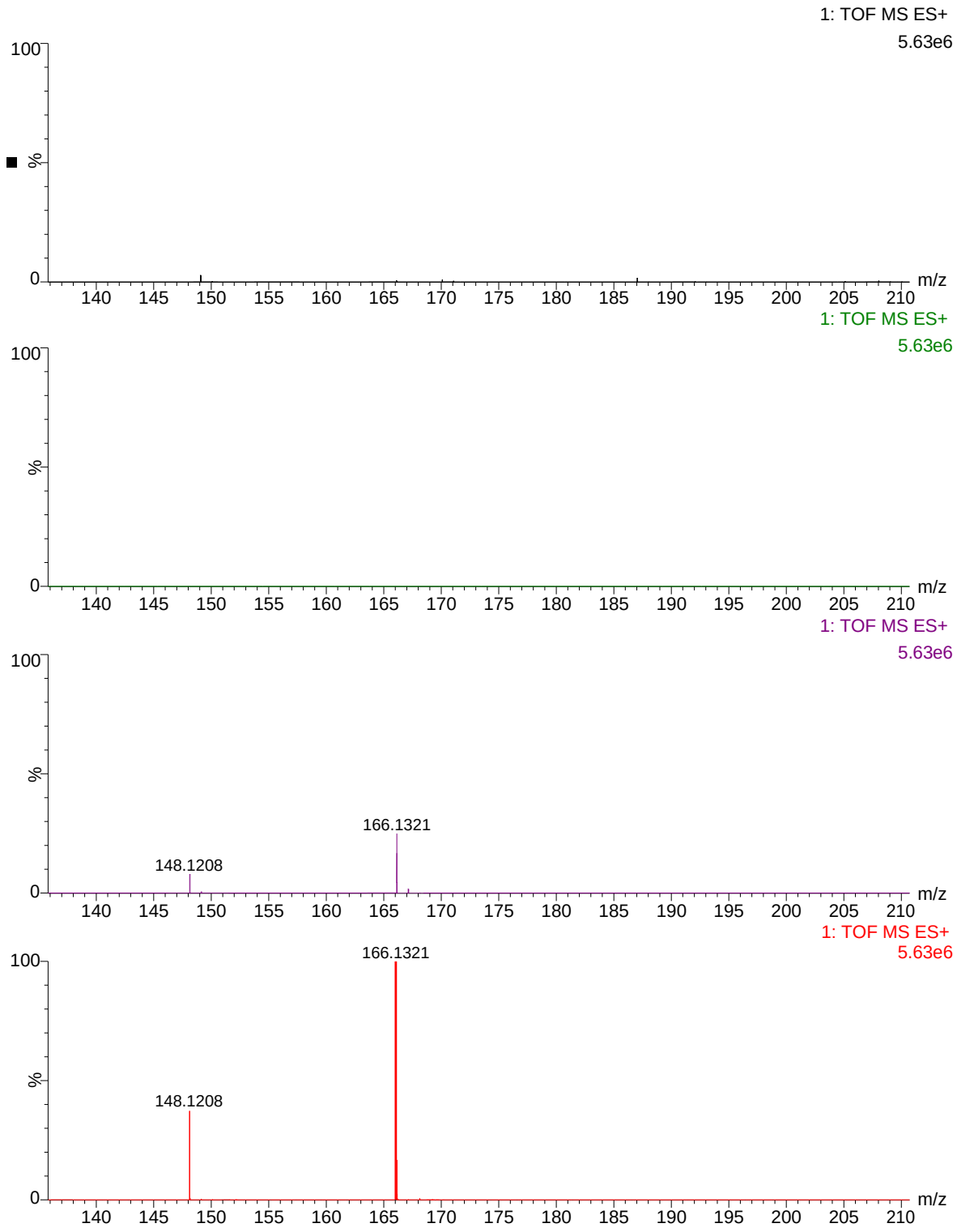

Figure 30: Mass spectra of ephedrine in drug-free bovine whole blood samples extracted by filtration pass-through extraction (A), mixed-mode solid phase extraction (B), molecular imprinted polymer-solid phase extraction (C), and in a 1 ng/mL neat standard mixture (D)

Table 16: Experimental data on ephedrine interference in aged bovine blood

SPE	Sample No.	Retention Time (min)	Ion Instrumental Response						Identified Analyte
			166 (m/z)	S/N	149 (m/z)	S/N	148 (m/z)	S/N	
MMSPE	1	---	0	0	0	0	0	0	-------
	2	---	0	0	0	0	0	0	-------
	3	---	0	0	0	0	0	0	-------
FPTE	1	---	0	0	0	0	0	0	-------
	2	---	0	0	0	0	0	0	-------
	3	---	0	0	0	0	0	0	-------
MIP-SPE	1	7.56	16669	817	564	191	7171	616	Ephedrine
	2	7.56	15485	907	541	231	6584	466	Ephedrine
	3	7.56	17632	1120	630	177	7449	745	Ephedrine
Mean			16595	948	578	200	7068	609	
STDEV			1075	155	46	28	441	139	

**S/N = signal to noise ratio; SPE, solid phase extraction; MM, mixed-mode; FPTE, filtration pass-through extraction; MIP, molecular imprinted polymer*

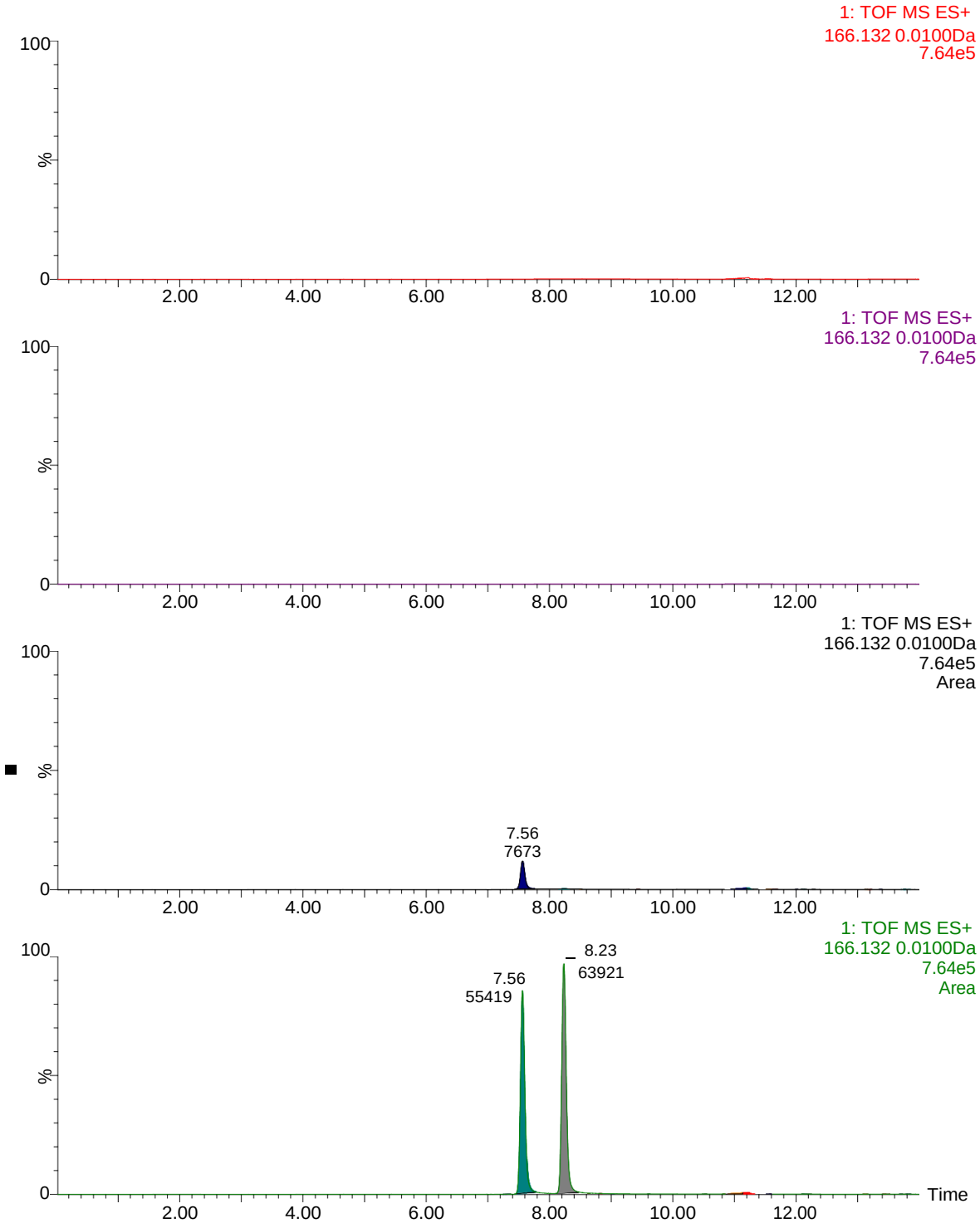

Figure 31: Extracted ion chromatograms of ephedrine by using the molecular ion m/z 166 in aqueous solutions (mobile phase A) extracted by filtration pass-through extraction (A), mixed-mode solid phase extraction (B), molecular imprinted polymer-solid phase extraction (C), and in a 1 ng/mL neat standard mixture (D).

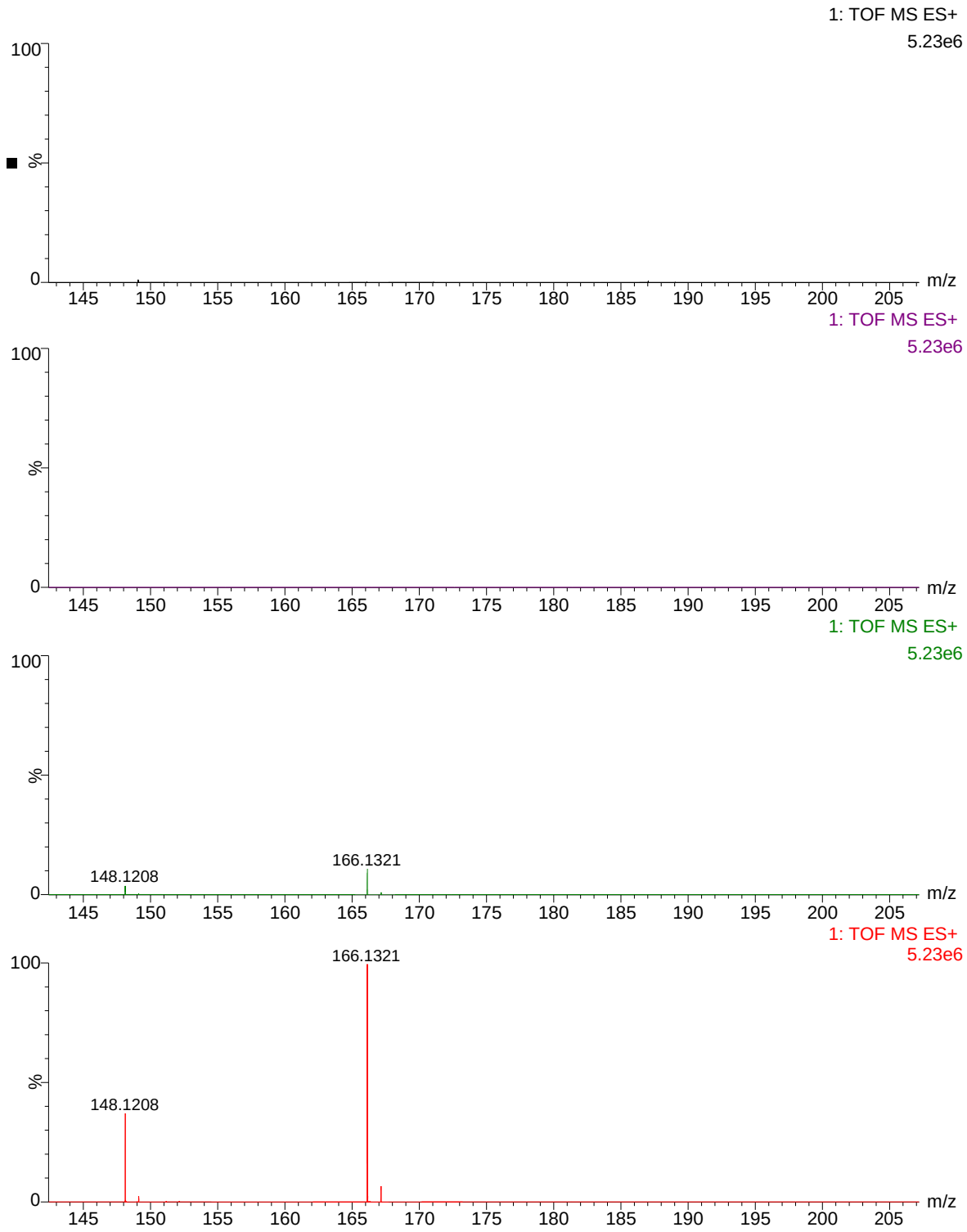

Figure 32: Mass spectra of ephedrine in aqueous solutions extracted by filtration pass-through extraction (A), mixed-mode solid phase extraction (B), molecular imprinted polymer-solid phase extraction (C), and in a 1 ng/mL neat standard mixture (D)

Table 17: Experimental data on ephedrine interference in in aqueous solutions

SPE	Sample No.	Retention Time (min)	Ion Instrumental Response						Identified Analyte
			166 (m/z)	S/N	149 (m/z)	S/N	148 (m/z)	S/N	
MMSPE	1	---	0	0	0	0	0	0	-------
	2	---	0	0	0	0	0	0	-------
	3	---	0	0	0	0	0	0	-------
FPTE	1	---	0	0	0	0	0	0	-------
	2	---	0	0	0	0	0	0	-------
	3	---	0	0	0	0	0	0	-------
MIP-SPE	1	7.56	7573	416	294	70	3533	309	Ephedrine
	2	7.56	9180	412	262	72	3380	319	Ephedrine
	3	7.57	9960	468	388	74	3890	345	Ephedrine
Mean			8904	432	314	72	3601	324	
STDEV			1075	155	46	28	441	139	

**S/N = signal to noise ratio; SPE, solid pahse extraction; MM, mixed-mode; FPTE, filtration pass-through extraction; MIP, molecular imprinted polymer*

3.4 Discussion

EPH, a toxicologically important analyte, was identified and observed to leach from a commercially available MIP across extracts of numerous drug-free aged animal WB and aqueous matrices (250 µL sample volume) in a phenomenon known as analyte bleeding. In such cases, template residues that are used to form the structure of the cavities in the polymeric particles are found to remain within the matrix of the designed polymer, despite extensive washing. This results in their leakage during sample extraction, and presence as a background interferent. This phenomenon can affect the detection accuracy of trace analytes, thereby significantly affecting forensic toxicological analysis [174, 176]. During validation, EPH interference was observed in the analysis of various drug-free aged animal WB matrices (Figures 22–24). To study the extent to which EPH interference affects the accuracy of the proposed analytical method, the ME of EPH was evaluated using two matrices of aged animal WB. It was observed that the apparent instrumental response for EPH at 20 ng/mL increased by more than 25% for both blood matrices. Due to the leaching of the template residue (EPH), ME crossed the acceptable levels at the low concentration level (20 ng/mL), but not at the medium (500 ng/mL), or high concentration level (1000 ng/mL) as shown in Table 14 and 15; these findings are graphically represented in Figure 25 and 26. Upon further investigation, the source of EPH was traced to the MIP-SPE template. Consultation with the vendor revealed that EPH was used as a template in the synthesis of amphetamines-specific MIPs. Due to the combination of imperfect washing and the high sensitivity of the UPLC-qTOF-MS method used, residual template molecules leached out during sample extraction were detected and registered as a EPH interference. This was demonstrated through analysis of numerous matrices of aged animal WB and an aqueous solution (mobile phase A) were extracted by MIP-SPE, MMSPE, and FPTE. Interestingly, EPH was not detected

in WB or aqueous samples that were extracted by MMSPE or FPTE (Figures 28–32). The identity of the interferent as EPH was confirmed based on three fragment ions of EPH at m/z 166, 149, and 148, their signal-to-noise ratios (S/Ns), and their retention times. The EIC, and mass spectrum of a neat standard of EPH matched with that of the interference compound in terms of the fragment ions formed and retention times. The S/Ns were above the lower acceptable limit (3:1) for all the three ions in the extracted aqueous and aged animal WB samples.

3.5 Conclusion

Although MIPs provide remarkable extraction selectivity, template leaching measurably interferes with the analysis of target analytes when instruments of very high sensitivity and selectivity are used; therefore, such an interference should be characterized and disclosed by all vendors.

Chapter 4

4. Validation of a Method to Identify and Quantify Selected ARDs in WB using UPLC-qTOF-MS after Extraction by MMSPE

4.1 Introduction

ARDs are common compounds implicated in drug abuse in Saudi Arabia. This drug abuse plays an important role in early mortality due to traffic accidents, violence, and overdose. Consequently, the entire Saudi society has been affected from abusing ARDs. Therefore, control of ARDs abuse is important. In forensic toxicology, analysis of ARDs may be utilized to identify those driving or performing other tasks under the influence of drugs, to clarify the manner and cause of death, and to identify individuals who have been exposed to drugs in the recent past. For purposes of estimation of the degree of drug toxicity, this analysis is best carried out by using blood samples, since blood drug concentrations are generally best correlated with the extent of toxicity.

Within the field of forensic toxicology, new analytical methods must undergo a process comprised of three stages prior to being adopted and incorporated within the laboratories' standard analytical methods. The three stages involve development, validation, and verification. It is crucial in forensic toxicological analysis to obtain reliable, consistent, and accurate measurements. Therefore, validation of the developed method is a prerequisite to analyzing actual samples in forensic casework. Validation involves performing a set of experiments to estimate the efficacy and reliability of an analytical method [176]. In forensic toxicological analysis, these experiments must be performed according to the most recent professional standards for the intended application. One example of such standards are those established by SWGTOX [176].

In this study, we report a validated analytical method to identify and quantify selected ARDs in WB using UPLC-qTOF-MS after extraction by MMSPE. The procedure requires 250 µL of WB to achieve a limit of quantification (LOQ) and detection (LOD) of 20 ng/mL for all analytes. Extraction recoveries of 63–90% and MEs of -21–9% were observed in aged animal WB samples. A quadratic polynomial equation was applied for fitting the calibration curves for all analytes. Satisfactory precisions below 20% and accuracies within 89–118% were obtained for all analytes.

4.2 Method

Method validation was done according to the standard practices established by SWGTOX [176].

4.2.1 Evaluation of Matrix Interferences (MIs): Selectivity

MIs were evaluated to confirm the absence of substances that may interfere with analyte detection in WB matrices. Five different types of aged animal and human drug-free WB matrices were pretreated and extracted in triplicate by following the MMSPE pretreatment and extraction method explained in section 2.4 (chapter 2). These extracted samples were analyzed for MIs by UPLC-qTOF-MS.

4.2.2 Evaluation of Matrix Effects (MEs): Ionization Suppression/Enhancement

MEs are defined as the direct or indirect alteration or interference in the instrument response due to the presence of co-eluting compounds that comprise the sample matrix [176]. Five different types of aged animal and human drug-free WB matrices were pretreated and extracted in triplicate by following the MMSPE pretreatment and extraction method explained in section 2.4 (chapter 2). The extracted drug-free samples were spiked with combined working standard and IS solutions in triplicate at concentrations of 20 (low), 500 (medium), 100 (high) ng/mL.

Spiked samples and corresponding neat standards were analyzed, and their instrumental responses were used to determine the magnitude of ME by using the following equation:

$$\%\mathbf{ME} = \frac{\text{Response}_{\text{spiked post-extracted sample}}}{\text{Response}_{\text{standard (working) solution}}} \text{ x } 100 \qquad \textit{(3)}$$

where,

ME less than 100 indicates suppression,

and ME greater than 100 indicates enhancement.

The acceptable range of ME is considered as 100 ± 25 = 75–125

MEs at each concentration level are represented as percentage increase or decrease in the peak areas of analytes in the samples relative to those of analytes in the neat standards.

4.2.3 Evaluation of Recovery

Recovery refers to the fraction of original analyte mass that is carried through the extraction process and is present in the final extract. It is measured as the ratio of analyte response in an extract to that of a drug-free extract after spiking the sample with the same mass of the analyte. Two different types of aged animal drug-free WB matrices were evaluated for recovery in triplicate at three concentration levels (low, medium, and high) in pre- and post-extraction spiked samples. Both samples were processed by following the MMSPE pretreatment and extraction method explained in section 2.4 (chapter 2). The samples were spiked with combined working standard and IS solutions in triplicate at concentrations of 20 (low), 500 (medium), and 1000 (high) ng/mL either before (pre-extraction spiked) or after (post-extraction spiked) extraction. The spiked samples were analyzed, and their instrumental responses were used to determine the magnitude of recovery by using the following equation:

$$\%\mathbf{RE} = \left(\frac{\text{Response}_{\text{pre-extraction spiked sample}}}{\text{Response}_{\text{post-extraction spiked sample}}} \right) \times 100 \qquad \textit{(4)}$$

4.2.4 Evaluation of Carryover

Carryover was evaluated by analyzing extracts of 250 µL of drug-free WB (n = 3) after analyzing a high-concentration calibrator (1000 ng/mL, n = 3) of the analytes. Both the samples were pretreated and extracted by the MMSPE extraction method described in section 2.4.

4.2.5 Evaluation of Calibration

Calibrators (250 µL) were prepared in drug-free aged bovine WB matrix at concentrations of 20, 40, 200, 500, 800, 1000 ng/mL by using combined working standard solutions each containing 125 ng of ISs (section 2.2). All samples were pretreated and extracted by the MMSPE extraction method (section 2.4) and analyzed by UPLC-qTOF-MS (sections 2.6, 2.7, and 2.8). Quantification was performed by measurement of the ratio of peak areas of the analytes relative to those of the corresponding deuterated analogs in the specific EICs; deuterated AMP was used for quantifying AMP and BMP, and deuterated EPH was used for quantifying EPH, PEPH, NEPH, and CAT. Calibration curves were constructed and assessed using quadratic regression (considered acceptable if $R^2 \geq 0.99$) of peak area ratios versus concentration on each of five different days. Each calibration curve was constructed using six calibrators in triplicate for each analyte. Furthermore, a batch of blind samples were analyzed in triplicate at two concentration levels along with the calibrators for purposes of assessment of analytical bias.

The working concentration range of the method was 20–1000 ng/mL for all analytes. The LOD was administratively defined as 20 ng/mL by using the lowest non-zero calibrator method (the calibrator with lowest concentration assayed with response that met precision criteria), due to the lack of toxicological significance of the analyte compounds at blood concentrations below 20

ng/mL. Fifteen samples with analytes at a concentration of 20 ng/mL were used to identify the LOD. All these samples were pretreated and extracted by following the MMSPE method (section 2.4). Similarly, the LOQ was also identified by following the same method for identifying LOD.

Analytical precision was measured as the coefficient of variation (%CV) of triplicate measurements at the assayed concentration range on each of five different days. It was considered acceptable when the %CV was ≤ 20%. Bias was determined after blinded analysis of triplicate samples at two different concentrations of each analyte per run. Bias was considered acceptable when the measured concentration was within 20% of the theoretical concentration.

4.2.6 Evaluation of Autosampler Stability

Analyte stability within the autosampler (maintained at 10°C) of the UPLC-qTOF-MS was evaluated by repeated injection of extracted samples at three different concentration levels (40, 500, and 1000 ng/mL; n = 3) after 0, 12, 24, and 36 h. Analytes were considered stable if the deviation in analyte response was within 20% of the response of the corresponding sample at t= 0 h

4.3 Results

UPLC-qTOF-MS data for samples prepared by MMSPE are summarized in Table 18 and shown in Figure 33.

4.3.1 Matrix Interferences (Selectivity and Specificity)

No MI was observed in the EICs at the retention times of the analytes in the five-different aged animal and human WB matrices (Table 19).

4.3.2 Matrix Effects (Ionization Suppression/Enhancement)

MEs (suppression/enhancement) were < 25 % for all analytes in the five different WB matrices assayed. Tables 20–24 show the ME values of all analytes in aged bovine, sheep, and

human WB matrices, respectively; Figures 34–38 graphically represent the respective mean ME values.

4.3.3 Recovery

Recovery ranged from 60–90% for all analytes in aged bovine (Table 25 and Figure 39) and sheep (Table 26 and Figure 40) WB matrices.

4.3.4 Carryover

Carryover was evaluated by analysis of three drug-free aged animal WB extracts directly after analyzing the high concentration calibrator (1,000 ng/mL, n = 3) samples. No carryover was observed upon visual inspection of the chromatograms and after the analysis of EICs.

4.3.5 Calibration of Analytical Response

Analytical response ratios were fit to calibrator concentrations using quadratic regression equations over a range of 20–1,000 ng/mL. Strong correlations ($R^2 > 0.99$) were observed on all five days. Table 27 shows the averaged calibration curve regression equations and correlation coefficients for all analytes. Averaged quadratic calibration curves are shown in Figures 41 (NEPH and CAT), 42 (EPH and PEPH), and 43 (AMP and BMP). The LOD and LOQ were determined to be 20 ng/mL for all analytes. Intra- and inter-day precision were 1.00–18.30% and 6.60–19.70%, respectively; they were deemed acceptable. The accuracy of the method was also acceptable (-11–18.25%). Table 28 summarizes the parameters determining analytical performance.

4.3.6 Stability of Analytes in Autosampler

The stability of the analytes in the autosampler was assessed at three different concentrations over 36 h. For all analytes, there was no change in response ratio in excess of 20% of the initial

response (t = 0 h), indicating that they remained stable while on the instrument waiting to be injected (Table 29).

Table 18: Analytical parameters of the analytes

Drug	Ionisation Mode	Molecular Ion (m/z)	Fragmented Ion (m/z) (± 0.01)	Retention Time (min) (± 0.05)
Amphetamine−d_{11}	Positive	147.1938	98.1078* /130.1653	8.76
Ephedrine−d_3	Positive	169.1568	136.1195 /151.1433*	7.30
Norephedrine	Positive	152.1180	115.0736 / 117.0736 /134.0975*	5.21
Cathine	Positive	152.1180	115.0736 / 117.0736 /134.0975*	5.90
Ephedrine	Positive	166.1378	115.0556 / 117.0713 / 148.1140* / 149.1160	7.31
Pseudoephedrine	Positive	166.1378	115.0556 / 117.0713 / 148.1140* / 149.1160	8.00
Amphetamine	Positive	136.1219	91.0553 / 119.0868*	9.05
β-methylphenethylamine	Positive	136.1219	91.0553 / 119.0868*	9.58

*Quantifier ions

Table 19: Evaluation of matrix interferences in five drug-free whole blood matrices after extraction.

Number	Whole Blood Matrix	Result
1	Bovine	No interference
2	Sheep	No interference
3	Human Sample 1	No interference
4	Human Sample 2	No interference
5	Human Sample 3	No interference

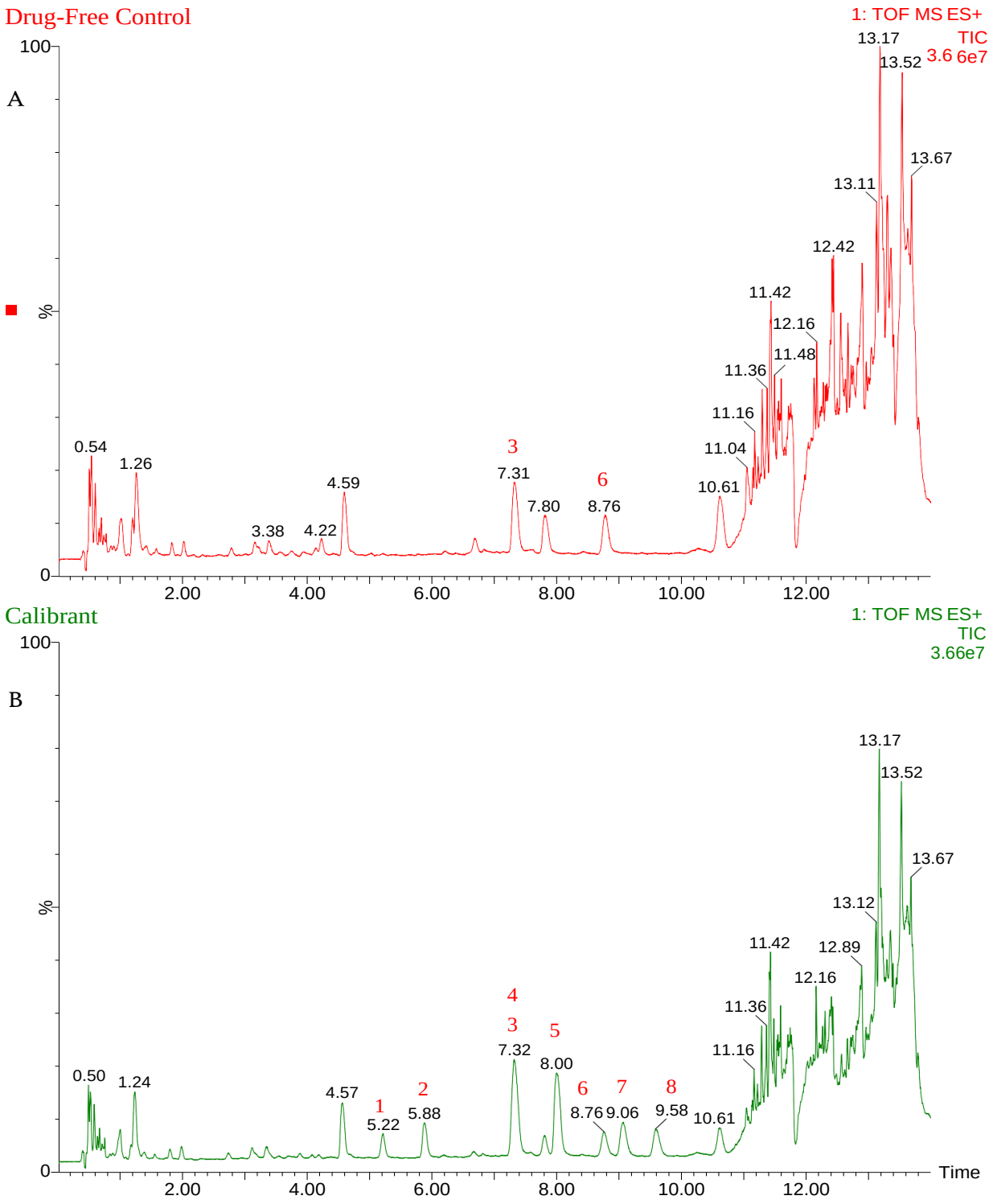

Figure 33: Total ion chromatogram of extracted aged animal whole blood; (A) drug-free control, and (B) spiked with 800 ng/mL of the combined working solution and 500 ng/mL of the internal standard solution; (1) norephedrine, (2) cathine, (3) ephedrine-d_3, (4) ephedrine, (5) pseudoephedrine, (6) amphetamine-d_{11},(7) amphetamine, and (8) β-methylphenethylamine

Table 20: Evaluation of matrix effects (%) of aged bovine whole blood on amphetamine-related drugs and deuterated analogues

Analyte	Concentration					
	Low 20 ng/mL	% CV	Medium 500 ng/mL	% CV	High 1000 ng/mL	% CV
Amphetamine−d_{11}	84 ± 3	3.57	87 ± 3	3.45	89 ± 1	1.12
Ephedrine−d_3	87 ± 5	5.75	88 ± 3	3.41	86 ± 6	6.98
Norephedrine	89 ± 3	3.37	90 ± 2	2.22	87 ± 1	1.15
Cathine	87 ± 3	3.45	91 ± 2	2.20	87 ± 2	2.30
Ephedrine	88 ± 10	11.36	86 ± 4	4.65	87 ± 7	8.05
Pseudoephedrine	86 ± 6	6.98	91 ± 2	2.20	91 ± 2	2.20
Amphetamine	93 ± 2	2.15	94 ± 2	2.13	92 ± 2	2.17
β-methylphenethylamine	93 ± 4	4.26	94 ± 1	1.06	91 ± 4	4.40

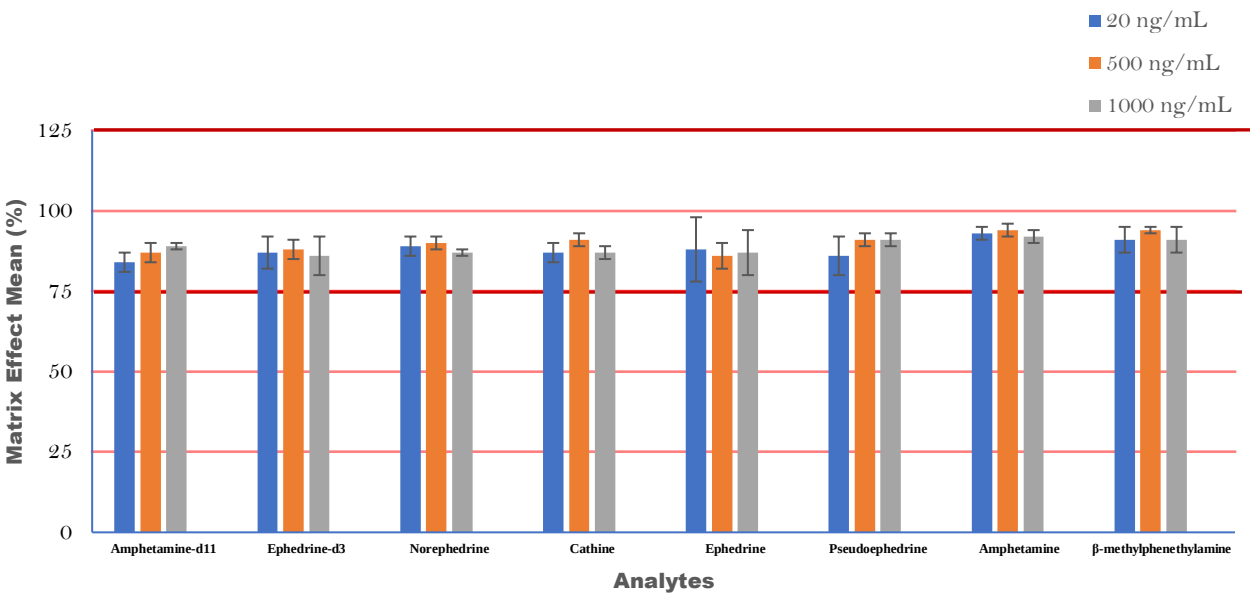

Figure 34: Matrix effects (%) measured in extracts of aged bovine whole blood spiked with amphetamine-related drugs, including two deuterated analogues, at three different concentration levels (20, 500 and 1000 ng/mL). The data shown represent the mean of triplicate analysis, error bars represent the standard error of mean, and red lines represent acceptable limits of matrix effects.

Table 21: Evaluation of matrix effects (%) of aged sheep whole blood on amphetamine-related drugs and deuterated analogues

Analyte	Concentration					
	Low 20 ng/mL	% CV	Medium 500 ng/mL	% CV	High 1000 ng/mL	% CV
Amphetamine−d_{11}	101 ± 8	7.92	101 ± 1	0.99	100 ± 1	1.00
Ephedrine−d_3	96 ± 9	9.38	106 ± 2	1.89	95 ± 4	4.21
Norephedrine	98 ± 3	3.06	100 ± 2	2.00	95 ± 1	1.05
Cathine	96 ± 1	1.04	99 ± 2	2.02	94 ± 1	1.06
Ephedrine	109 ± 5	4.59	98 ± 3	3.06	98 ± 1	1.02
Pseudoephedrine	109 ± 3	2.75	104 ± 1	0.96	95 ± 2	2.11
Amphetamine	101 ± 6	5.94	100 ± 2	2.00	99 ± 2	2.02
β-methylphenethylamine	102 ± 7	6.86	99 ± 1	1.01	99 ± 3	3.03

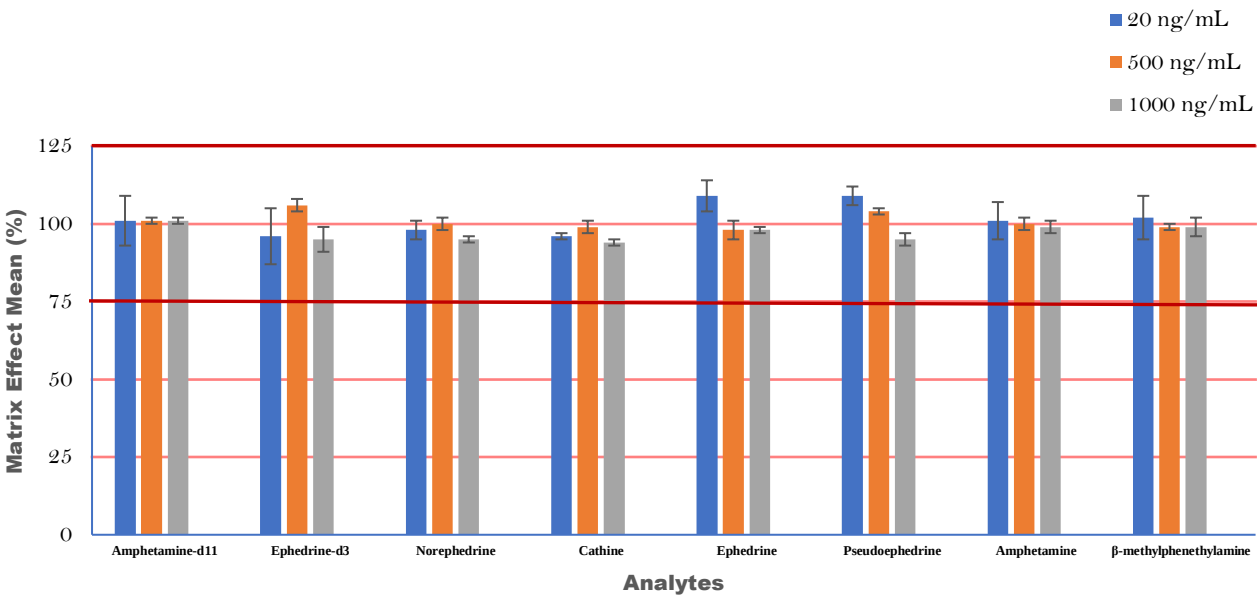

Figure 35: Matrix effects (%) measured in extracts of aged sheep whole blood spiked with amphetamine-related drugs, including two deuterated analogues, at three different concentrations (20, 500 and 1000 ng/mL). The data represent the mean of triplicate analysis, error bars represent the standard error of mean, and red lines represent acceptable limits of matrix effects.

Table 22: Evaluation of matrix effects (%) of human whole blood (Source 1) on amphetamine-related drugs and deuterated analogues

Analyte	Concentration					
	Low 20 ng/mL	% CV	Medium 500 ng/mL	% CV	High 1000 ng/mL	% CV
Amphetamine−d_{11}	87 ± 3.0	3.45	81 ± 2.7	3.33	85 ± 4.4	5.18
Ephedrine−d_3	89 ± 3.3	3.71	81 ± 2.4	2.96	83 ± 3.0	3.61
Norephedrine	83 ± 4.5	5.42	80 ± 1.0	1.25	82 ± 2.9	3.54
Cathine	86 ± 2.2	2.56	81 ± 2.5	3.09	82 ± 2.2	2.68
Ephedrine	87 ± 3.2	3.68	81 ± 2.2	2.72	79 ± 1.0	1.27
Pseudoephedrine	89 ± 1.9	2.13	82 ± 1.1	1.34	81 ± 1.0	1.23
Amphetamine	88± 5.2	5.91	83 ± 1.2	1.45	85 ± 1.0	1.18
β-methylphenethylamine	93 ± 4.7	5.05	86 ± 1.0	1.16	86 ± 0.2	0.23

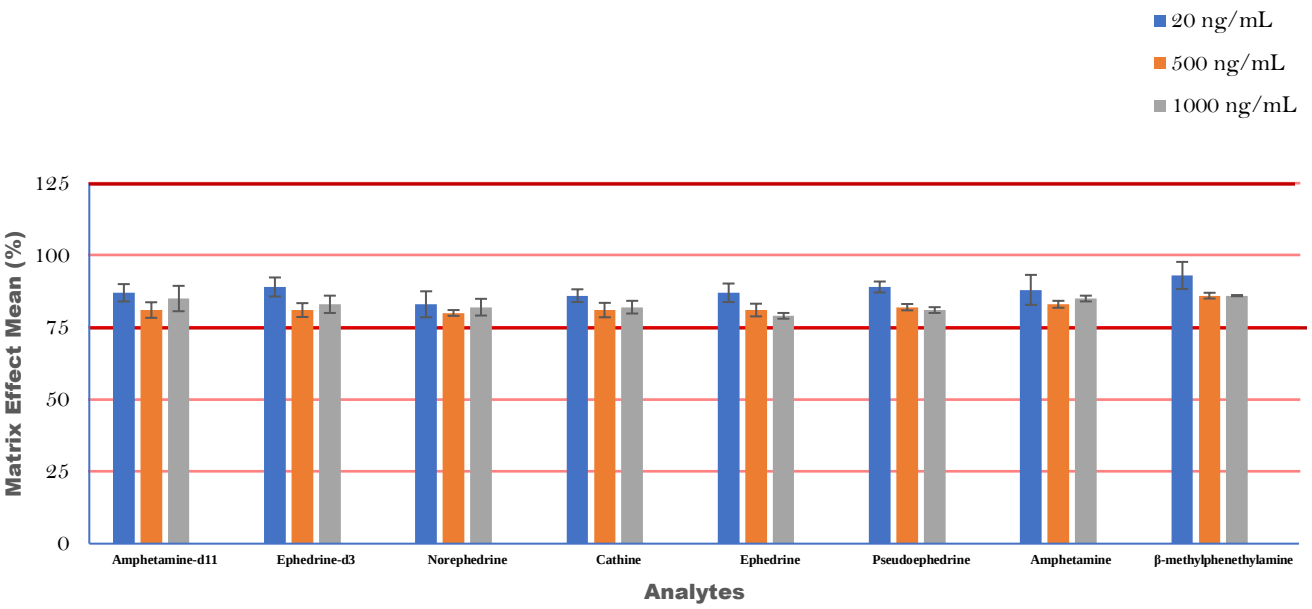

Figure 36: Matrix effects (%) measured in extract of human whole blood (Source 1) spiked with amphetamine-related drugs, including two deuterated analogues, at three different concentrations (20, 500 and 1000 ng/mL). The data represent the mean of triplicate analysis, error bars represent the standard error of mean, and red lines represent acceptable limits of matrix effects.

Table 23: Evaluation of matrix effects of human whole blood (Source 2) on amphetamine-related drugs and deuterated analogues

Analyte	Concentration					
	Low 20 ng/mL	% CV	Medium 500 ng/mL	% CV	High 1000 ng/mL	% CV
Amphetamine−d_{11}	87 ± 4	4.60	89 ± 4	4.49	88 ± 2	2.27
Ephedrine−d_3	93 ± 6	6.45	89 ± 6	6.74	87 ± 3	3.45
Norephedrine	91 ± 2	2.20	92 ± 4	4.35	91 ± 2	2.20
Cathine	88 ± 2	2.27	91± 1	1.10	91 ± 1	1.10
Ephedrine	91 ± 2	2.20	89 ± 5	4.49	88± 2	2.27
Pseudoephedrine	89 ± 2	2.25	90 ± 4	4.44	89 ± 2	2.25
Amphetamine	84± 3	3.57	91 ± 1	1.10	98 ± 3	3.06
β-methylphenethylamine	85 ± 4	4.71	94 ± 2	2.13	99 ± 0.1	0.10

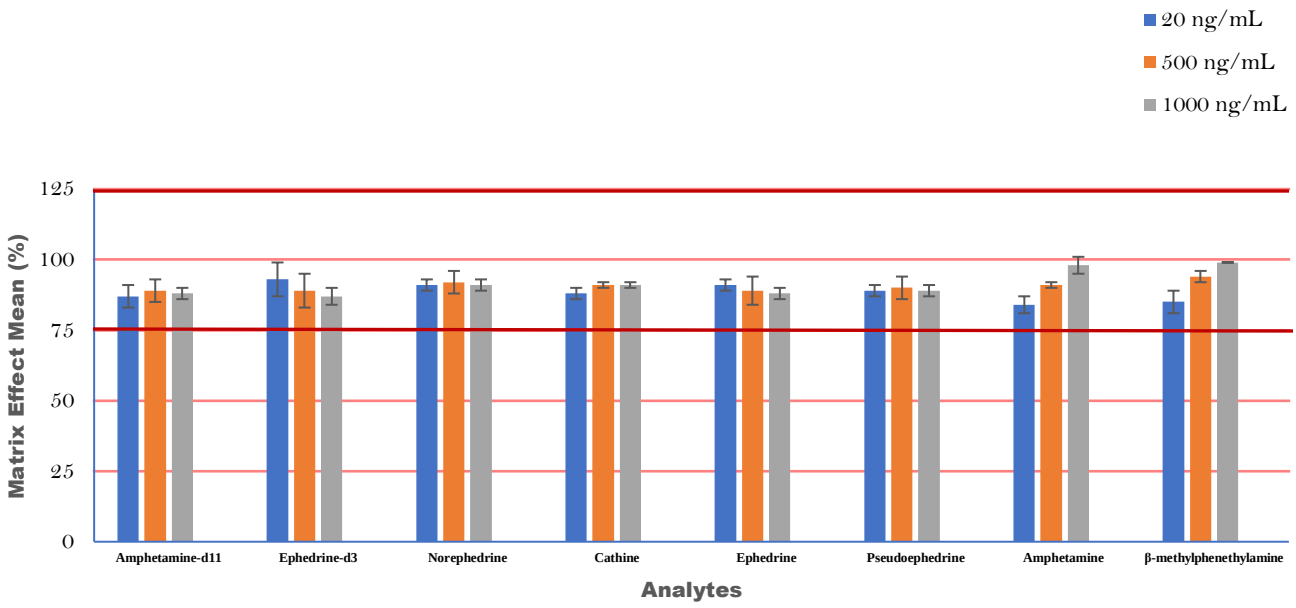

Figure 37: Matrix effects (%) measured in extract of human blood (Source 2) spiked with amphetamine-related drugs, including two deuterated analogues, at three different concentrations (20, 500 and 1000 ng/mL). The data represent the mean of triplicate analysis, error bars represent the standard error of mean, and red lines represent acceptable limits of matrix effects.

Table 24: Evaluation of matrix effects of human whole blood (Source 3) on amphetamine-related drugs and deuterated analogues

Analyte	Concentration					
	Low 20 ng/mL	% CV	Medium 500 ng/mL	% CV	High 1000 ng/mL	% CV
Amphetamine−d_{11}	82 ± 1	1.22	89 ± 2	2.25	90 ± 1	1.11
Ephedrine−d_3	84 ± 4	4.76	89 ± 1	1.12	92 ± 2	2.17
Norephedrine	83 ± 5	6.02	92 ± 2	2.17	95 ± 1	1.05
Cathine	82 ± 3	3.66	93± 3	3.23	96 ± 4	4.17
Ephedrine	84 ± 2	2.38	90 ± 1	1.11	91± 2	2.20
Pseudoephedrine	83 ± 2	2.41	90 ± 2	2.22	93 ± 3	3.23
Amphetamine	83± 2	2.41	97 ± 4	4.12	101 ± 2	1.98
β-methylphenethylamine	89 ± 4	4.49	97 ± 4	4.12	101 ± 0.2	0.20

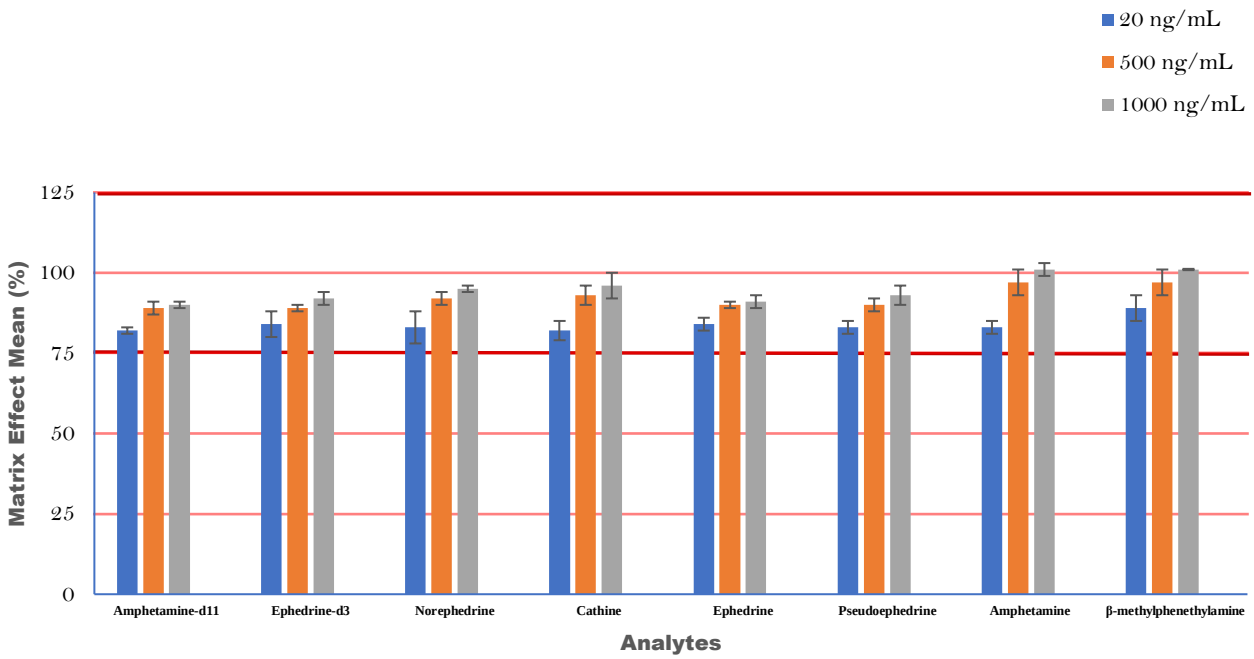

Figure 38: Matrix effects (%) measured in extract of human blood (source 3) spiked with amphetamine-related drugs, including two deuterated analogues, at three different concentrations. The data represent the mean of triplicate analysis, error bars represent the standard error of mean, and red lines represent acceptable limits of matrix effects.

Table 25: Evaluation of recovery (%) of amphetamine-related drugs and deuterated analogues from aged bovine whole blood

Analyte	Concentration					
	Low 20 ng/mL	% CV	Medium 500 ng/mL	% CV	High 1000 ng/mL	% CV
Amphetamine−d_{11}	70 ± 3	4.29	70 ± 1	1.43	71 ± 2	2.82
Ephedrine−d_3	77 ± 4	5.19	77 ± 1	1.30	77 ± 4	5.19
Norephedrine	71 ± 3	4.23	72 ± 2	2.78	76 ± 1	1.32
Cathine	68 ± 3	4.41	71 ± 2	2.82	77 ± 1	1.30
Ephedrine	71 ± 4	5.63	75 ± 1	1.33	77 ± 7	9.09
Pseudoephedrine	68 ± 3	4.41	75 ± 4	5.33	90 ± 5	5.56
Amphetamine	70 ± 3	4.29	80 ± 1	1.25	80 ± 2	2.50
β-methylphenethylamine	65 ± 4	6.15	73 ± 1	1.37	75 ± 1	1.33

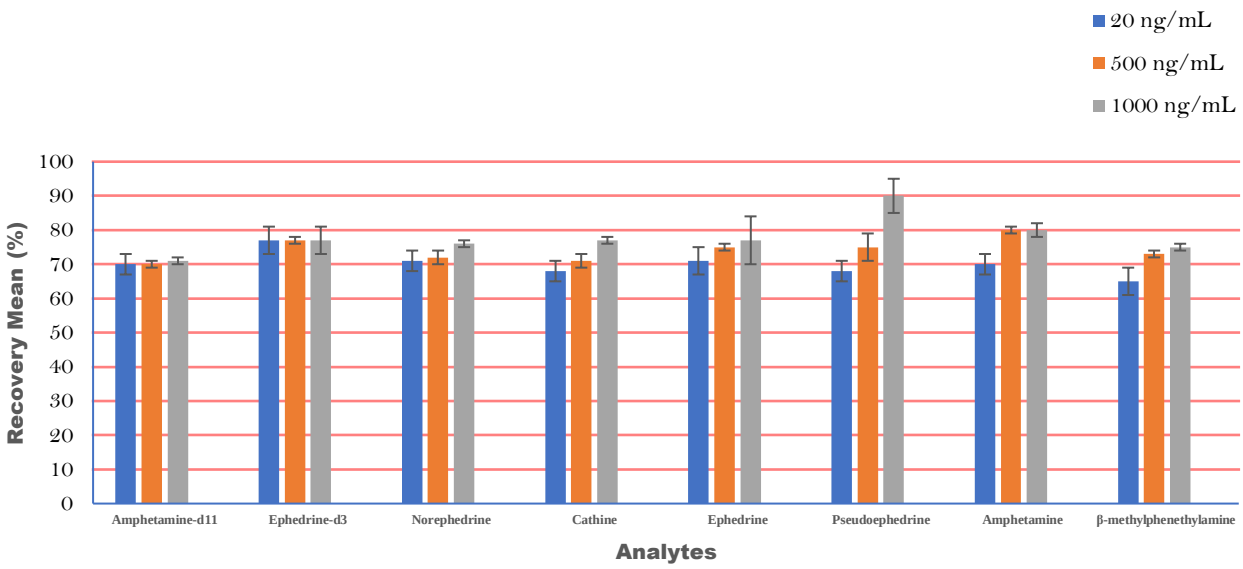

Figure 39: Recovery (%) of amphetamine-related drugs, including two deuterated analogues at three different concentrations from extract of spiked aged bovine whole blood. The data represent the mean of triplicate analysis, and error bars represent the standard error of mean.

Table 26: Evaluation of recovery (%) of amphetamine-related drugs and deuterated analogues from aged sheep whole blood

Analyte	Concentration					
	Low 20 ng/mL	% CV	Medium 500 ng/mL	% CV	High 1000 ng/mL	% CV
Amphetamine−d_{11}	60 ± 7	11.67	62 ± 7	11.29	61 ± 6	9.84
Ephedrine−d_3	70 ± 12	17.14	77 ± 4	5.19	90 ± 6	6.67
Norephedrine	70 ± 5	7.14	70 ± 5	7.14	81 ± 8	9.88
Cathine	67 ± 7	10.45	67 ± 4	5.97	79 ± 7	8.86
Ephedrine	65 ± 5	7.69	67 ± 5	7.46	70 ± 1	1.43
Pseudoephedrine	63 ± 2	3.17	68 ± 2	2.94	87 ± 1	1.15
Amphetamine	69 ± 3	4.35	72 ± 6	8.33	74 ± 4	5.41
β-methylphenethylamine	60 ± 2	3.33	68 ± 6	8.82	70 ± 6	8.57

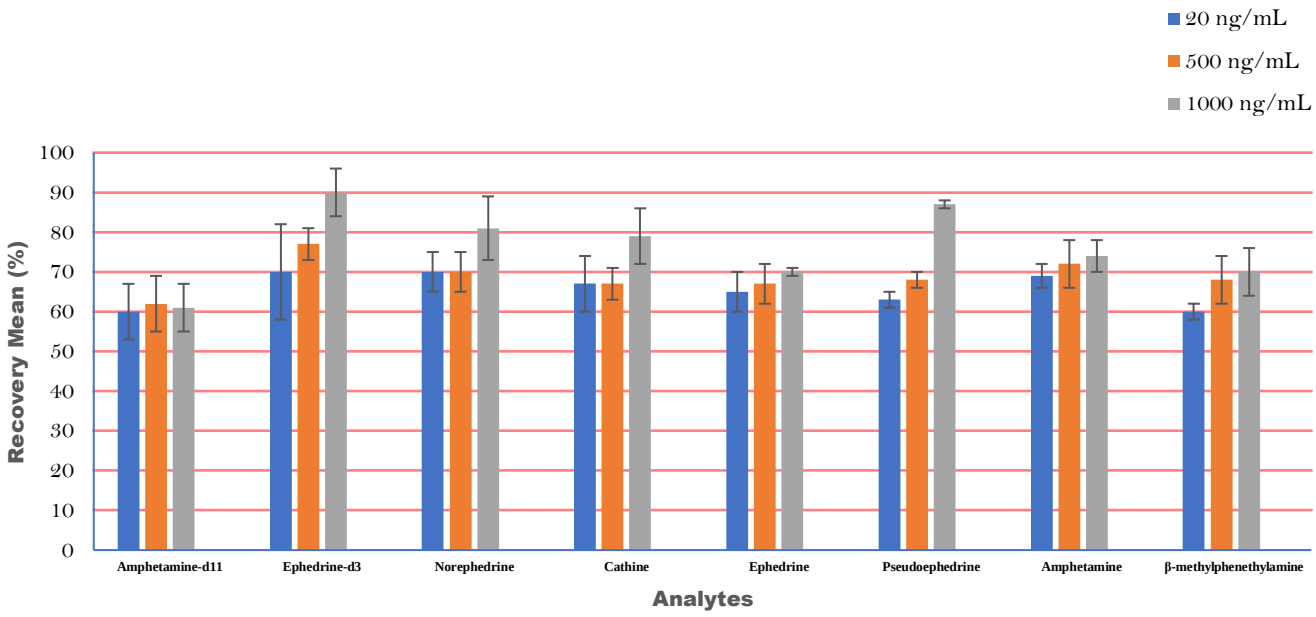

Figure 40: Recovery (%) of amphetamine-related drugs, including two deuterated analogues, at three different concentrations from extract of spiked aged sheep whole blood. The data represent the mean of triplicate analysis, and error bars represent the standard error of mean.

Table 27: Averaged curve regression equations and correlation coefficients of the analytes in aged bovine whole blood

Analyte	Linearity ng/mL	Regression Equation	R^2
Norephedrine	20 – 1000	$y = 8\,x\,10^{-9}C^2 + 0.0002\,C - 0.002$	0.9998
Cathine	20 – 1000	$y = 6\,x\,10^{-9}C^2 + 0.0003\,C - 0.0039$	0.9994
Ephedrine	20 – 1000	$y = -2\,x\,10^{-7}C^2 + 0.0018\,C - 0.0198$	0.9994
Pseudoephedrine	20 – 1000	$y = -8\,x\,10^{-7}C^2 + 0.003\,C - 0.0219$	0.9998
Amphetamine	20 – 1000	$y = -1\,x\,10^{-7}C^2 + 0.0006\,C + 0.00004$	0.9999
β-methylphenethylamine	20 – 1000	$y = -1\,x\,10^{-7}C^2 + 0.0005\,C - 0.0013$	1

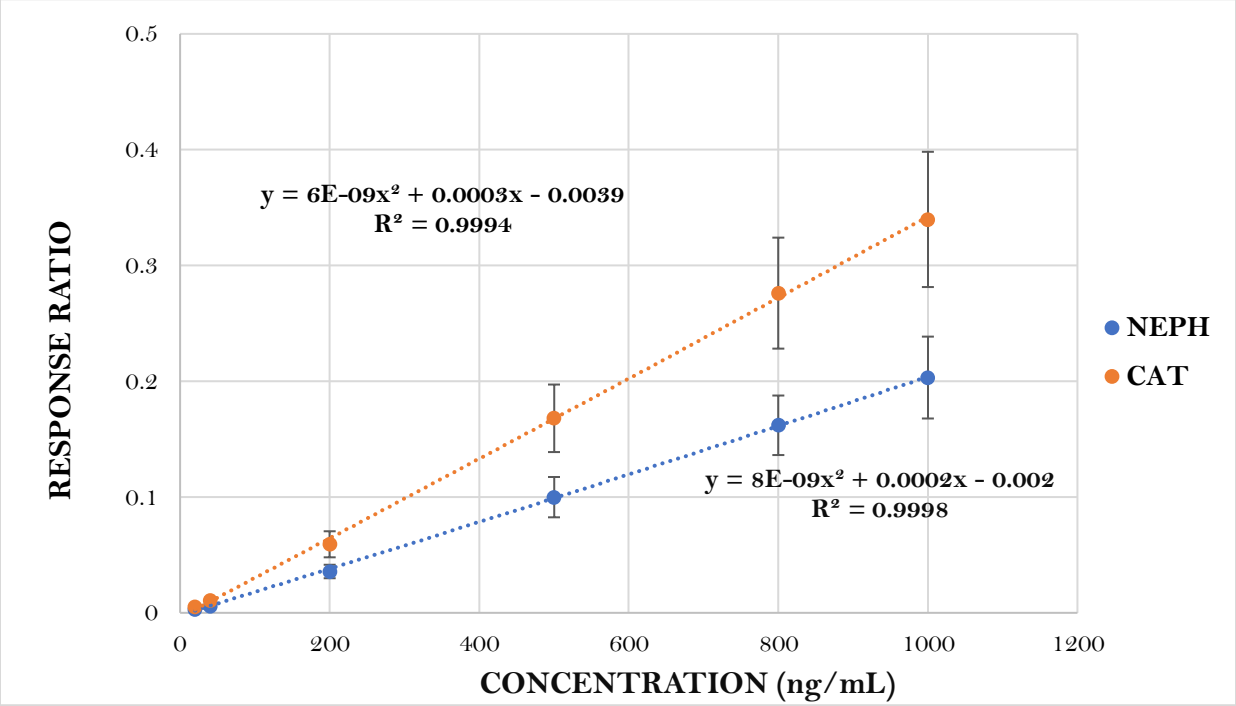

Figure 41: Averaged quadratic calibration curves of norephedrine and cathine

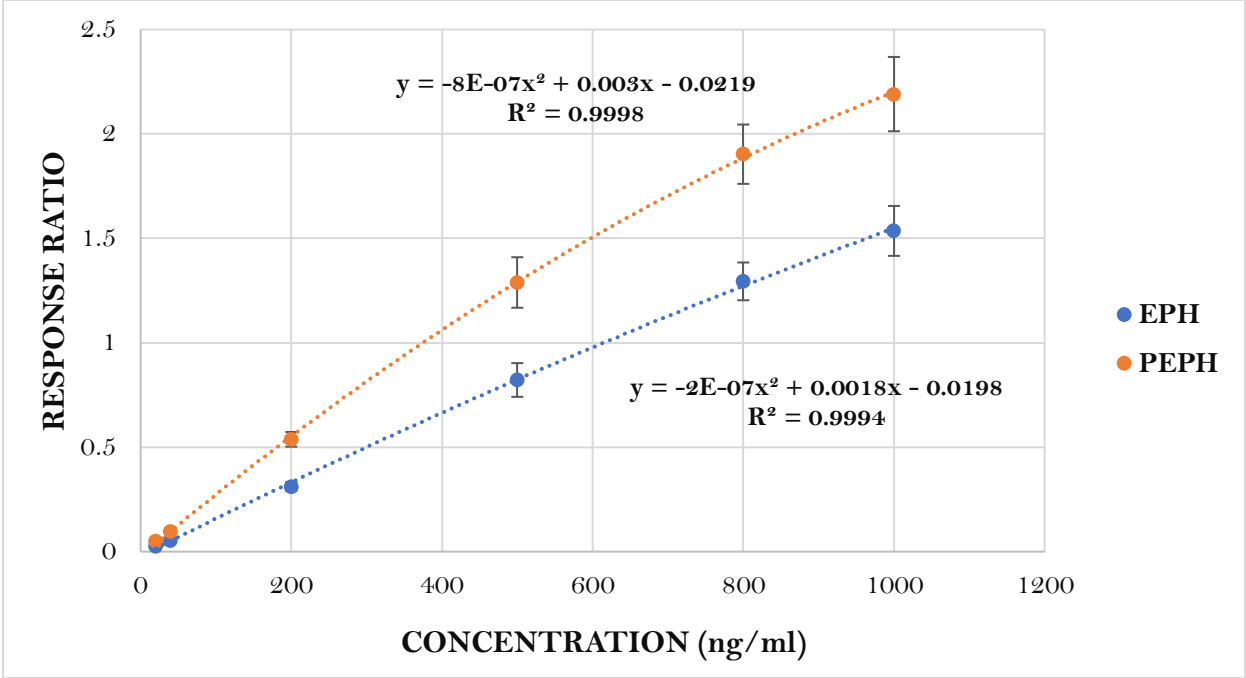

Figure 42: Averaged quadratic calibration curves of ephedrine and pseudoephedrine

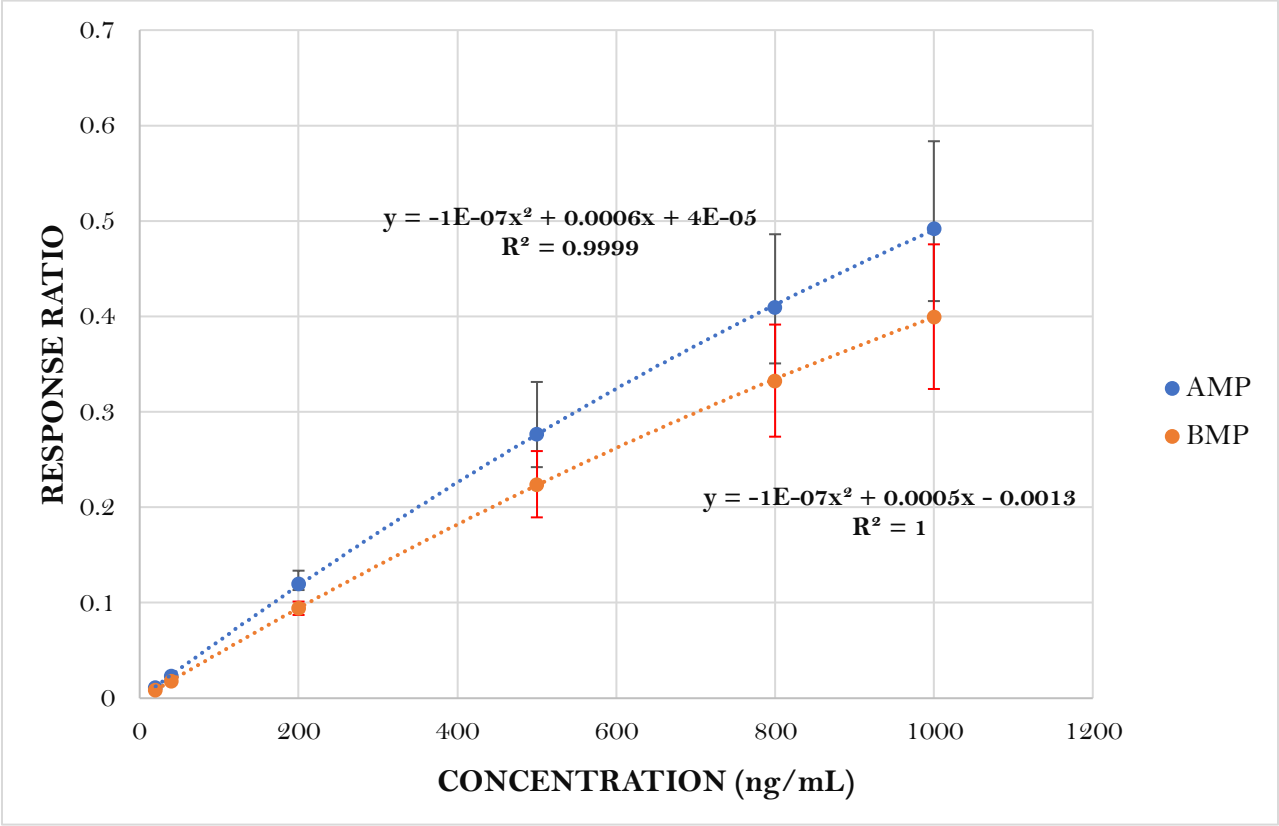

Figure 43: Averaged quadratic calibration curves of amphetamine and β-methylphenylamine.

Table 28: Summary of analytical performance parameters

Drug	Limit of detection (LOD, ng/mL)	Limit of quantitation (LOQ, ng/mL)	Within-Run Precision (CV, %) acceptance criteria: ≤20%) [# failed]	Between-Run Precision (CV, %) acceptance criteria: ≤20%) [# failed]	Bias (%) (acceptance criteria: ≤20%) [# failed]
Norephedrine	20	20	1.17–18.10 [0/90]	15.86–18.99 [0/30]	-4.72-18.25 [0/10]
Cathine	20	20	1.60–13.20 [0/90]	16.2–18.98 [0/30]	-5.00-15.00 [0/10]
Ephedrine	20	20	1.00–11.54 [0/90]	5.31–9.81 [0/30]	-6.90-8.40 [0/10]
Pseudoephedrine	20	20	1.06–12.01 [0/90]	3.50–9.38 [0/30]	-10.82-7.16 [0/10]
Amphetamine	20	20	1.00–18.3 [0/90]	7.95–19.70 [0/30]	-7.98-3.40 [0/10]
β-methylphenethylamine	20	20	1.50–15.78 [0/90]	6.60–18.95 [0/30]	-11.00-9.00 [0/10]

Analyses were performed using five different sets of extractions of analyte standard mixtures ranging from 20 to 1,000 ng/mL over six non-zero calibration points; each standard concentration was analyzed in triplicate. LOD, limit of detection; LOQ, limit of quantitation

Table 29: Analyte stability data for amphetamine-related drugs at three different concentrations while resident on autosampler (10 ºC) over 36 h.

Drug	(CV, %) (acceptance criteria: ≤20%)								
	40 ng/mL			500 ng/mL			1000 ng/mL		
	12 hours	24 hours	36 hours	12 hours	24 hours	36 hours	12 hours	24 hours	36 hours
Norephedrine	5.32	5.32	5.32	1.62	1.35	1.83	2.63	2.63	2.38
Cathine	5.42	1.76	2.34	2.6	4.62	2.22	2.39	1.29	1.16
Ephedrine	2.24	2.37	6.04	1.39	1.07	1.12	1.36	3.35	3.48
Pseudoephedrine	1.56	2.57	2.94	0.57	0.98	1.2	4.22	7.26	7.77
Amphetamine	0.32	0.32	0.32	2.98	2.62	5.45	1.51	3.24	4.17
β-methylphenethylamine	0.30	0.18	0.92	2.81	2.77	5.89	2.46	4.2	4.81

4.4 Discussion

This study was conducted to develop and validate a qualitative and quantitative method to determine ARDs in WB by UPLC-qTOF-MS after extracting the samples by MMSPE. Validation of the analytical method was based on standards established by SWGTOX [176]. To optimize the extraction process, several experiments were performed, including the evaluation of different precipitation agents, modes of SPE, and conditions of UPLC-qTOF-MS analysis. Samples of WB were precipitated using MeOH and ACN, alone or in combination. Based on visual inspection of the supernatant (i.e., clarity), ACN was deemed to be the most suitable precipitation agent in the pretreatment step of WB samples. After evaluating two types of SPE platforms for the extraction step (chapter 2), MMSPE was found to be superior to MIP-SPE because it did not elicit any interference to response associated with key analytes (chapter 3).

The six selected ARDs included two pairs of diastereomers (NEPH and CAT, and EPH and PEPH) and one pair of positional isomers (AMP and BMP). Therefore, fragmentation patterns for each pair of isomers were expected to be very similar or indistinguishable. To overcome this analytical challenge, chromatographic resolution of the ARDs was crucial. Accordingly, a pseudo-isocratic elution method was developed in which the composition of the UPLC mobile phase was varied at very shallow gradients (from 0% B to 5% B over 9 min) to facilitate the complete baseline resolution of the isomeric analytes (Figure 33 and Tables 12, 18).

Rapid, alternating acquisition of MS spectra at low (LE) and high (HE) collision energies during qTOF-MS analysis was performed in the MS^E mode. Ions from intact molecules were generally and predominantly detected at LE, whereas more extensive fragmentation data was acquired at HE. In a single injection, this technique enables the acquisition of ions from precursor molecules and their fragment ions [177]. Low capillary voltage (0.8 kV) facilitated the

detection of low-molecular-mass ARDs (135–168 Da) with optimum sensitivity. Similarly, the cone voltage was also set to a low voltage (20 V) as shown in Table 12. The analytical method was optimized for these parameters (Table 18).

Both isomer pairs, NEPH and CAT, and EPH and PEPH, formed $[M+H]^+$ ions with m/z 152 and 166, respectively. Consequently, by losing water from their molecular ions $[M+H-H_2O]^+$, the isomer pairs formed fragments with m/z 134 and 148, respectively. NEPH and CAT also yielded $[M+H-H_2O-NH_2]^+$ with m/z 117 after subsequently losing ammonia, whereas EPH and PEPH yielded $[M+H-H_2O-NH-CH_3]^+$ with m/z 117 after losing methylamine. Moreover, $[M+H-H_2O-NH_2-H_2]^+$ with m/z 115 was formed by both isomer pairs due to the loss of H_2 [178]. Ephedrine-d_3 yielded $[M+H]^+$, $[M+H-H_2O]^+$, and $[M+H-H_2O-CH_3]^+$ with m/z 169, 151, and 136, respectively [178]. AMP and BMP displayed the same fragmentation pattern. They formed $[M+H]^+$ with m/z 136. Subsequently, they formed $[M+H-NH_2]^+$ with m/z 119 by losing ammonia and tropylium ion $[M+H-NH_2-CH_3-CH]^+$ with m/z 91 as a result of a β-C-C cleavage. Amphetamine-d_{11} formed $[M+H]^+$, $[M+H-NH_2]^+$, and $[M+H-NH_2-CD_3-CD]^+$ with m/z 147, 130, and 98, respectively (see appendix A).

The developed method was validated by evaluating MIs, MEs, recovery, carryover, autosampler stability, and calibration to measure bias, intra- and inter-day accuracy, and precision. Five types of drug-free WB matrices (Table 19) were extracted and analyzed without the addition of ISs. Each sample was analyzed to confirm the absence of MIs by monitoring the quantifier and qualifier ions of the analytes of interest at their respective retention times; no MI was detected in the five WB matrices.

Changes (enhancement or suppression) of analyte responses due to matrix effects (MEs) must be less than 25%as per SWGTOX guidelines. MEs of the five different WB matrices on the

responses of all analytes at all concentration levels assayed were less than 25% (with %CV ≤ 20%). The majority of the ME values were negative for bovine, and human source 1, 2, and 3 WB matrices, indicating ion suppression as shown in Tables 20, 22, 23, and 24, respectively. However, ion enhancement was observed in the sheep WB matrix as shown by positive ME values (Table 21). Recovery was evaluated using aged bovine and sheep WB matrices; it was 65–90% for all analytes extracted from bovine WB (Table 25), whereas it was 60–90% for all analytes extracted from sheep WB (Table 26) at all concentration levels (with %CV ≤ 20%). Low recovery values, especially at low analyte concentrations, were observed. These low recovery values might be due to the loss of analytes because of the polarity and volatility of ARDs. The deactivation of any utilized glass apparatus during the extraction and preventing the protonated amine group of ARDs from interacting with the hydroxyl group of glass silicone could increase analyte recovery and reduce ME. This remedial step was not incorporated in this study due the high cost of silanized glass tubes. Therefore, further experiments are required to verify its benefits.

Analyte carryover may compromise the accuracy of qualitative or quantitative analysis. ARDs were evaluated for carryover by analyzing drug-free WB extracts immediately following the analysis of the corresponding upper calibrator (1000 ng/mL) in triplicate. None of the analytes in this study displayed carryover effects.

Accuracy and precision were determined by constructing calibration curves for each analyte on each of five separate days and running two blind samples (one high (640-960 ng/mL) and one low (32-48 ng/mL unknown concentration samples) with each curve. The curves were produced using calibrators prepared in triplicate at 20, 40, 200, 500, 800, and 1000 ng/mL. The LOQ was determined to be the lowest point on the curve that demonstrated a precision of ≤ 20% and an

S/N ratio ≥ 10. The LOD was determined to be equal to the LOQ as the lowest concentration that was measured on the curve (the lowest non-zero calibrator method). R^2 values (0.999–1) that were observed for each curve showed a good fit; each curve was fit with a quadratic regression equation. Table 27 shows the averaged regression equations and correlation coefficients of five curves for the analytes in aged bovine WB. Figures 41, 42, and 43 show the averaged quadratic calibration curves of NEPH and CAT, EPH and PEPH, and AMP and BMP, respectively.

The concentration of each unknown blind sample was calculated using the equation of the line of best fit, and bias was determined by comparing the calculated and theoretical concentrations by using the following equation:

$$\text{Bias (\%) at Concentration}_x = \left[\frac{\text{Grand Mean of Calculated Concentration}_x\text{-Theoretical Concentration}_x}{\text{Theoretical Concentration}_x}\right] \times 100 \qquad \textbf{(5)}$$

Bias values up to 20% are permissible as per SWGTOX guidelines [176]. The high and low concentration blind samples for all analytes exhibited acceptable bias values, indicating that the method is reliable at both the high and low ends of the curve. Bias results of 10 blind and calibrator samples analyzed on five separate days are shown for each analyte in Table 28.

Precision, expressed as %CV, is the closeness of agreement between a series of measurements obtained from multiple samples of the same homogenous sample population [176]. Imprecision can lead to inaccurate quantitative results. SWGTOX guidelines state that the %CV shall not exceed 20% at any concentration level. Intra- and inter-run precisions were calculated. Intra-run precision was calculated using the values obtained in each run after triplicate analyses at each concentration as follows:

$$\text{Intra-run \%CV} = \left[\frac{\text{Standard deviation of a single run of samples}}{\text{Mean calculated value of a single run of samples}}\right] \times 100 \qquad \textbf{(6)}$$

Inter-run precision was calculated using the values obtained in each run after triplicate analyses at each concentration as follows:

$$\text{Inter-run \%CV} = \left[\frac{\text{Standard deviation of the grand mean for each concentration}}{\text{Grand mean for each concentration}}\right] \times 100 \qquad (7)$$

The %CV for all analytes at all six concentrations were within the acceptable precision limit (≤ 20%). Table 28 presents the results of the accuracy and precision of the assay.

The stability of each analyte while samples resided in the autosampler was assessed. Stability is defined as the ability of an analyte to resist chemical change in a matrix under specific conditions for given time intervals [176]. It is a measure of the time for which an analyte can remain under those conditions before the interpretation of its concentration is affected; a change in response beyond ± 20% from the initial response indicates a loss of analyte stability. The relative change in response was measured at three concentrations (40, 500, and 1000 ng/mL) in triplicate at 0, 12, 24, and 36 h. The samples were maintained in the autosampler at 10°C. All analytes were stable throughout the period of evaluation as shown in Table 29, indicating that ARDs can reliably be quantified for at least 36 h under the autosampler conditions used here.

4.5 Conclusion

This work involved development and validation of a method for quantitative analysis of selected ARDs by UPLC-qTOF-MS in WB after extraction by MMSPE. The method was validated according to the standard practices of SWGTOX. The validation experiments demonstrated that the assay has acceptable accuracy and precision for use in forensic toxicology. Additionally, the study demonstrated the utility of UPLC-qTOF-MS for the qualitative and

quantitative determination of ARDs in WB. Consequently, it holds potential for screening and quantification studies in forensic toxicology.

Chapter 5

5.0 Determination of β-methylphenethylamine and Its Metabolites in Whole Blood of Rats Using MMSPE and UPLC-qTOF-MS

5.1 Introduction

BMP is a recreational drug that was synthesized in the 1930s as an alternative analog of AMP [95, 96]; it is a positional isomer of AMP. Figure 24 shows the chemical structures of AMP and BMP [96]. Pharmacologically, BMP acts as a DA-receptor agonist, facilitating DA release and inhibiting DA reuptake from the synaptic cleft, but to a lesser extent than AMP does. The metabolism of BMP is poorly understood, and the efficacy and safety of BMP have never been evaluated in humans. Hence, its use as an ingredient in weight loss products and dietary supplements has been banned by the FDA [96]. To our knowledge, no pharmacokinetic study of BMP has been performed in animals. Therefore, one of the main goals of this project was to partially investigate the metabolic pathway of BMP in rats.

In this study, the validated analytical assay described in Chapter 4 for the identification and quantification of selected ARDs in WB by MMSPE and UPLC-qTOF-MS was used to determine BMP concentrations and to identify any of its metabolites in cardiac WB from rats exposed to BMP. There was one newly detected metabolite of BMP, which is proposed to be 1-amino-2-phenylpropan-2-ol. This proposed metabolite structure was determined through its fragmentation pattern by using the MS^E acquisition mode of qTOF-MS. Further experiments are required to confirm the proposed chemical structure of this newly detected metabolite of BMP.

5.2 Method

5.2.1 Drug Administration to Rats and Blood Sampling

Male Sprague-Dawley rats (230–250 g, n = 12) were provided by Charles River Laboratories (St-Constant, QC, Canada). The animals were housed in an environmentally controlled breeding room at the Laurentian University Animal Care Facility and were acclimated to the laboratory conditions for 3 days. Adult male Sprague-Dawley rats were housed in groups of three in cages with ¼″ bedding (Harlan Teklad, Indianapolis, IN, USA) under a 12-h light/dark cycle at a temperature of 20 ºC. The animals were provided free access to water and Harlan Teklad laboratory diet 8640. The animal procedures used in this study were approved by the Laurentian University Animal Care Committee. Twelve adult male Sprague-Dawley rats were randomly assigned to four groups (n = 3 each): a control group, in which the rats did not receive BMP; a low-dose group where the rats received a dose of 10 mg/kg of BMP (i.p.); and two high-dose groups where rats were injected with a dose of 30 mg/kg (i.p.). The rats from the low-dose and one of the two high-dose groups were euthanized by CO_2 asphyxiation, within 20 min. Those from the other high-dose group were euthanized by CO_2 asphyxiation 90 min post-injection. Perimortem blood samples were obtained from the rat heart (cardiac puncture). The blood was collected in sodium fluoride vacutainer tubes obtained from BD (Mississauga, ON, Canada).

5.2.2 Sample Pretreatment and Extraction

The collected cardiac WB samples were pretreated and extracted following the MMSPE extraction method (see 2.4). These extracted samples were analyzed by the validated assay for selected ARDs using UPLC-qTOF-MS (see Chapter 4).

5.2.3 Concentration Determination

Two standard curves were constructed using six calibrators samples in duplicate for each analyte. Calibrators were prepared in a drug-free rat cardiac WB matrix (control group). Rat WB

calibrators (250 μL) were assayed at concentrations of 20, 40, 200, 500, 800, and 1,000 ng/mL using a combined working standard solution, with addition of 125 ng ISs to each calibrant. Quantification was performed based on the ratio of the integrated area under EIC of BMP to that of amphetamine-d_{11} using specific quantifier ions (see Table 30).

5.2.4 Detection and Identification of Metabolites

The identification process of the BMP metabolite was carried out by comparison with drug-free samples. Molecular or fragmented ions uniquely found in LE mass spectral profiles of BMP-dosed samples were considered potential metabolites and were used for subsequent analysis by examining their HE mass spectral profiles.

5.3 Results

The UPLC-qTOF-MS data for BMP in rat drug-free perimortem WB samples prepared by MMSPE are summarized in Table 30 and are shown in Figure 44.

5.3.1 Concentration Determination

BMP concentrations were fit with quadratic regression lines, and concentration dependence was assessed over a range of 20–1,000 ng/mL. The results showed a strong correlation (R^2 > 0.99). Table 34 shows the averaged calibration curve regression equation and correlation coefficient, and Figure 45 shows the averaged quadratic calibration curve. The BMP concentrations in the rat cardiac WB of the three groups (low, high, and high delayed groups) were determined using the averaged quadratic regression equation of the two constructed standard curves (see Figures 46 and 47). The determined concentrations of BMP are shown in Table 31. All determined concentrations (22–899 ng/mL) were within the validated working range of the assay (20–1,000 ng/mL).

5.3.2 Metabolite Detection and Identification

A molecular or fragmented ion uniquely found in LE mass spectral profiles of BMP-dosed samples was considered the potential metabolite and was used for subsequent analysis by examining their HE mass spectral profiles. A fragmented ion was detected with a relatively high instrumental response in the high-dose group samples, whereas its intensity was low in the low-dose and delayed high-dose samples. Figures 48 and 49 show the EIC and mass spectral profiles of the detectable metabolite, respectively. A comparative approach was used to compare EICs and mass spectra of the proposed metabolite with those of NOR (Figures 50, 51, and 52) and CAT (Figures 50, 53, and 54). Based on the metabolic pathway of AMP, a metabolic pathway of BMP was proposed as shown in Figure 55. The proposed metabolite was assumed to be 1-amino-2-phenylpropano-2-ol. Figures 56, 57 and 58, 59 show the chemical structure of the proposed metabolite and its fragmentation patterns, respectively.

Table 30: Analytical parameters of β-methylphenethylamine and amphetamine-d_{11}

Drug	Ionization Mode	Molecular Ion (*m/z*)	Fragmented Ion (*m/z*) (± 0.01)	Retention Time (min) (± 0.05)
Amphetamine-d_{11}	Positive	147.1938	98.1000*/130.1653	9.43
β-methylphenethylamine	Positive	136.1219	91.0553/119.0868*	10.28

**Quantifier ion*

Table 31: Regression equation and correlation coefficient of a beta-methylphenethylamine concentration curve in rat perimortem whole blood

Analyte	Linear Range (ng/mL)	Regression Equation	R^2
β-methylphenethylamine	20–1,000	$y = -9\ x\ 10^{-8}C^2 + 0.0005\ C + 0.003$	0.9995

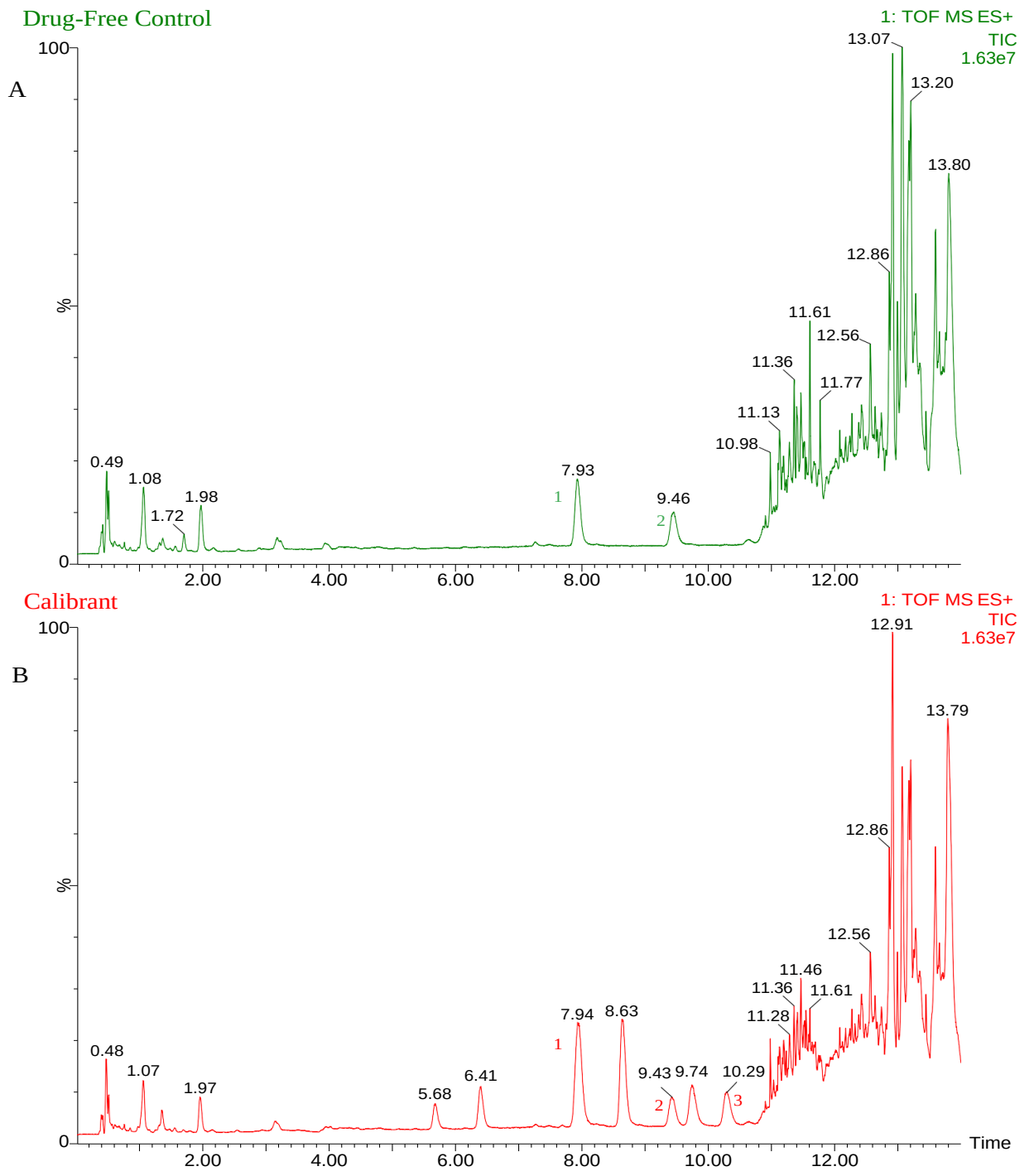

Figure 44; Total ion chromatogram of extracted rat postmortem whole blood; (A) drug-free control, and (B) spiked with 800 ng/mL of the combined working solution and 500 ng/mL of the internal standard solution; (1) ephedrine-d_3, (2) amphetamine-d_{11} and (3) β-methylphenethylamine.

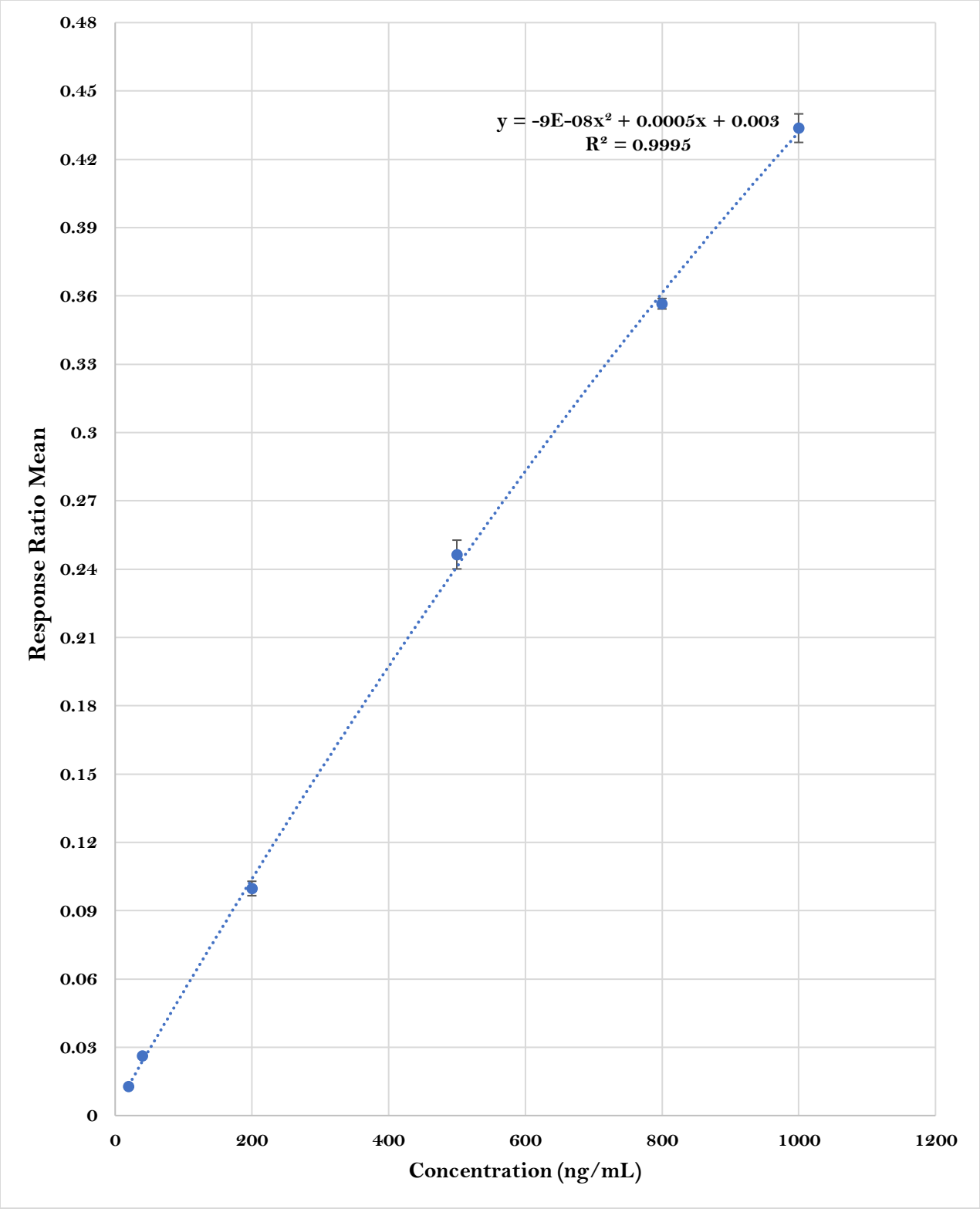

Figure 45: Averaged quadratic calibration curve of β-methylphenethylamine. Error bars represent the standard error of the mean of the response ratio of duplicate samples at each concentration level

Table 32: Concentrations of β-methylphenethylamine in perimortem whole-blood (rat, n=9) samples

Dose	Calculated Concentration (ng/mL)	Average (ng/mL)	STDEV (ng/mL)
Low Dose			
Rat 1	132		
Rat 2	96	104	25
Rat 3	85		
High Dose			
Rat 1	868		
Rat 2	841	869	29
Rat 3	899		
High Delayed Dose			
Rat 1	40		
Rat 2	22	31	9
Rat 3	32		

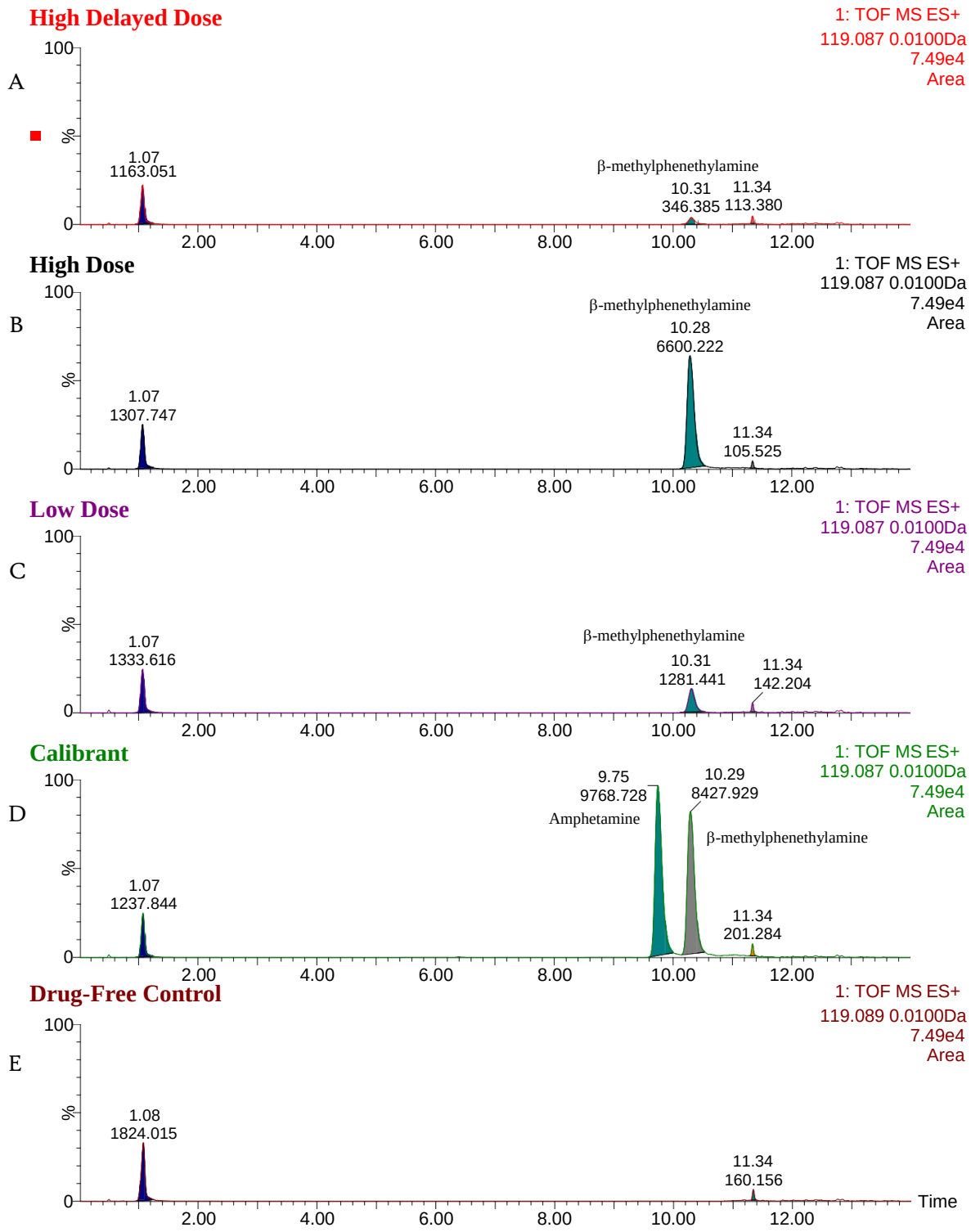

Figure 46: Extracted ion chromatograms (A–E) obtained using the molecular ion m/z 119 for β-methylphenethylamine from extracts of perimortem whole-blood (rat) samples: (A) high delayed-dose, (B) high-dose, and (C) low-dose; (D) calibrant at a concentration of 1,000 ng/mL; (E) drug-free control

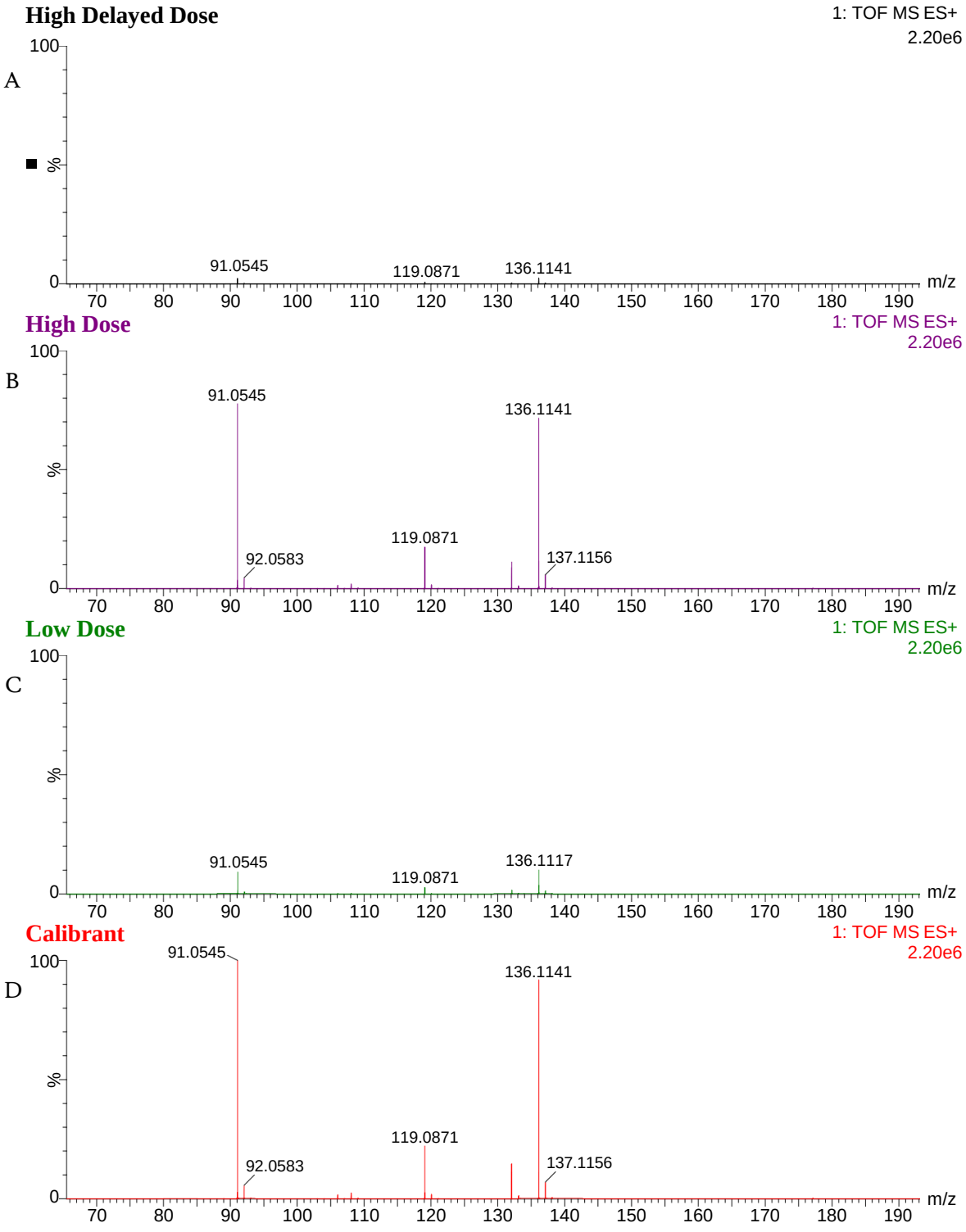

Figure 47: Mass spectral profile (A–D) of β-methylphenethylamine in extracts of perimortem whole-blood samples: (A) high delayed -dose, (B) high-dose, and (C) low-dose; (D) calibrant at a concentration of 1,000 ng/mL

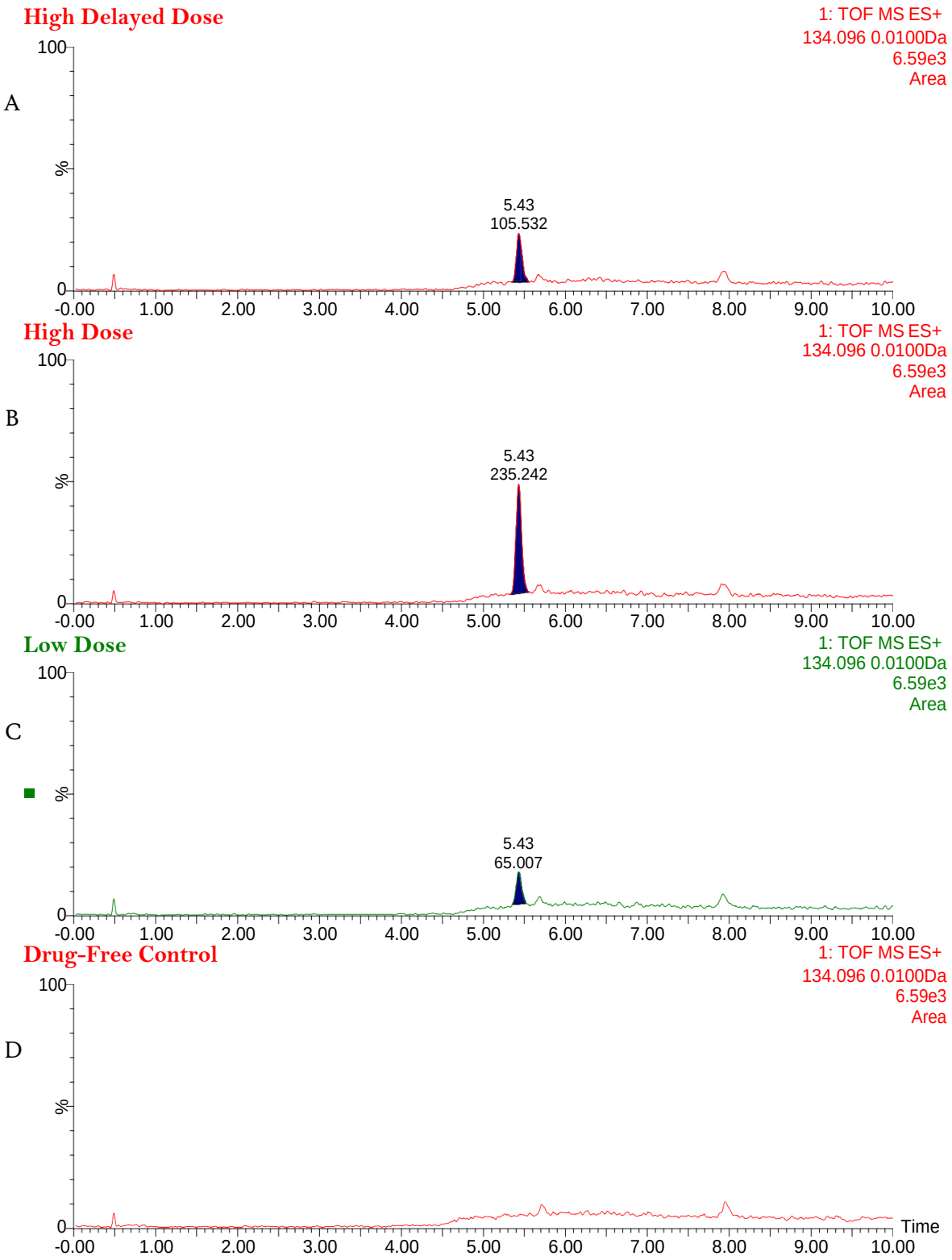

Figure 48: Extracted ion chromatograms (A–D) obtained using the fragmented ion m/z 134 for β-methylphenethylamine in extracts of perimortem whole-blood samples: (A) high delayed-dose, (B) high-dose, and (C) low-dose; (D) drug-free control.

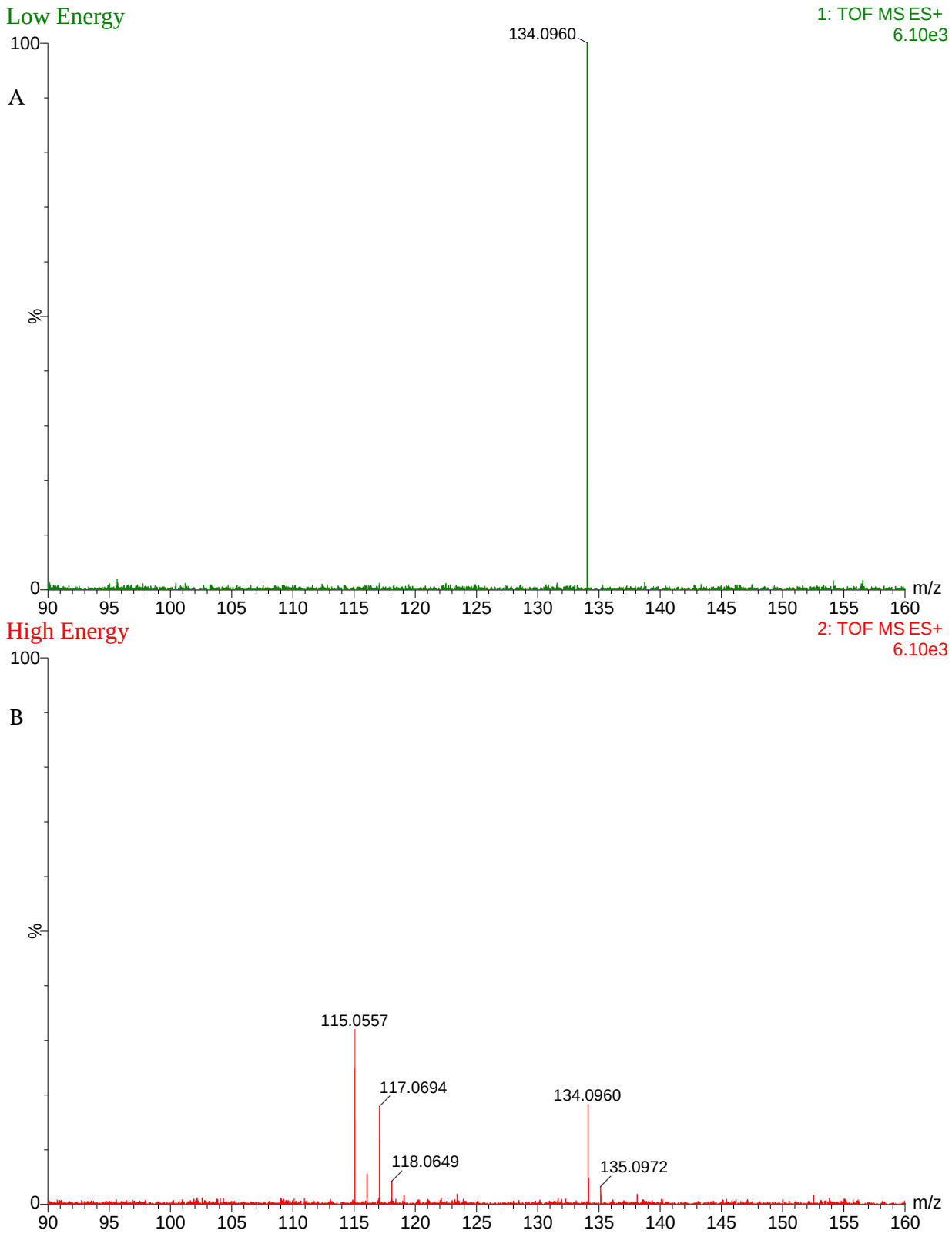

Figure 49: Mass spectra of the proposed metabolite of β-methylphenethylamine obtained at low energy (A) and high energy (B).

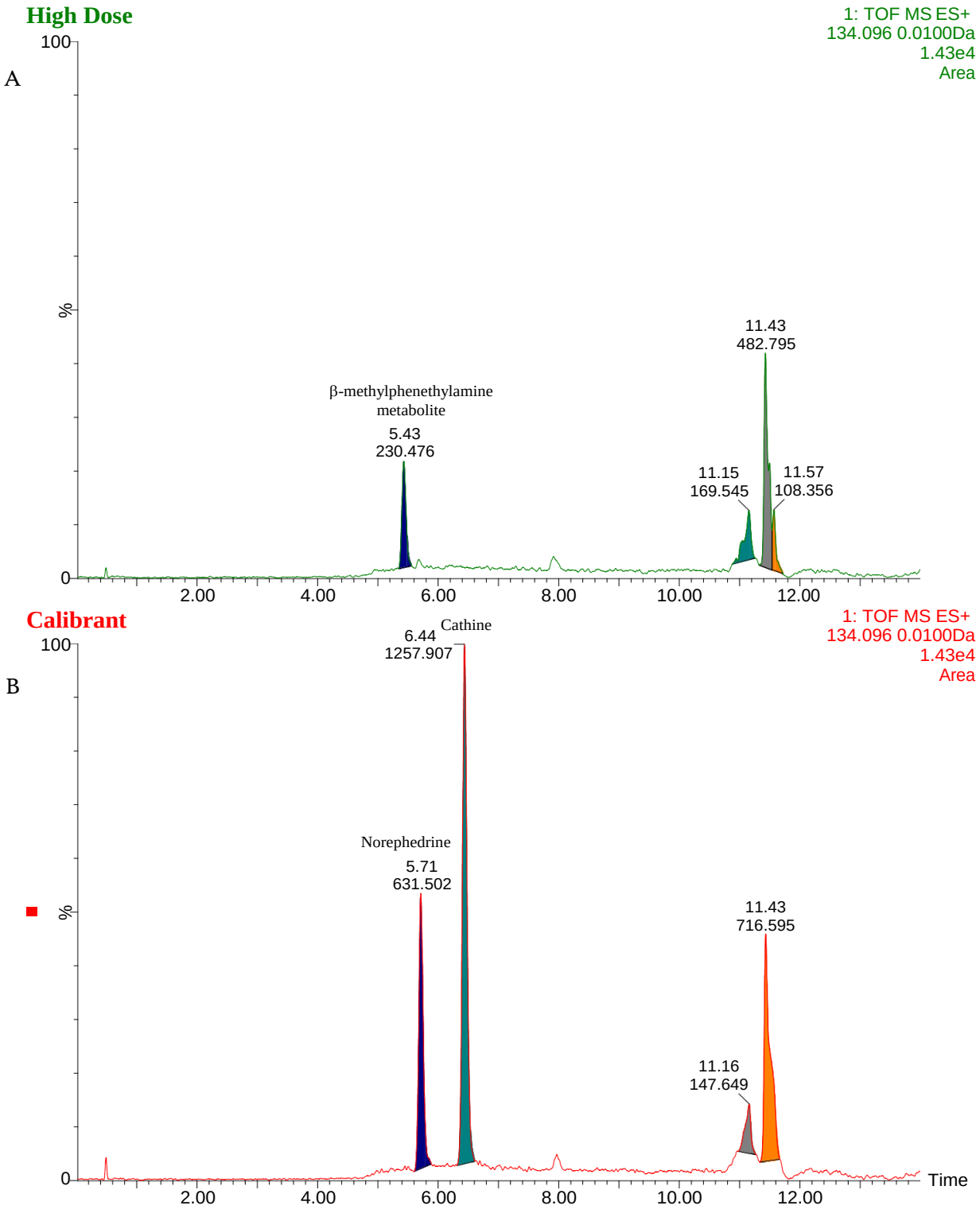

Figure 50: Extracted ion chromatograms obtained using the fragmented ion m/z 134 for (A) the metabolite of β-methylphenethylamine in extracts of the high-dose rat perimortem whole-blood samples and (B) norephedrine and cathine at a concentration of 20 ng/mL in the calibrant.

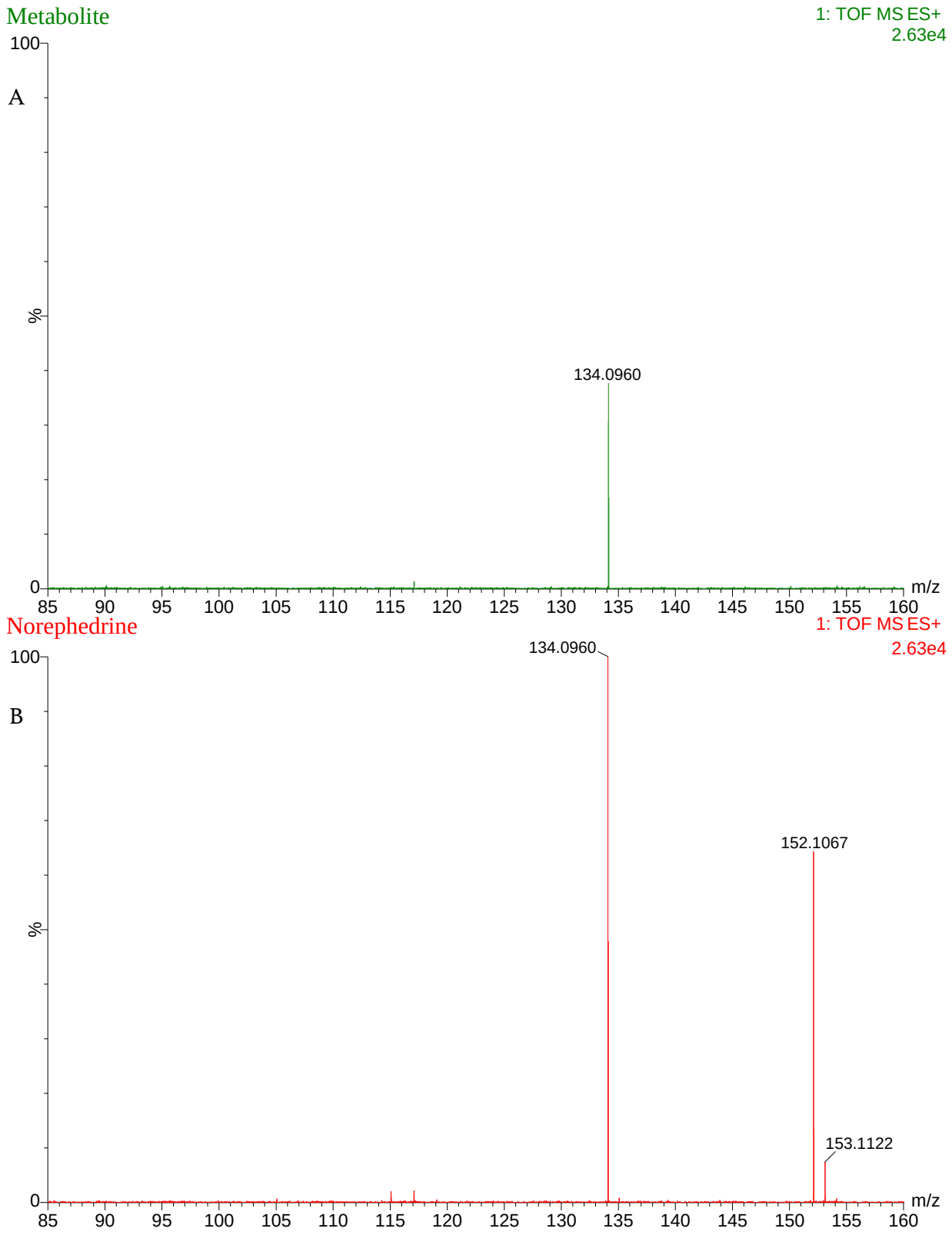

Figure 51: Mass spectra obtained at low energy for (A) the proposed metabolite of β-methylphenethylamine and (B) norephedrine at a concentration of 20 ng/mL.

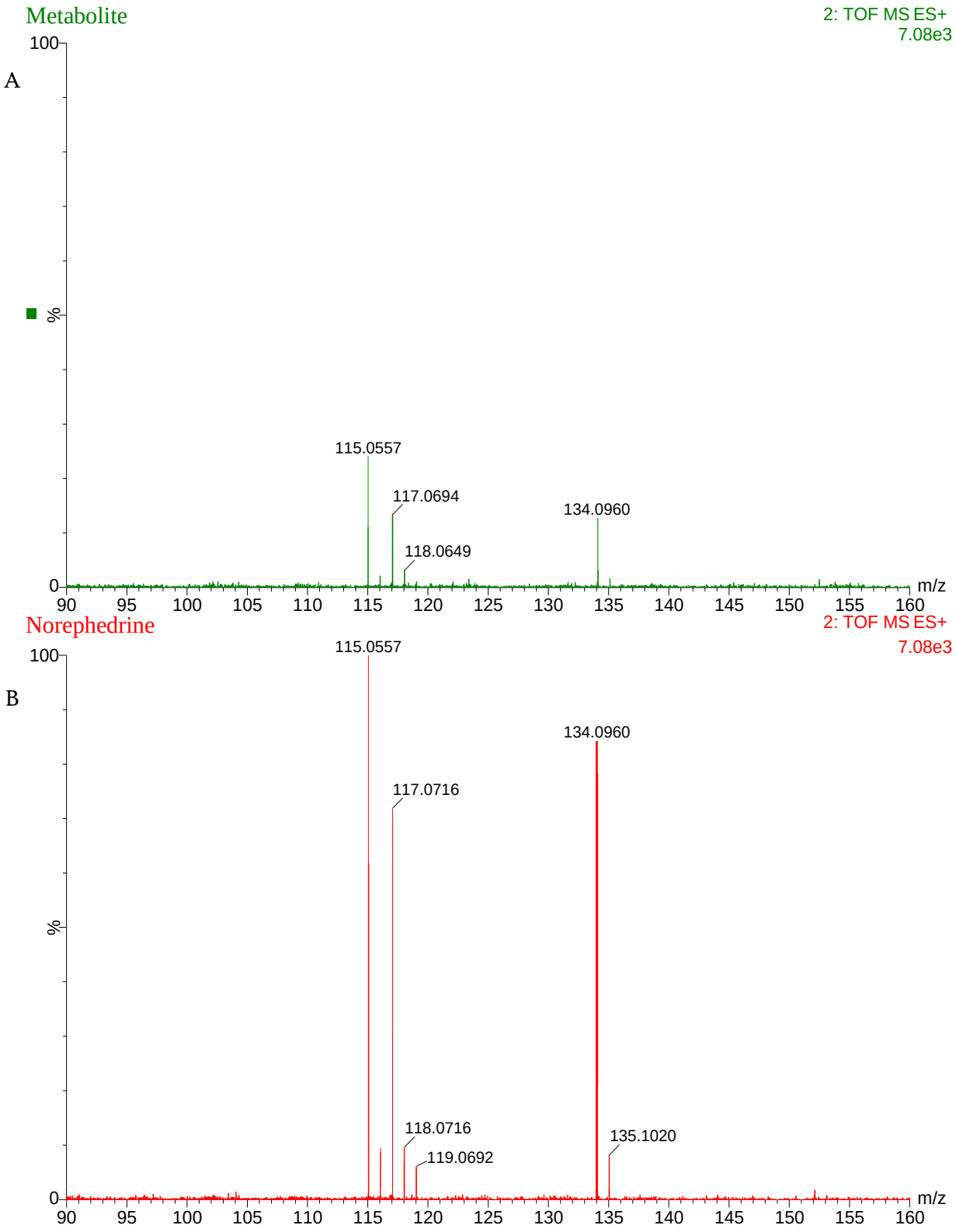

Figure 52: Mass spectra obtained at high energy for (A) the proposed metabolite of β-methylphenethylamine and (B) norephedrine at a concentration of 20 ng/mL.

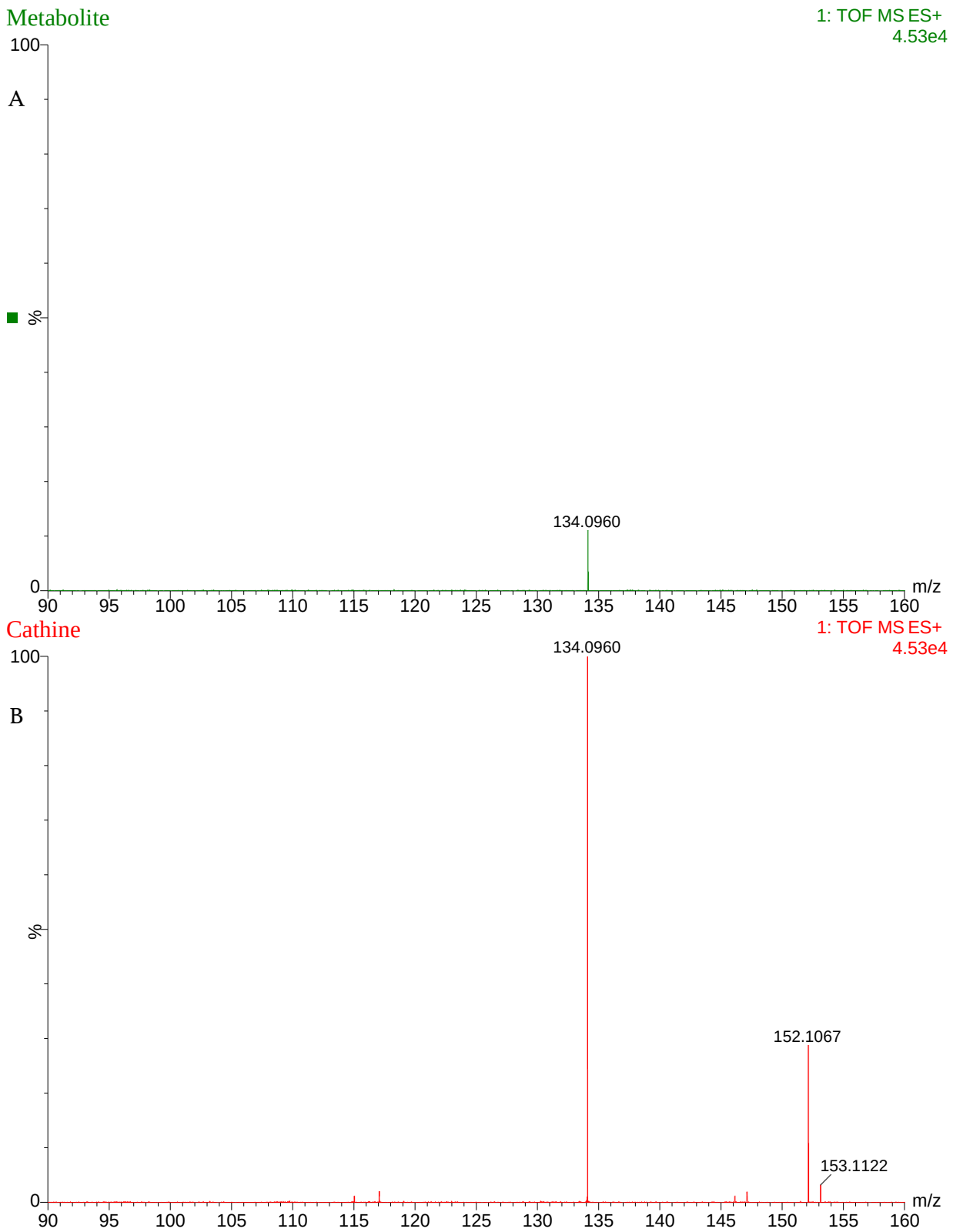

Figure 53: Mass spectra obtained at low energy for (A) the proposed metabolite of β-methylphenethylamine and (B) cathine at a concentration of 20 ng/mL.

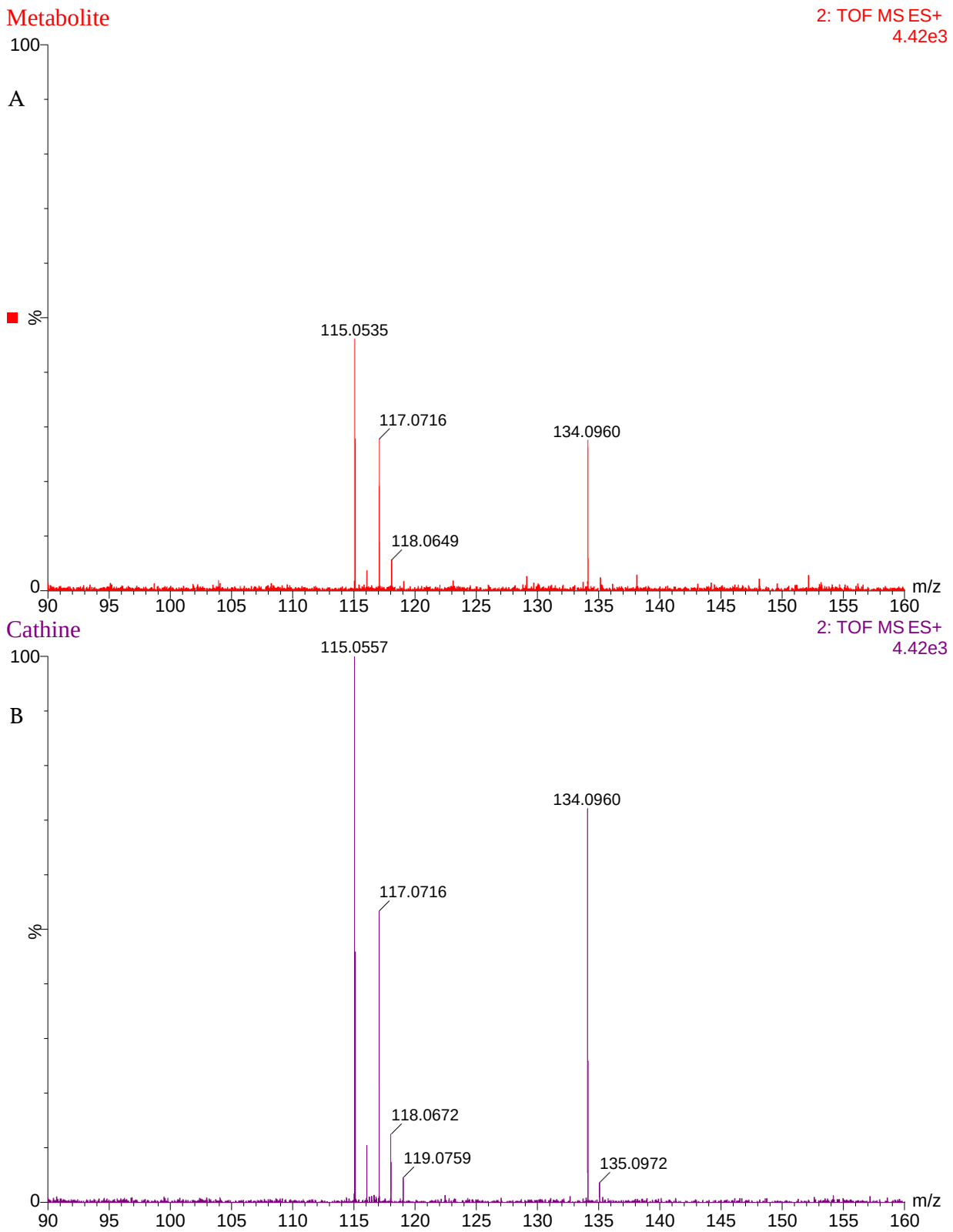

Figure 54: Mass spectra obtained at high energy for (A) the proposed metabolite of β-methylphenethylamine and (B) cathine at a concentration of 20 ng/mL.

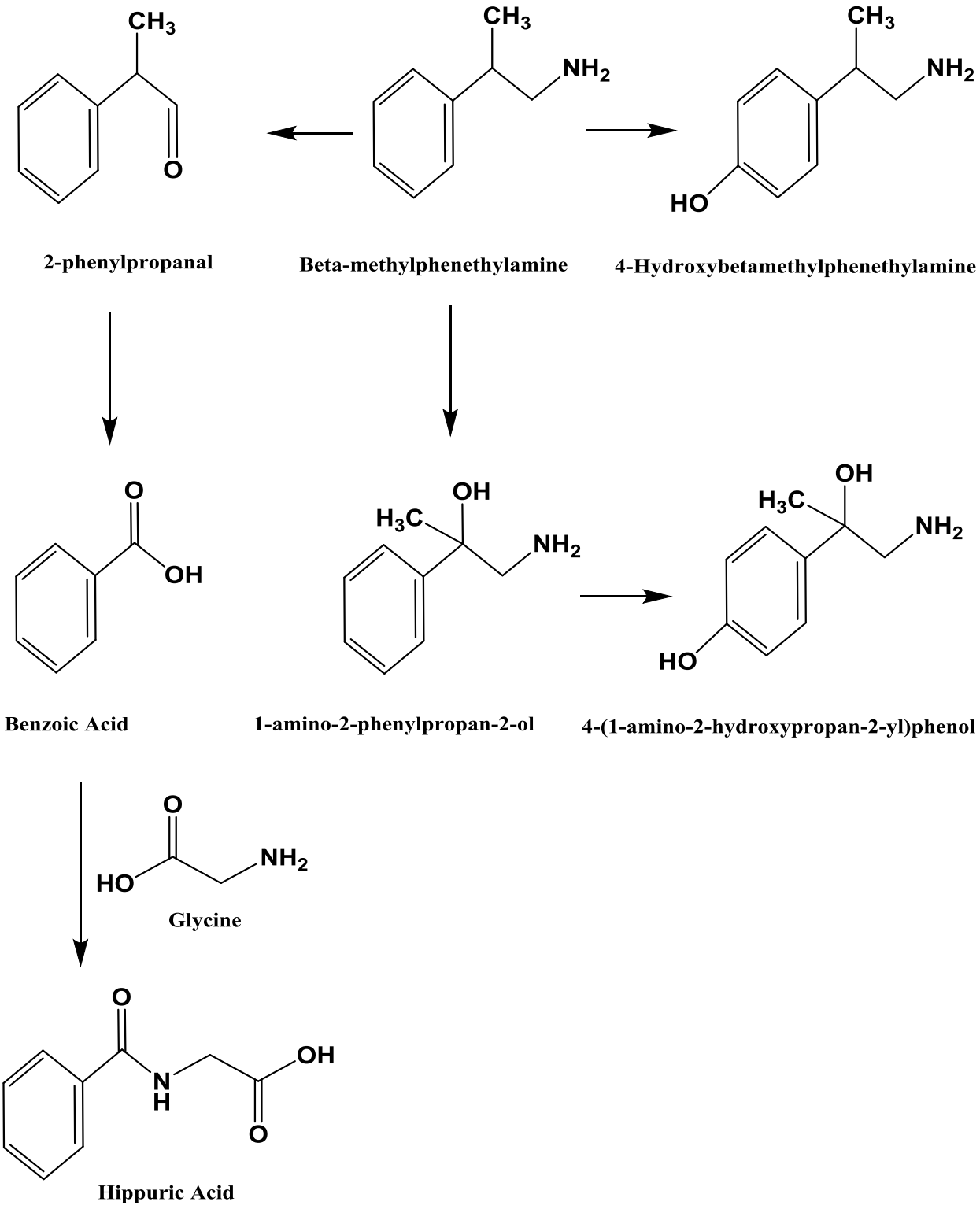

Figure 55: Proposed metabolic pathway of β-methylphenethylamine.

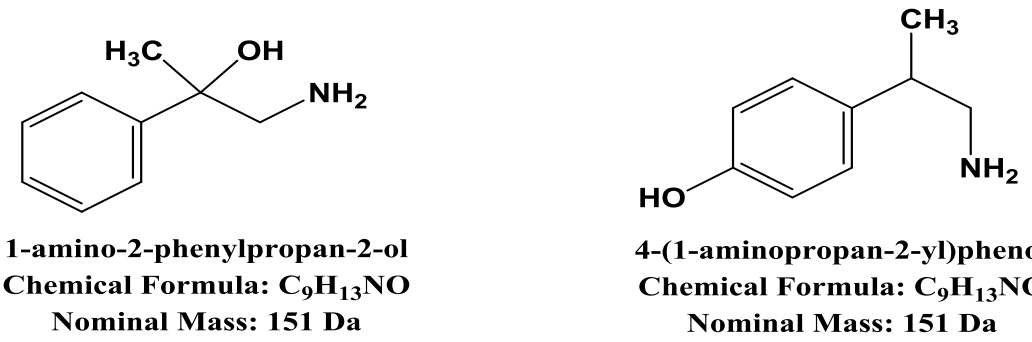

1-amino-2-phenylpropan-2-ol
Chemical Formula: $C_9H_{13}NO$
Nominal Mass: 151 Da

4-(1-aminopropan-2-yl)phenol
Chemical Formula: $C_9H_{13}NO$
Nominal Mass: 151 Da

Figure 56: Proposed chemical structures of the putative metabolites of β-methylphenethylamine.

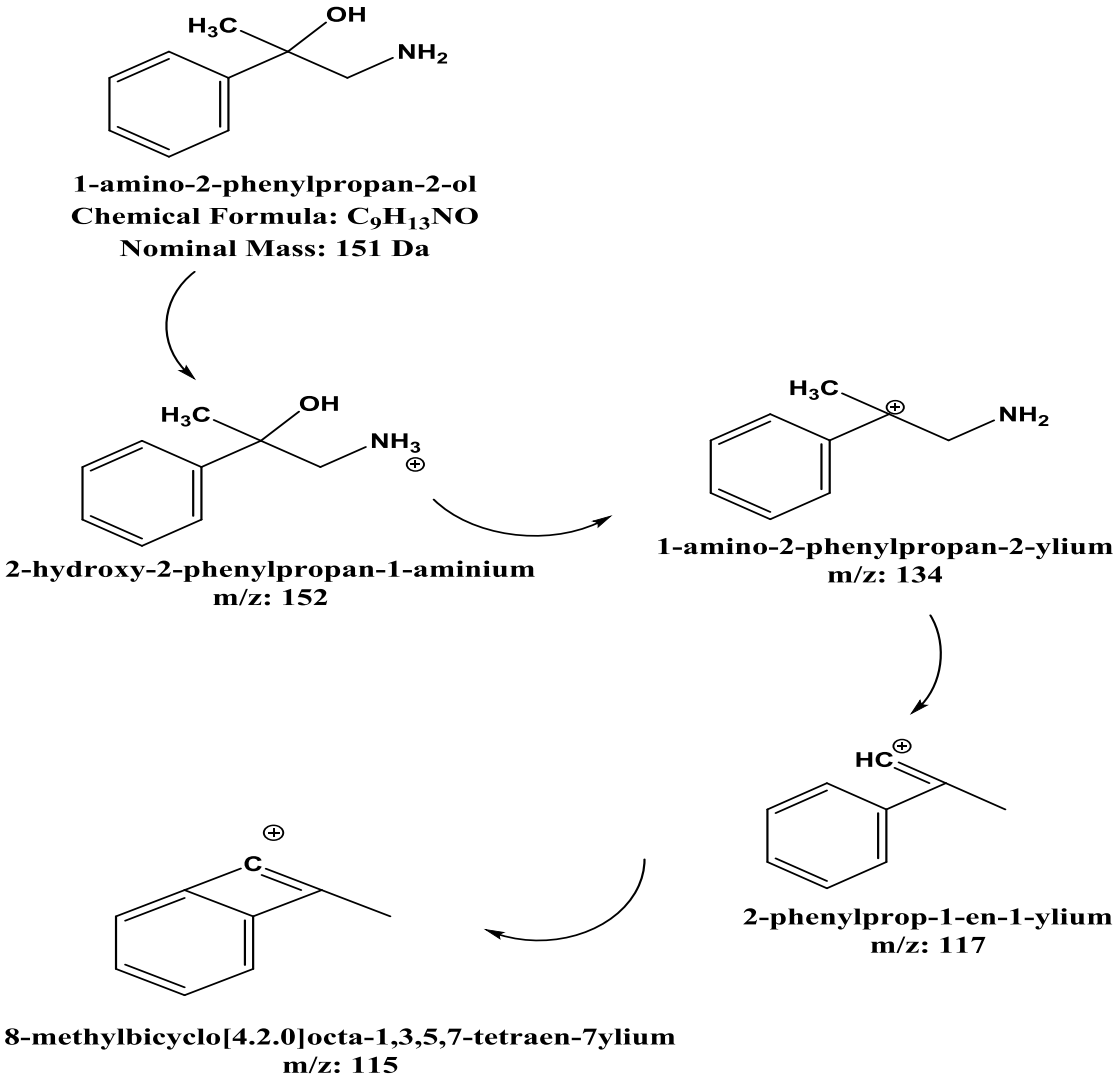

Figure 57: Proposed fragmentation pattern of the metabolite of β-methylphenethylamine.

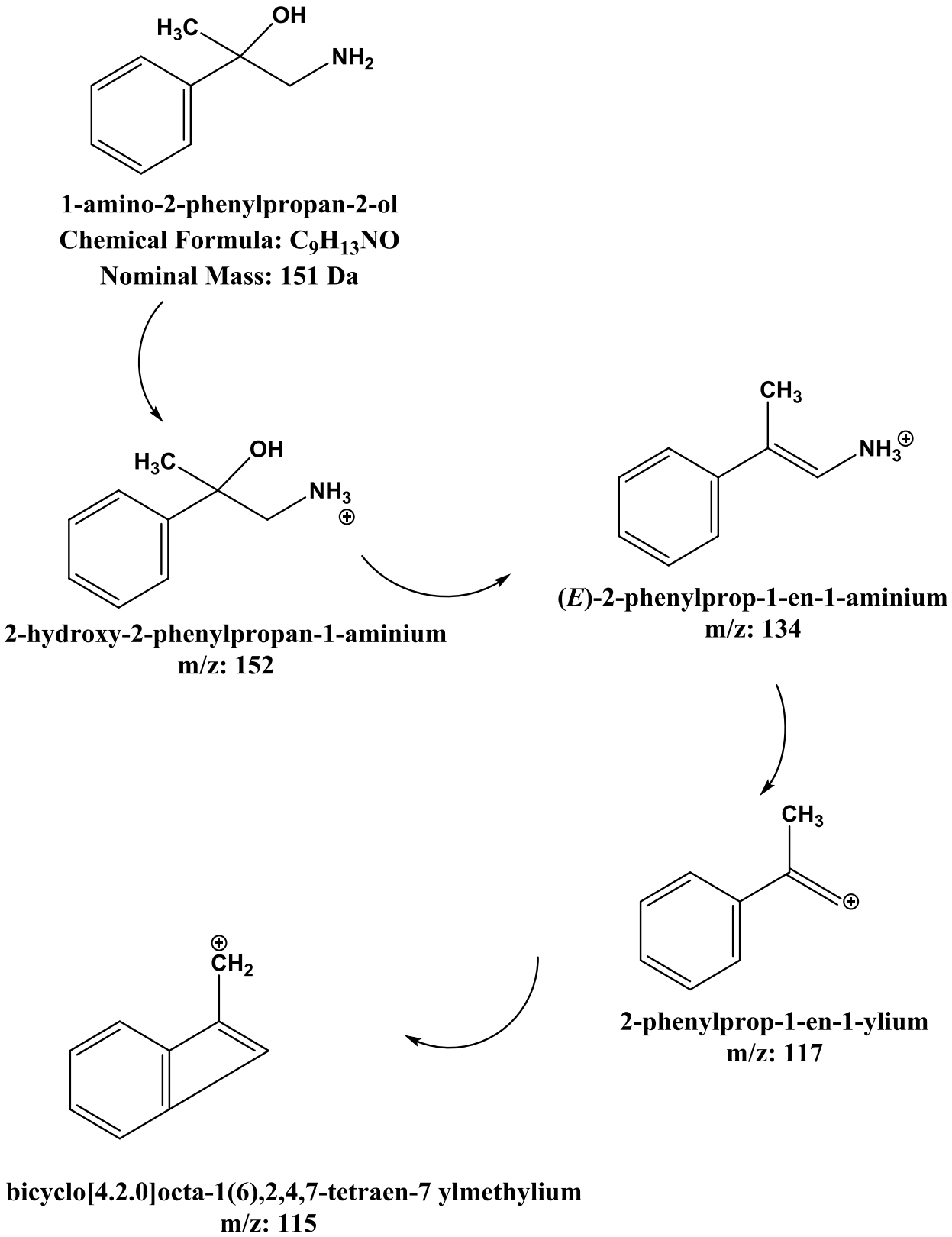

Figure 58: Second proposed fragmentation pattern of the metabolite of β-methylphenethylamine.

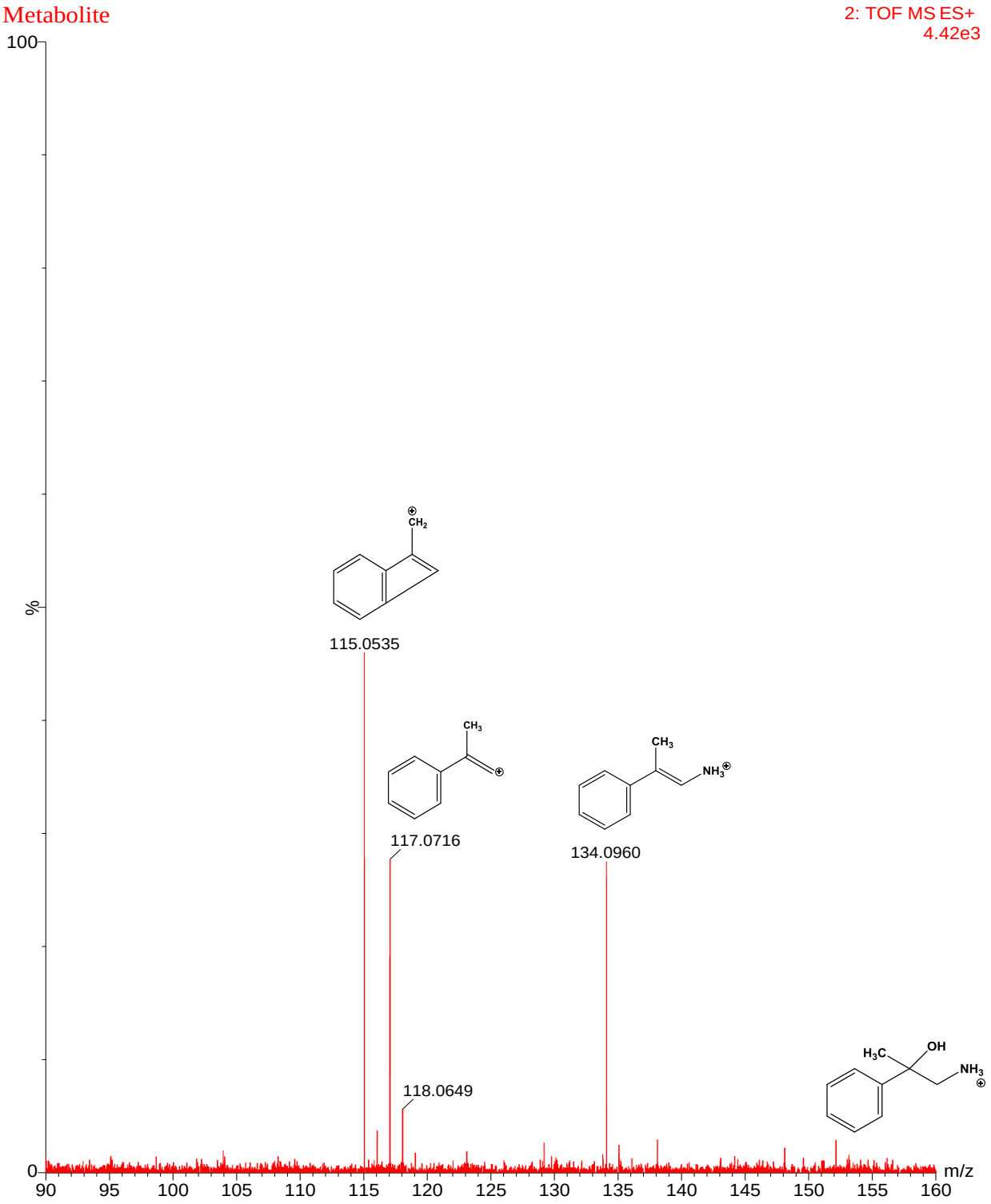

Figure 59: Proposed fragmentation pattern of the metabolite of β-methylphenethylamine presented on the mass spectral profile of β-methylphenethylamine, obtained at high energy.

5.4 Discussion

The validated analytical assay for the identification and quantification of selected ARDs in WB using MMSPE and UPLC-qTOF-MS was applied to the determination of BMP concentrations and detecting its metabolite in rat cardiac WB in this study. Post-injection rat WB samples were pretreated and extracted following the MMSPE pretreatment and extraction method (see 2.4). The extracted samples were analyzed using the validated analytical procedure described in Chapter 4.

The identification of BMP in rat WB was based on agreement between the putative compound and BMP (calibrator) in relative intensity at *m/z* 136, 119, and 91and retention time. The EIC (m/z = 119) and mass spectrum of a calibrant sample (positive control) corresponded to those from a sample derived from a drug-positive rat in terms of the relative instensity of the fragment ions formed and retention times. The S/N ratios were above the lower acceptable limits of 3:1 for *m/z* 136 and 91(qualifiers ions) and 10:1 for m/z 119 (quantifier ion) in all drug-postive rat WB samples. BMP quantification was based on the averaged standard curve using drug-free cardiac rat WB (control group), fit with a quadratic regression equation (R^2 = 0.9995); Table 30, Figure 45. The measured concentrations of BMP are shown in Table 35. The highest determined concentration of BMP was 899 ng/mL in a sample obtained from the high-dose group, whereas the lowest determined concentration was 22 ng/mL in a sample collected from the high delayed-dose group. Both the highest and lowest determined concentrations were within the validated working range of the assay (20-1,000 ng/mL). Interestingly, the high delayed-dose samples (collected 90 min post-injection) showed a sharp decline in the concentration levels of BMP (31 ng/mL ± 9 ng/mL) compared to the high-dose samples (collected within 20 min of injection), which showed very high concentration levels of BMP (869 ng/mL ± 29 ng/mL). This finding

proved that BMP has a short half-life of elimination from the rat blood. Further experiments are required to precisely estimate the half-life of BMP.

The main purpose of this study was to apply the validated method to authentic samples from subjects exposed to BMP and to identify one or more BMP metabolites. A theoretical metabolic pathway of BMP is proposed in Figure 55. This metabolic pathway was proposed based on the published metabolic pathway of AMP [173]. According to this theoretical metabolic pathway, 4-hydroxy-β-methylphenethylamine (4-HYDROXY), 1-amino-2-phenylpropan-2-ol (1-AMINO), and 4-(1-amino-2-hydroxypropan-2-yl) phenol (4-PHENOL) were proposed to be the metabolites of BMP. These proposed metabolites may be expected to be detectable by the analytical method proposed here, whereas 2-phenylpropanol, benzoic acid, and hippuric acid may not be detectable in positive ionization mode. A method for detection of putative metabolites by negative ionization mode was not developed in this work.

The metabolite identification process was carried out through manual and automated searches. The manual search process was performed using Masslynx® software, through search for molecular ions of common metabolite products (e.g., hydroxylation products). As was observed through analysis of the EICs corresponding to [M+H] (i.e., m/z = 152; hydroxylated metabolite of BMP) or [M+H+16] (e.g., m/z = 168; doubly hydroxylated metabolite of BMP), no detectable compounds were observed. Considering the fragmentation phenomena of the molecular ions of analytes included in validation within the qTOF-MS used, it is reasonable to anticipate similar patterns with any observed BMP metabolites.

The ion focusing system used in the XEVO-G2XS qTOF-MS is known as the StepWave® (see Figure 4) system, which plays a significant role in transferring ions from the ion source to the first mass filter (quadrupole). The StepWave® uses a relatively high electric field to guide

ions toward the first mass filter. Such an electric field may lead to "in-source" fragmentation of certain analytes prior to reaching the mass selector, especially at a low concentration level, leading to low sensitivity of detection of the molecular ion of an analyte. This phenomenon of in-source fragmentation could explain the underlying reason for the inability to detect the molecular ions of the theoretically proposed metabolites. Interestingly, a compound producing the ion with *m/z* 134 was detectable in all extracts from drug-positive rats at HE and LE but not in those from the drug-free controls. Figures 48 and 49 show EICs (m/z = 134) and mass spectral profiles from extracts of drug-positive and drug-negative rats. The presence of a compound forming this ion in extracts from the drug-positive animals was demonstrated using the automated Metabolite Identification feature of the UNIFI® software. Unfortunately, UNIFI® was not able to conclusively determine the identity of the proposed metabolite, even though the software was able to detect the compound. Furthermore, a search through the scientific libraries of the UNIFI® software yielded more than 100 candidate compounds. Most of these candidate compounds were excluded based on their chemical structures and compositions (chemical formula and nominal mass). Two candidates underwent comparison with the proposed metabolite at the level of mass spectral profiles. These candidate compounds were 4-hydroxyamphetamine and NOR. Since NOR was included in the validated method, its EIC and mass spectra at HE and LE were compared with those of the detectable metabolite, as shown in Figures 51, 52, and 53, respectively. There was agreement between the spectra of NOR and the proposed metabolite in the HE and LE mass spectra (Figure 52). However, the ion with *m/z* 152 was not detectable in the mass spectrum of the proposed metabolite, probably due to in-source fragmentation, as suggested earlier. Surprisingly, the HE mass spectra of CAT and the proposed metabolite were in good agreement, as shown in Figure 54. These findings support the idea that

the proposed metabolite might be a positional isomer of phenylpropanolamine (NOR and CAT). Experimentally, this proposition was strengthened by comparison of the retention times of the proposed metabolite and NOR, which were 5.43 and 5.71 min, respectively, as shown in Figure 50. This degree of resolution is consistent with that of the positional isomers included in the validated method (i.e. AMP and BMP). Accordingly, the metabolite of BMP was proposed to be 1-AMINO (see Figure 56) which is the corresponding positional isomer of NOR in the proposed metabolic pathway of BMP (see Figure 55). Two fragmentation patterns were proposed for 1-AMINO, as shown in Figures 57, 58, and 59. However, 4-HYDROXY could not be excluded as a candidate metabolite of BMP. Since a reference standard for 4-HYDROXY was not available for inclusion in this study, further investigation could not be carried out. Thus, further experiments are required to confirm the identity of the detected metabolite of BMP as 1-AMINO or 4-HYDROXY, or to exclude both candidates. This confirmatory study can be carried out by analyzing neat standards, and spiked WBs of 1-AMINO and 4-HYDROXY and comparing their mass spectra (HE and LE) with those of the metabolite of BMP detected in this study.

5.5 Conclusion

The validated analytical method for the identification and quantification of selected ARDs in WB using MMSPE and UPLC-qTOF-MS was verified by determining BMP concentrations and detecting its metabolite in rat cardiac WB in this study. Additionally, the study demonstrated the utility of UPLC-qTOF-MS for metabolite identification owing to its MS^E scanning mode feature.

Chapter 6

6.0 Conclusion

6.1 General Conclusions

A highly sensitive analytical method developed for selected ARDs was proven to be reliable for the detection and identification of a trace amount of EPH leaching from MIP-SPE. Although MIPs provide remarkable extraction selectivity by most analytical standards, the template compound leaching observed in this work measurably interfered with the analysis of one of the target analytes as a result of the high sensitivity and selectivity of the instrument and method used. Therefore, vendors should be wary of the potential for such interferences given that increasing sensitivity and mas resolution of LC-MS technology, and should be appropriately disclosed. Second, this study presents a validated method for the identification and quantification of selected ARDs by UPLC-qTOF-MS in WB after extraction by MMSPE. The method was validated according to the standard practices of SWGTOX, and. therefore, it can be utilized in forensic toxicology. Finally, the validated analytical assay was applied to measurement of BMP in WB of rats exposed to the drug, as well as to detection and potential identification of a putative BMP metabolite in rat cardiac WB.

6.2 Future Work

WB is one of the most complicated biological matrices available in forensic toxicology. Additionally, the chemical properties of ARDs add more complexity to the analytical approach for the detection of these drugs in WB. Therefore, further research is required to assist with and evaluate some of the challenges (e.g. the effects of non-silanized glass during sample preparation on detection of ARDs) faced during development and validation stages of this analytical method.

The research presented here used aged WB in developing a method for the identification and quantification of selected ARDs. This study was performed on aged animal WB matrices because of our limited access to aged human WB. This type of study should be expanded to include aged human WB.

Metabolite identification is another complex issue, requiring advanced techniques and analytical strategies, especially when the detectable metabolite has never been reported in the literature, as was the case in the analysis of WB of BMP-exposed animals. The proposed metabolite of BMP needs further research to confirm its chemical identity and structure.

Appendix A

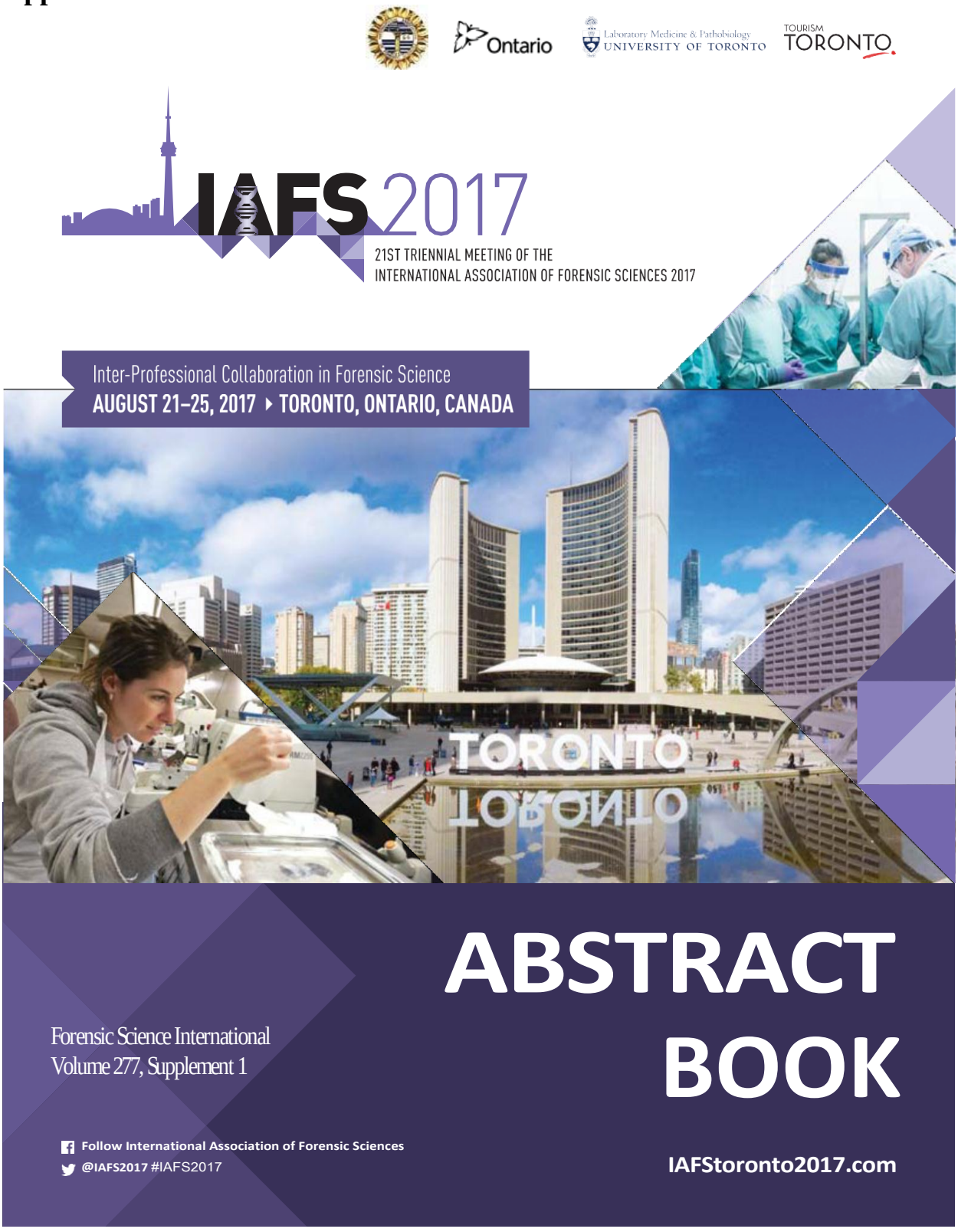
Ontario
Laboratory Medicine & Pathobiology
UNIVERSITY OF TORONTO
TOURISM TORONTO
IAFS 2017
21ST TRIENNIAL MEETING OF THE
INTERNATIONAL ASSOCIATION OF FORENSIC SCIENCES 2017
Inter-Professional Collaboration in Forensic Science
AUGUST 21–25, 2017 ▸ TORONTO, ONTARIO, CANADA
TORONTO
ABSTRACT BOOK
Forensic Science International
Volume 277, Supplement 1
Follow International Association of Forensic Sciences
@IAFS2017 #IAFS2017
IAFStoronto2017.com

Forensic Science International 277 (2017) 1–257

Contents lists available at ScienceDirect

Forensic Science International

journal homepage: www.elsevier.com/locate/forsciint

FATAL BRONCHOVASCULAR FISTULA VISUALIZED THROUGH POST MORTEM COMPUTED TOMOGRAPHY ANGIOGRAPHY

Philipp Hinderberger, Barbara Fliss, Michael J. Thali, Wolf Schweitzer
Institute of Forensic Medicine, University of Zurich, Zurich/SWITZERLAND

False aneurysm of the pulmonary artery complicated by bronchovascular fistula formation represents a rare life threatening condition. We report a case of fatal hemoptysis after formation of a bronchial fistula in the late postoperative period after sleeve lobectomy. Cause of death was determined by external post-mortem examination, post mortem computed tomography (PMCT) and angiography (PMCTA) without conventional autopsy.

Disclosure: All authors have declared no conflicts of interest.

DETERMINATION OF LSD AND 25H-NBOME BY SQUARE WAVE VOLTAMMETRY

Marcelo F. de Oliveira, Erica N. Oiye, Maria Fernanda M. Ribeiro, Juliana M.T. Katayama
Department of Quimica - FFclrp, Universidade de São Paulo, Ribeirão Preto - SP/BRAZIL

A new class of psychoactive designer drugs, N-Benzyl- substituted phenethylamines known as NBOMes ("N-bomb" or "Smiles") has been highlighted among seized drugs, and it englobes a great variety of substances, as the 25H-NBOMe. Apart from its detection, it is essential to differentiate these new drugs from others as the most common form of consumption of NBOMe is in blotter, similarly to those found for LSD (lysergic acid diethylamide). Besides, the detection of these drugs must be sensitivity, fast and specific. In order to comply with these characteristics, voltammetric analysis holds an important role in forensic scenario. The present work focuses on the detection of both of the drugs by a unique Square Wave Voltammetric methodology. The measurements were performed on a glassy carbon electrode as the working electrode in a methanolic solution containing $LiClO_4$0, 1 mol.L^{-1} as supporting electrolyte. The experimental parameters used were: step potential of 0.005V, frequency of 25Hz and amplitude of 0.02 V. In this experimental condition, it was possible to detect LSD in 2.57 10^{-7} mol L^{-1} and the quantification of 25H-NBOMe allows to reach concentration level of 4.25 10^{-6} mol L^{-1}. In the first drug, the present methodology only identifies LSD, which implies in a qualitative analysis; when 25H-NBOMe is analyzed, qualitative and quantitative results are achieved. After considering the extraction process applied for blotter samples, concentrations values around 10μg of LSD or 25H-NBOMe are enough to result the oxidative peaks observed in 1.12V (LSD) and 1.35 V (25H-NBOMe). From the same Square Wave Voltammetric methodology, it is possible to differentiate LSD and the new psychoactive drug 25H-NBOMe in less than 1 minute of analysis. These reliable results observed after a simulation in blotter extraction allow the application of this electroanalysis in the routine of forensic laboratories.

Disclosure: All authors have declared no conflicts of interest.

CERVICAL INJURIES IN DROWNING CASES

Marwa Boussaid[1], Mohamed Amine Mesrati[1], Meriem Belhadj[2], Nidhal Hadj Salem[2], Ali Chadly[2], Abir Aissaoui[1]
[1]*Forensic Medicine, Tahar Sfar University Hospital of Mahdia, Mahdia/TUNISIA,*
[2]*Forensic Medicine, Fattouma Bourguiba University Hospital, Monastir/TUNISIA*

Introduction: Discovery of bruises in the muscles of the neck and a fracture of the hyoid bone in a body recovered from water make the diagnosis as well as the determination of the manner of death difficult. **Aim:** The aim of this work is to report a case of a drowned body with cervical injuries and to highlight the importance of not misinterpreting these findings. **Case report:** A 39-year-old female was found dead, the face down in a well filled with water up to 3 meters whose height is 6 meters. She was mentally disturbed and had a history of suicide attempts in the same place and in the same way. The autopsy revealed bruises in the muscles of the neck and a bruise associated with a fracture of the left horn of the hyoid bone. **Conclusion:** In the case reported here, these lesions were explained by the impact of the fall from a high place and the cervical hyperextension or hyper-flexion due to mechanical asphyxia.

Disclosure: All authors have declared no conflicts of interest.

DENTAL AGE ASSESSMENT AMONG TUNISIAN CHILDREN USING THE DEMIRJIAN METHOD

Abir Aissaoui[1], Mohamed Amine Mesrati[1], Meriem Belhadj[2], Marwa Boussaid[1], Nidhal Hadj Salem[2], Ali Chadly[2]
[1]*Forensic Medicine, Tahar Sfar University Hospital of Mahdia, Mahdia/TUNISIA,*
[2]*Forensic Medicine, Fattouma Bourguiba University Hospital, Monastir/TUNISIA*

Introduction: Since Demirjian system of estimating dental maturity was first described; many researchers from different countries have tested its accuracy among diverse populations. Some of these studies have pointed out a need to determine population-specific standards. **Aim:** The aim of this study is to evaluate the suitability of the Demirjian's method for dental age assessment in Tunisian children. **Materials and Methods:** This is a prospective study previously approved by the Research Ethics Local Committee of the University Hospital Fattouma Bourguiba of Monastir (Tunisia). Panoramic radiographs of 280 healthy Tunisian children of age 2.8–16.5 years were examined with Demirjian method and scored by three trained observers. **Statistical Analysis Used:** Dental age was compared to chronological age by using the analysis of variance (ANOVA) test. Cohen's Kappa test was performed to calculate the intra- and inter-examiner agreements. **Results:** Underestimation was seen in children aged between 9 and 16 years and the range of accuracy varied from −0.02 to 3 years. The advancement in dental age as determined by Demirjian system when compared to chronological age ranged from 0.3 to 1.32 year for young males and from 0.26 to 1.37 year for young females (age ranged from 3 to 8 years). **Conclusions:** The standards provided by Demirjian for French-Canadian children may not be suitable for Tunisian children. Each population of children may need their own specific standard for an accurate estimation of chronological age.

Disclosure: All authors have declared no conflicts of interest.

will be presented, by reviewing the different steps and various parameters influencing such a statistical approach, and the overall relevance and impact of such outcomes for law enforcement, security and public policy will be discussed.

Disclosure: All authors have declared no conflicts of interest.

SUITCASE CONCEALMENT: AN ANALYSIS OF THE TAPHONOMIC PROCESSES AND THEIR EFFECT ON PMI ESTIMATION

A. Skylar Joseph, Gary W. Reinecke, Ian R. Dadour
Anatomy and Neurobiology, Forensic Anthropology Program, Boston University School of Medicine, Boston/MA/UNITED STATES OF AMERICA

In cases of homicide, suitcases provide concealment and may ease the transport of a body with minimal likelihood for detection. In order to create a minimum post-mortem interval estimate (mPMI), it is first necessary to understand the unique taphonomic processes that occur when a body is concealed within a suitcase. In this study, the experimental carcasses consisted of pig (*Sus scrofa*) heads, which were concealed within either hard shell plastic suitcases, or fabric suitcases; the control pig heads were left on the surface of the ground to decompose naturally. Starting on day three of each study period, and continuing every other day until day 15, three suitcases of each type were removed from the field for analysis of the entomological activity inside the suitcases and the decompositional stage of the pig head. Additionally, the ambient temperature and the temperature inside each type of suitcase was recorded by temperature data loggers throughout the duration of each study period. The study was repeated twice, once in May and once in August 2016. Temperature comparisons revealed that the hard shell plastic suitcases reached significantly (<0.001) hotter temperatures than both the ambient temperature and the temperature inside the fabric suitcases. Insect activity began immediately on the control samples during both study periods; however, during study one, insect activity was not present inside the fabric suitcases until days 3-5, and did not occur inside the hard shell suitcases until days 5-7. During study two, insect activity inside both types of suitcases was present by day 3, but not guaranteed to occur until day 4 or later. Some differences in insect species were noted between the controls and the suitcases, as well as between both types of suitcases. Most notable was the presence of a number of fly species that are generally associated with late decomposition inside the suitcases. Additionally, while beetles were present on the control samples, none were found inside the suitcases. All control samples mummified within days, while all of the experimental samples experienced wet decomposition often resulting in skeletonization by day 15. This study has shown that, not only does concealment within a suitcase change the taphonomic history of the body enclosed, but that the type of suitcase also influences the taphonomic factors that the body will experience. Ultimately, this study will aid in the ability to better predict the mPMI for cases in which a body is concealed within a suitcase.

Disclosure: All authors have declared no conflicts of interest.

DETERMINING A NEW METHOD FOR ESTIMATING THE PMI OF DECOMPOSED REMAINS FOUND IN TEMPERATE AUSTRALIAN

Stephanie J. Marhoff-Beard[1], Hayley Green[1], Shari Forbes[2]
[1]*School of Science and Health, Western Sydney University, Penrith/NSW/AUSTRALIA,* [2]*Centre for Forensic Science, University of Technology, Sydney, Sydney/NSW/AUSTRALIA*

At present, a reliable method for estimating the post-mortem interval (PMI) of decomposed remains in an Australian context using taphonomic changes occurring during decomposition alone is currently unavailable. Decomposition rates of human remains are climate dependent, therefore the current published methods developed internationally may not be useful for determining PMI in Australian environments. The aim of this study was to assess the validity of previously published methods in a temperate Australian climate and develop a method that is more appropriate in an Australian context. Between 2014 and 2016, pig carcasses, as an analogue for human remains, were left to decompose on a soil surface during the seasons of Summer and Winter (8 pigs per season, 32 in total) in Greater Western Sydney. Soft tissue changes were recorded at regular intervals during each season and scored according to previously published methods. Temperature data was recorded daily using data loggers and an onsite weather station. A new Western Sydney specific model for determining PMI was also developed using all new data collected. This presentation will discuss the validity of using published methods in determining PMI in an Australian environment and how they compare to the accuracy of the newly developed Western Sydney method.

Disclosure: All authors have declared no conflicts of interest.

ANALYTICAL INTERFERENCE IN MOLECULARLY-IMPRINTED POLYMER SPE (MIP-SPE) AND UPLC-QTOF-MS

Ahmad Alamir[1], Heather Cornthwaite[2], James Watterson[3]
[1]*Department of Chemistry & Biochemistry, Laurentian University, Sudbury/ON/CANADA,* [2]*Biomolecular Sciences Program, Laurentian University, Sudbury/ON/CANADA,* [3]*Department of Forensic Science, Laurentian University, Sudbury/ON/CANADA*

Molecularly imprinted polymers (MIPs) provide a medium with high selectivity binding sites for analytes with specific structural features. Accordingly, MIPs have been promoted as selective solid-phase extraction (SPE) media for extractions of targeted analytes that may serve to minimize matrix effects while providing desirable reagent and pH stability. A key limitation of MIP-SPE, however, is the bleeding and detection of residual template molecules from the polymer matrix detected by more sensitive instrument platforms. Here we report template bleeding and interference with analysis of selected amphetamine-related stimulants (ARSs) in aged/post-mortem blood by UPLC-qTOF-MS. Ephedrine (EPH), a toxicologically important analyte, was observed to leach from a commercially available MIP across extracts of numerous drug-free blood and aqueous matrices (250 uL sample volume), increasing apparent instrument EPH response by more than 25% at real EPH concentrations of 20 ng/mL. Mixed-mode SPE (MMSPE) and Filtration Pass-Through Extraction (FPTE) analyses of various drug-free aqueous and decomposed blood matrices confirmed the MIP as the source of the EPH interference. While the extraction selectivity provided by MIP technology is remarkable, the potential for template leeching as a significant source of interference of selected analytes may be very high and should be characterized and disclosed by all vendors.

Disclosure: All authors have declared no conflicts of interest.

HOMICIDAL DEATH INVESTIGATION AT WORKPLACE – THE MALAYSIAN EXPERIENCE.

Faridah Nor
Pathology, Universiti Kebangsaan Malaysia Medical Centre, Kuala Lumpur/MALAYSIA

Violence and crime are becoming quite common nowadays. Such deaths are of public interest, particularly to family members and relatives. This is a case of a 41-year old male, who was severely beaten to death at his workplace, and was investigated consequently. Further discussion revealed multiple injuries and the implicated objects used, which formed a learning experience. The employers have statutory responsibilities for enforcement of a method to control the risk of peer group pressure, and to help reassure that risks to workers are properly curb, and criteria adopted such that corrective actions are taken to wrongdoers.

Disclosure: All authors have declared no conflicts of interest.

Analytical Interference in Molecularly-Imprinted Polymer SPE (MIP-SPE) and High-Resolution LC-MS (UPLC-qTOF-MS)

Ahmad Alamir, Heather Cornthwaite and James Watterson
Forensic Toxicology Research Laboratory, Department of Forensic Science
Laurentian University, 935 Ramsey Lake Road, Sudbury, ON, P3E 2C6

INTRODUCTION

Molecularly imprinted polymers (MIPs) provide a medium with highly selective binding sites for analytes with specific structural features [1]. Accordingly, MIPs have been promoted as highly selective solid-phase extraction (SPE) media for extraction of targeted analytes to minimize matrix effects while providing desirable reagent pH stability. A key limitation, however, is the bleeding and detection of residual template molecules from the polymer matrix detected by a highly sensitive instrument platform [2].

Here we report MIP template bleeding and interference in the analysis of selected amphetamine-related stimulants (ARSs) in aged blood by Ultra Performance Liquid Chromatography Quadrupole Time of Flight Mass Spectrometry (UPLC-qTOF-MS). Ephedrine (EPH), a toxicologically important analyte, was observed to leach from a commercially available MIP product across numerous extracts of various drug-free blood and aqueous matrices, increasing apparent instrument EPH response by more than 25% at real EPH concentrations of 20 ng/mL. During the validation experiments, matrix interference, ephedrine interference was observed in analysis of various drug-free aged whole blood matrices. This ephedrine-interference has been intensively investigated to identify the source of ephedrine.

METHOD

Analytes were extracted from aged animal drug-free blood, or aqueous matrices (250 µL sample volume) in triplicate by MIP-SPE (Amphetamines MIP, 25 mg, Biotage Corp, Uppsala, SE), Mixed Mode SPE (MMSPE, Oasis MCX, 30 mg, Water Corp, Milford, MA, USA) and Filtration-Pass Through Extraction (FPTE, HLB Prime 100 mg, Waters Corp, Milford, MA, USA)

MIP-SPE Extraction Procedure:

Portions (250 µL) of drug-free whole blood or aqueous sample were mixed with 1 mL of 10 mM ammonium acetate (pH 7), followed by an addition of 1 mL of acetonitrile (ACN). The mixtures were vortexed and centrifuged at 5000 rpm for 15 min at room temperature and the supernatants were decanted into clean tubes. The MIPs-SPE procedure was carried out on an SPE vacuum manifold. The cartridges were conditioned with 1 mL of methanol (MeOH), and equilibrated with 1 mL of 10 mM ammonium acetate (pH 7). Supernatants were loaded under gravity, and cartridges were washed twice with 1 mL of water and once with 1 mL of ACN/distilled (60:40, v/v). Cartridges were then dried for 10 min at -40 kPa, washed with 1 mL of acetic acid/ACN (1:100, v/v), and dried again for 30 sec at -10 kPa. The analytes of interest were then eluted with 2 mL of formic acid/MeOH (1:100, v/v). The eluates were evaporated to dryness under vacuum centrifugation at a temperature of 30 °C, and residues were reconstituted in 200 µL of mobile phase A solution (5 mM ammonium formate + 0.1 % (v/v) formic in water). Reconstituted residues were subjected to UPLC-qTOF-MS analysis.

MMSPE Extraction Procedure:

Drug-free whole blood or aqueous samples (250 µL) were mixed sequentially with 1 mL volumes of 0.1 M HCl and ACN. The mixtures were vortexed and centrifuged at 5000 rpm for 15 min at room temperature and the supernatants were decanted into clean tubes. MMSPE was carried out by using Oasis MCX 96-well plates. Supernatants were loaded under gravity, and SPE wells were washed sequentially with 1 mL of 0.1 M HCl, 1 mL MeOH and 1 mL 5% ammonia. The wells were dried under vacuum for 10 min, then the analytes were eluted with 1 mL of 5% ammonia in MeOH. The eluted solutions were evaporated to dryness under vacuum centrifugation at a temperature of 30 °C, and residues were reconstituted in 200 µL of mobile phase A solution. Reconstituted residues were submitted for UPLC-qTOF-MS analysis.

METHOD cont'd

FPTE Extraction Procedure:

Drug-free whole blood (250 µL) or aqueous samples were diluted with 1 mL of MeOH. The mixtures were then mixed with 1 mL of ACN. The mixtures were vortexed and centrifuged at 5000 rpm for 15 min at room temperature and the supernatants were decanted into clean tubes. FPTSPE was carried out by using HLB Prime 96-well plate. Supernatants were directly loaded under gravity into the SPE wells. The eluted solutions were collected and evaporated to dryness under vacuum centrifugation at a temperature of 30 °C. Dry residues were reconstituted in 200 µL of mobile phase A solution and was submitted for UPLC-qTOF-MS analysis.

UPLC Conditions:

A Waters Acquity UPLC with a binary mobile phase system equipped with a HSS T3 column (2.1 mm x 100 mm, 1.8 µm) was utilized in this work. UPLC was run as pseudo-isocratic for 9 mins (5 mM ammonium formate, 0.1% (v/v) formic acid in 100 to 95:5 water:ACN) for baseline resolution.

qTOF-MS Settings:

Mass spectrometry was performed on a Waters Acquity UPLC equipped with a Waters Xevo G2-XS-qTOF-MS (Waters Corp., Milford, MA). Data were acquired in sensitivity mode under positive electrospray ionization with resolution > 20,000 at full width half maximum. The acquisition range was from m/z 50 to 601, using a scan time of 0.1 sec. Capillary voltage and cone voltage were set to 0.8 kV and 20 V, respectively. The source temperature was 140 °C, the desolvation gas flow was set to 900 L/h at a temperature of 250 °C and the cone gas was set to 50 L/h. Data acquisition was achieved using MS^E mode, with low collision energy set to 4.0 eV, and the high-energy ramp ranged from 10–40 eV.

Matrix Effect (ME) Calculation:

ME = Spiked Post Extract Instrumental Response / Neat Standard Instrumental Response

ME less than 1 indicates suppression
ME greater than 1 indicates enhancement

Acknowledgements:

The authors would like to acknowledge the Saudi Ministry of Education and Health, Saudi Culture Bureau in Ottawa, and Laurentian Forensic Toxicology Lab for their financial support of this work.

RESULTS

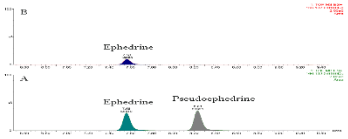

Figure 1: Extracted ion chromatogram of ephedrine molecular ion 166.1321 m/z of a neat standard mix at the concentration of 1 ng/mL (A), and drug-free animal blood sample extracted by MIP-SPE (B).

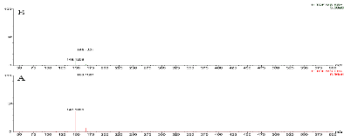

Figure 2: Ephedrine mass spectrum of a neat standard mix at the concentration of 1 ng/mL, (A) and (B) ephedrine mass spectrum of a drug-free animal blood sample extracted by MIP-SPE.

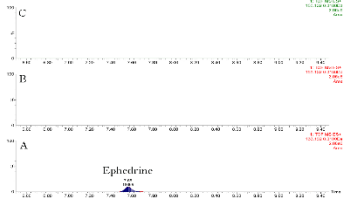

Figure 3: Extracted ion chromatogram of ephedrine molecular ion 166.1321 m/z of a drug-free animal sample extracted by MIP-SPE (A), MMSPE (B), and FPTE (C).

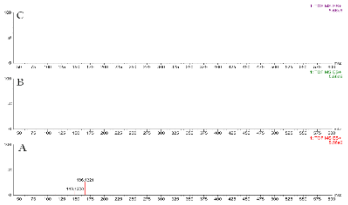

Figure 4: Mass spectrum of a drug-free animal sample extracted by MIP-SPE (A), MMSPE (B), and FPTE (C).

DISCUSSION AND CONCLUSION

EPH, a toxicologically important analyte, was identified and observed to leach from a commercially available MIP across extracts of numerous drug-free blood and aqueous matrices (250 uL sample volume), increasing apparent instrument EPH response by more than 25% at real EPH concentrations of 20 ng/mL.

While the extraction selectivity provided by MIP technology is remarkable, the potential for template leaching is a significant source of interference and should be characterized and disclosed by all vendors.

References:

[1] Vasapollo G, Sole RD, Mergola L, et al (2011) Molecularly Imprinted Polymers: Present and Future Prospective. International Journal of Molecular Sciences 12:5908 5945. doi:10.3390/ijms12095908

[2] Haupt K (2003) Peer Reviewed: Molecularly Imprinted Polymers: The Next Generation. Analytical Chemistry. doi: 10.1021/ac031385h

Appendix B

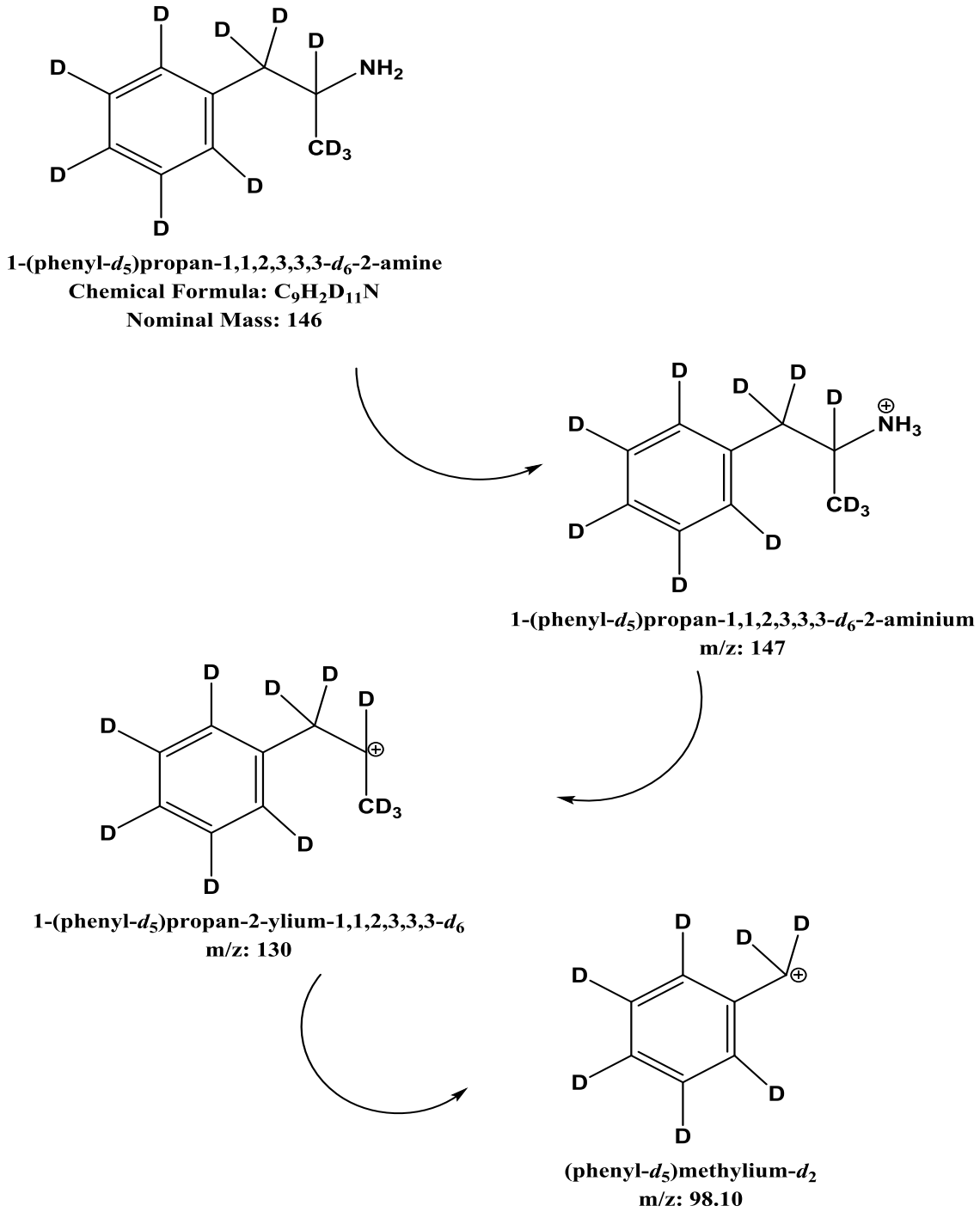

Figure 1: Structure proposals of the molecular ion and some of the fragment ions in the product ion mass spectra of amphetamine-d_{11}

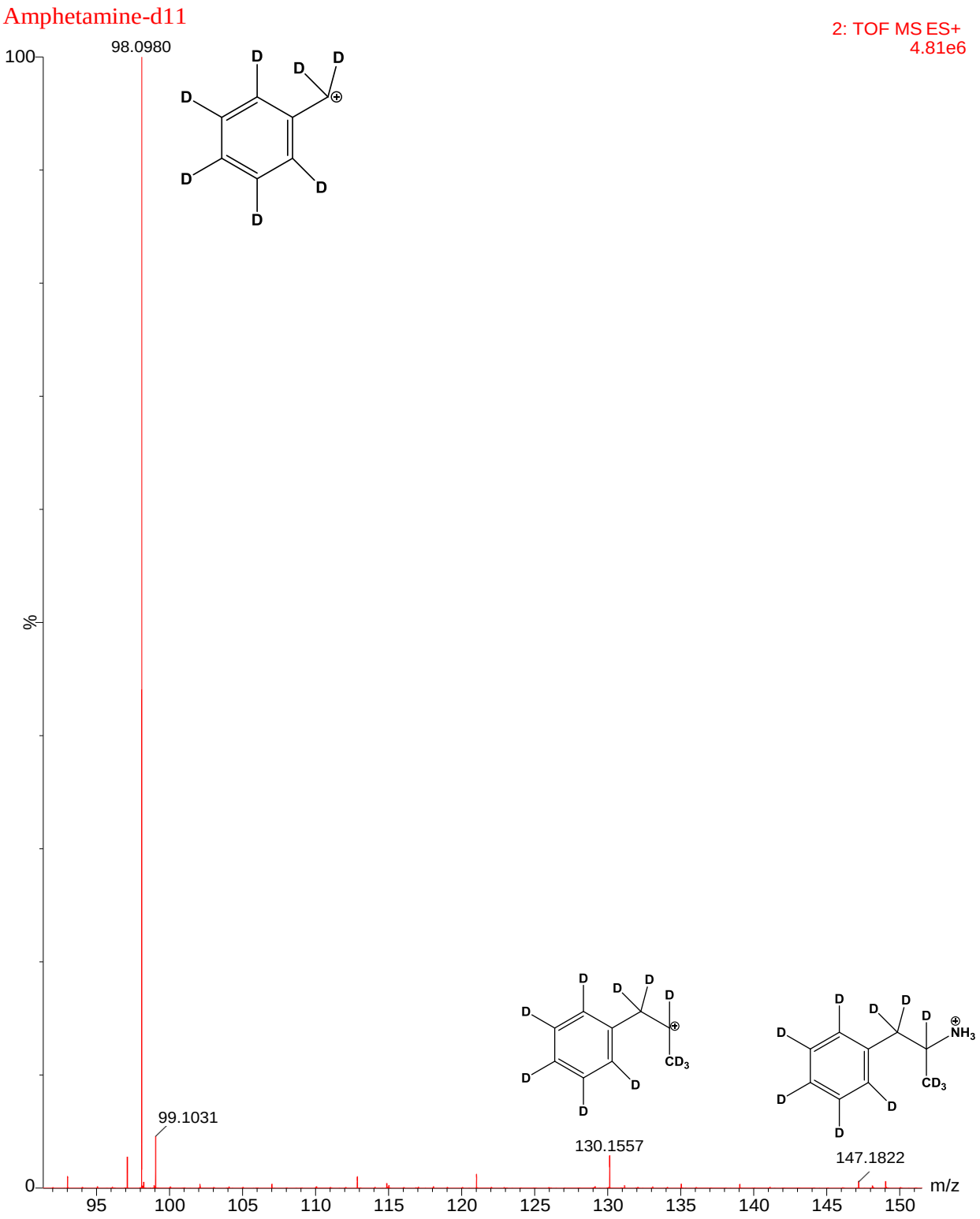

Figure 2: MS^E (HE) spectra of amphetamine-d_{11}

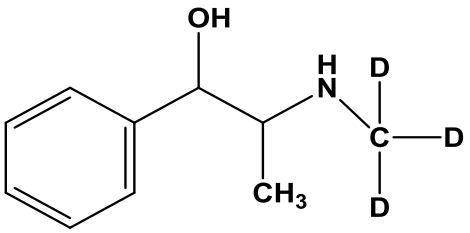

2-((methyl-d_3)amino)-1-phenylpropan-1-ol
Chemical Formula: $C_{10}H_{12}D_3NO$
Nominal Mass: 168.13

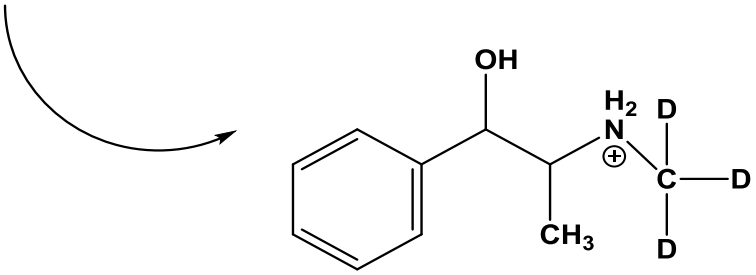

1-hydroxy-*N*-(methyl-d_3)-1-phenylpropan-2-aminium
m/z: 169

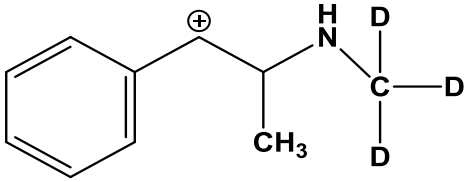

2-((methyl-d_3)amino)-1-phenylpropan-1-ylium
m/z: 151

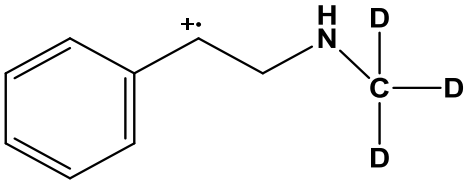

m/z: 136

Figure 3: Structure proposals of the molecular ion and some of the fragment ions in the product ion mass spectra of ephedrine-d_3

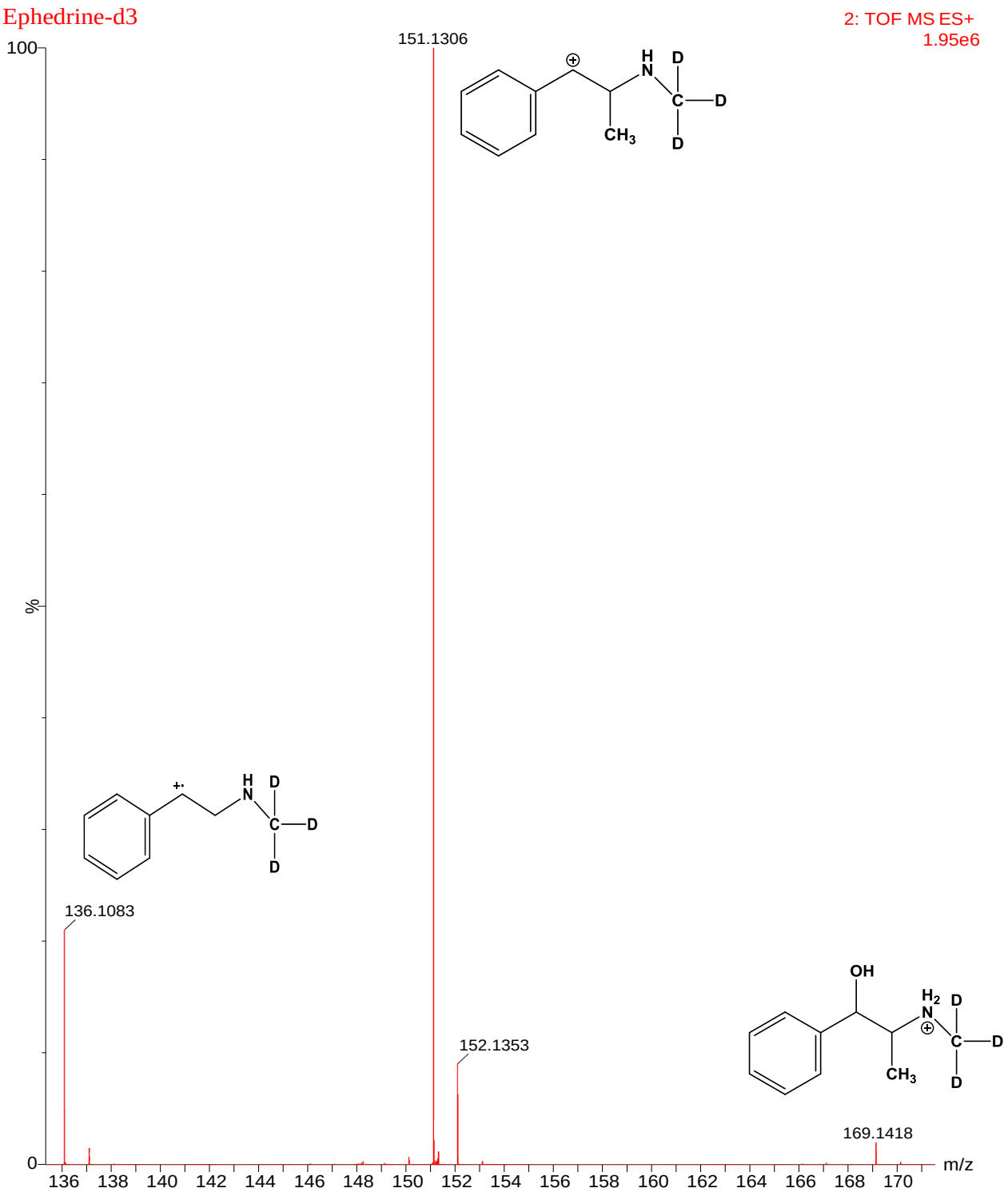

Figure 4: MS^E (HE) spectra of ephedrine-d_3

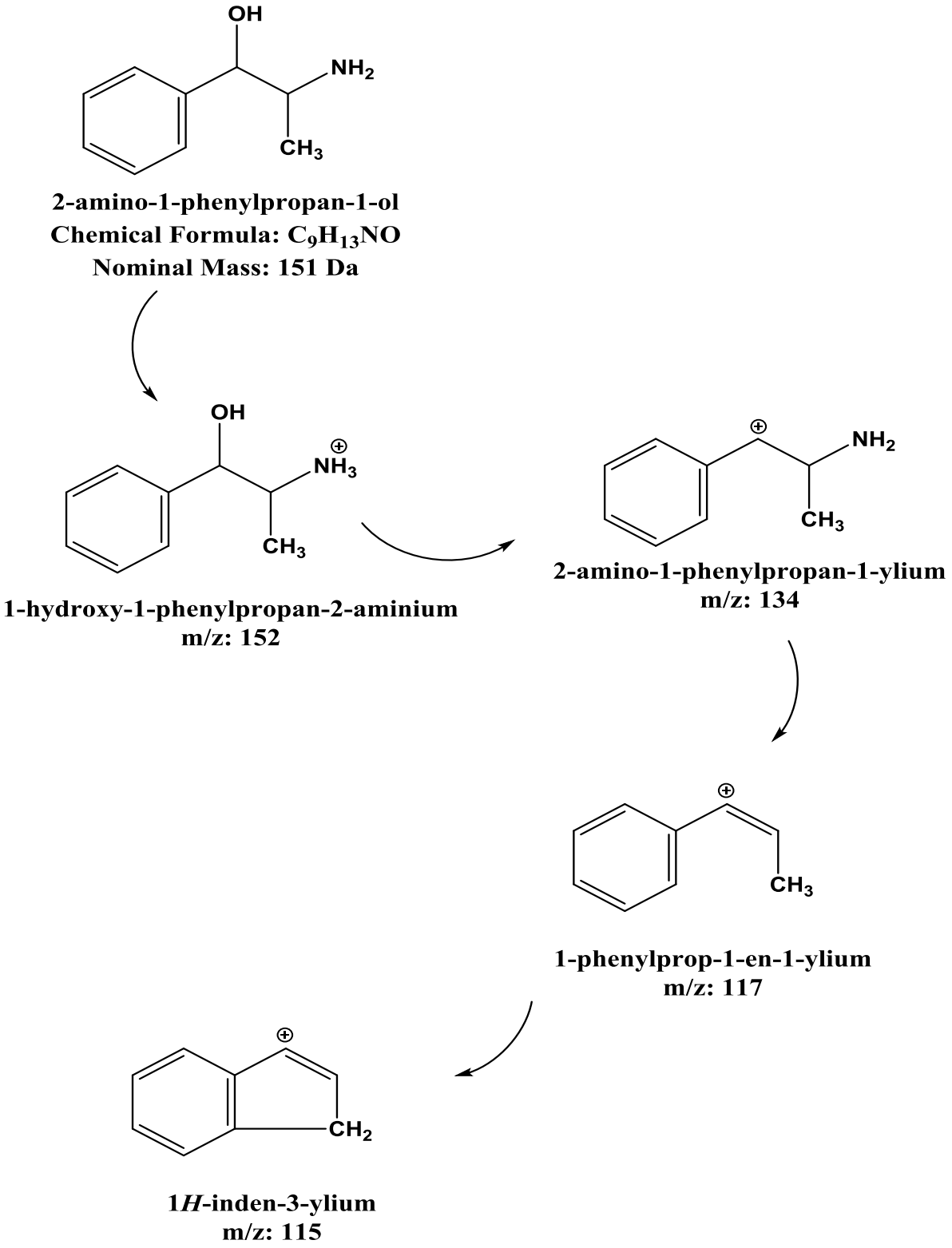

Figure 5: Structure proposals of the molecular ion and some of the fragment ions in the product ion mass spectra of phenylpropanolamine (norephedrine and cathine)

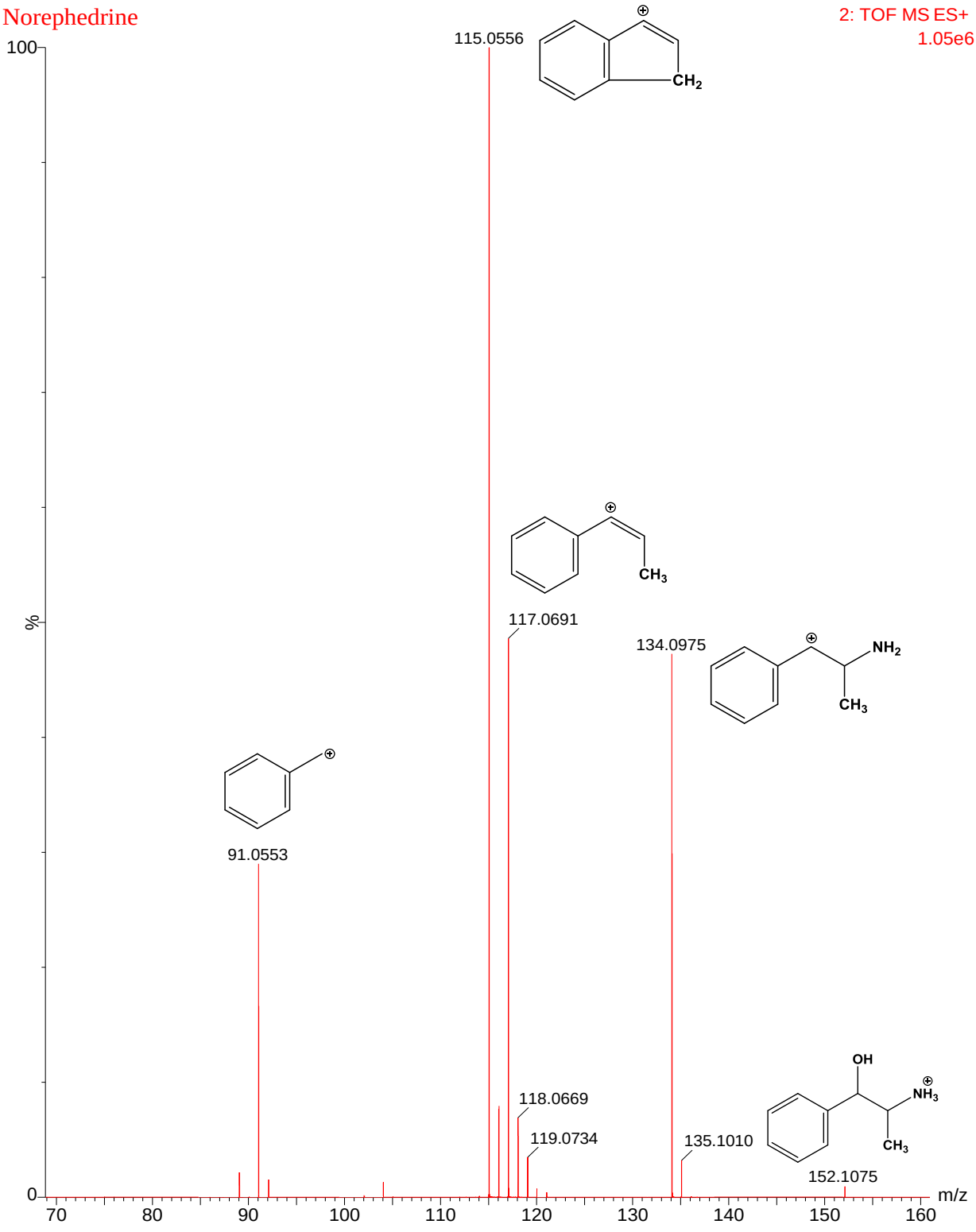

Figure 6: MS^E (HE) spectra of norephedrin

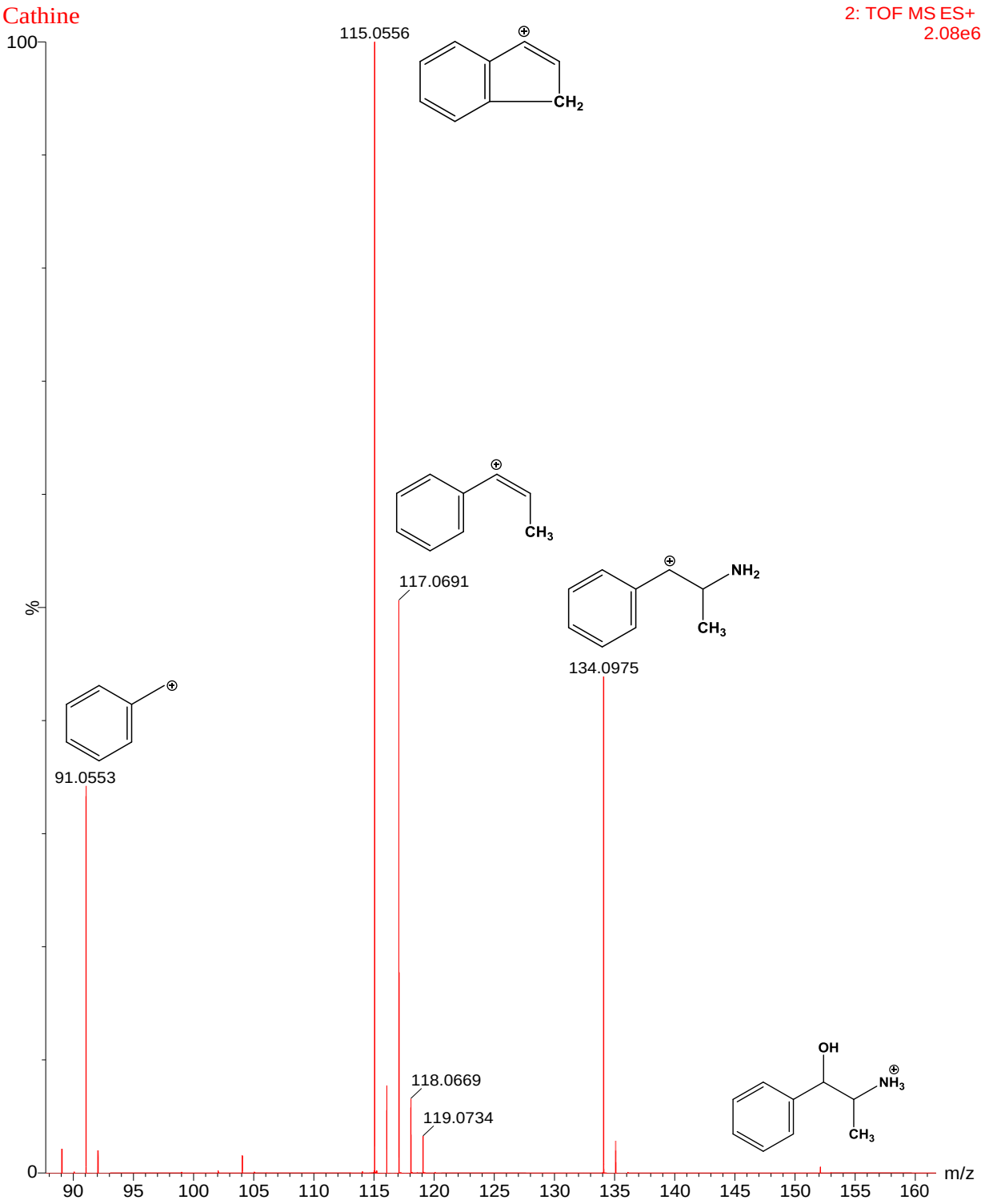

Figure 7: MS^E (HE) spectra of cathine

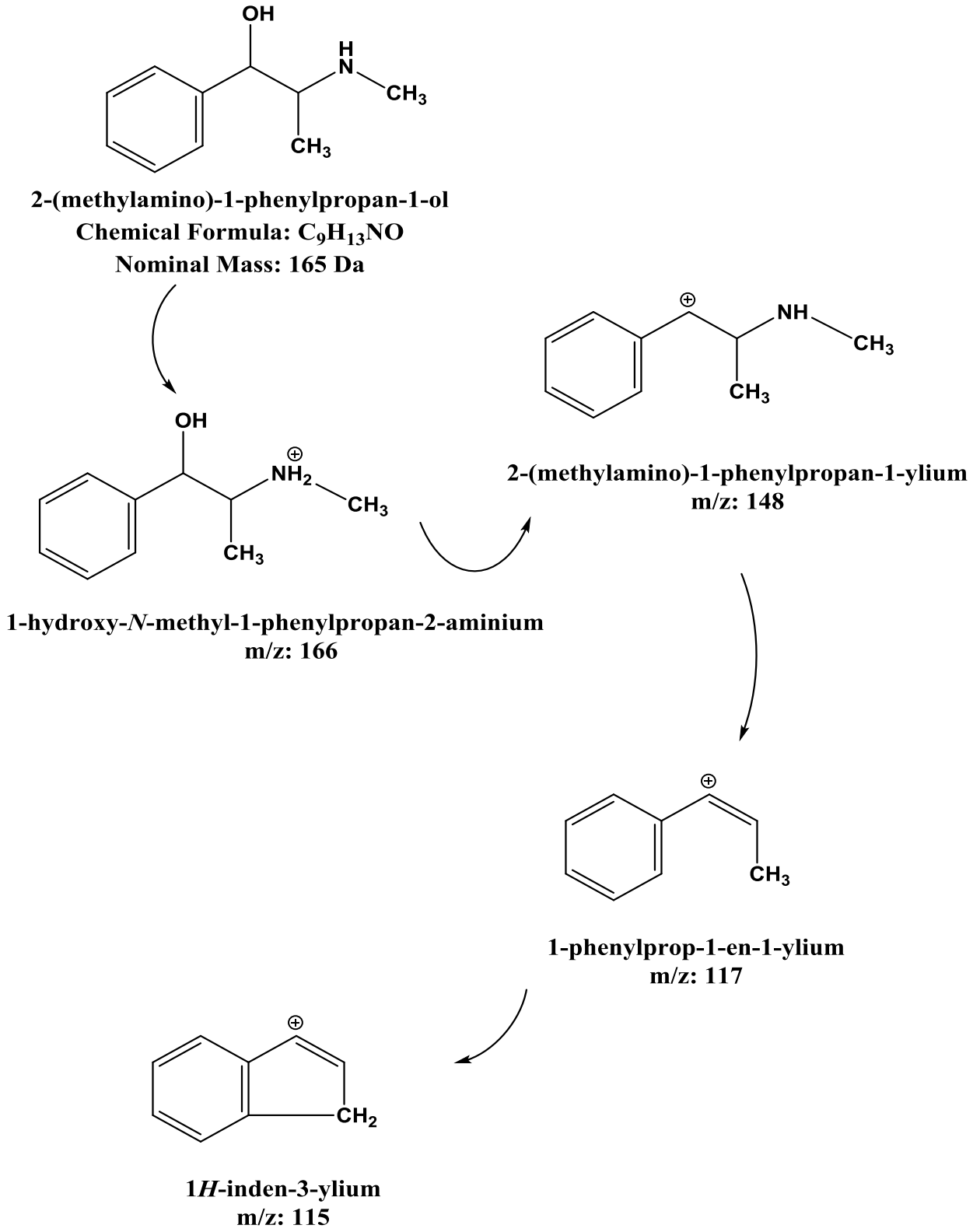

Figure 8: Structure proposals of the molecular ion and some of the fragment ions in the product ion mass spectra of methyl phenylpropanolamine (ephedrine and pseudoephedrine)

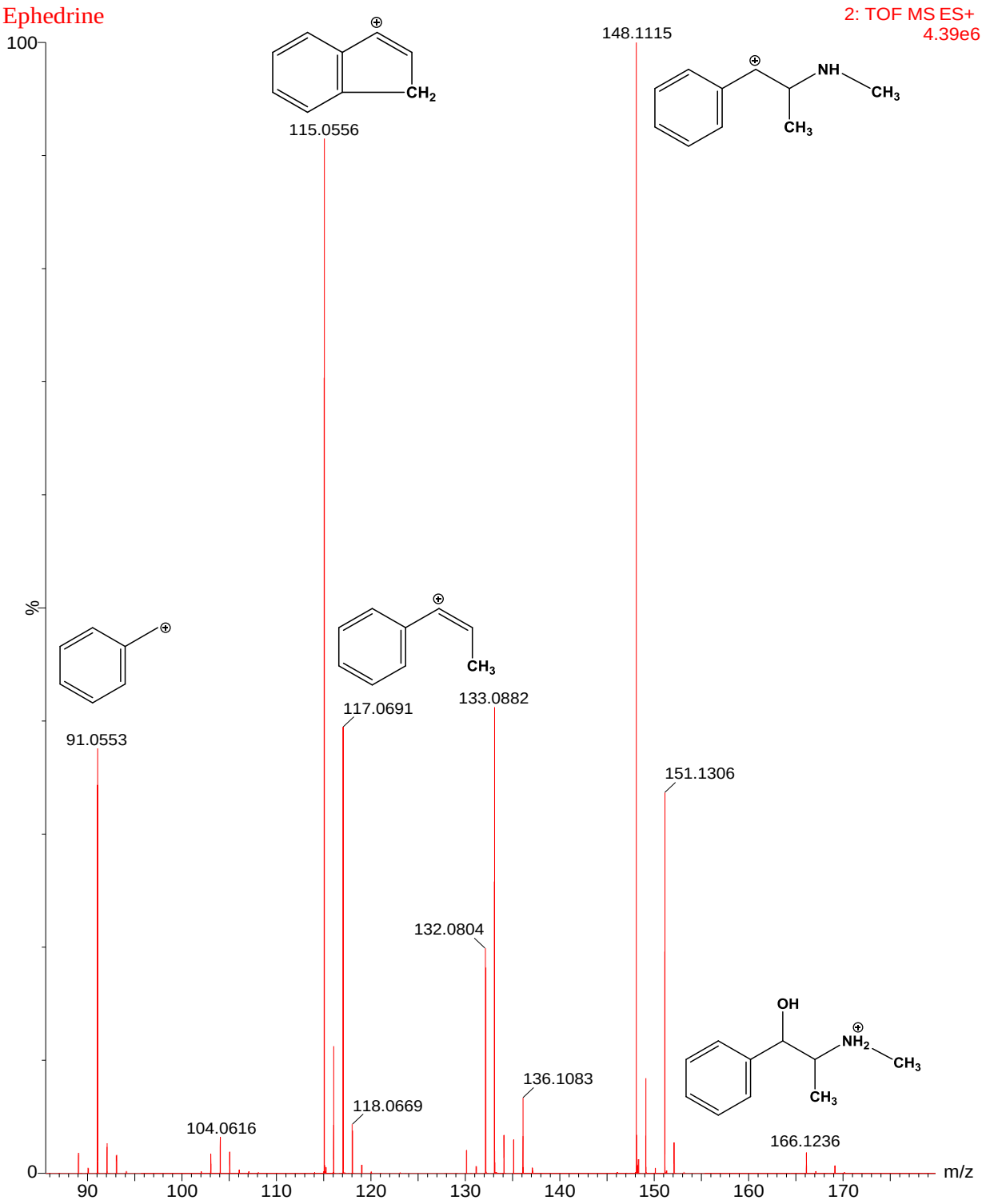

Figure 9: MS^E (HE) spectra of ephedrine

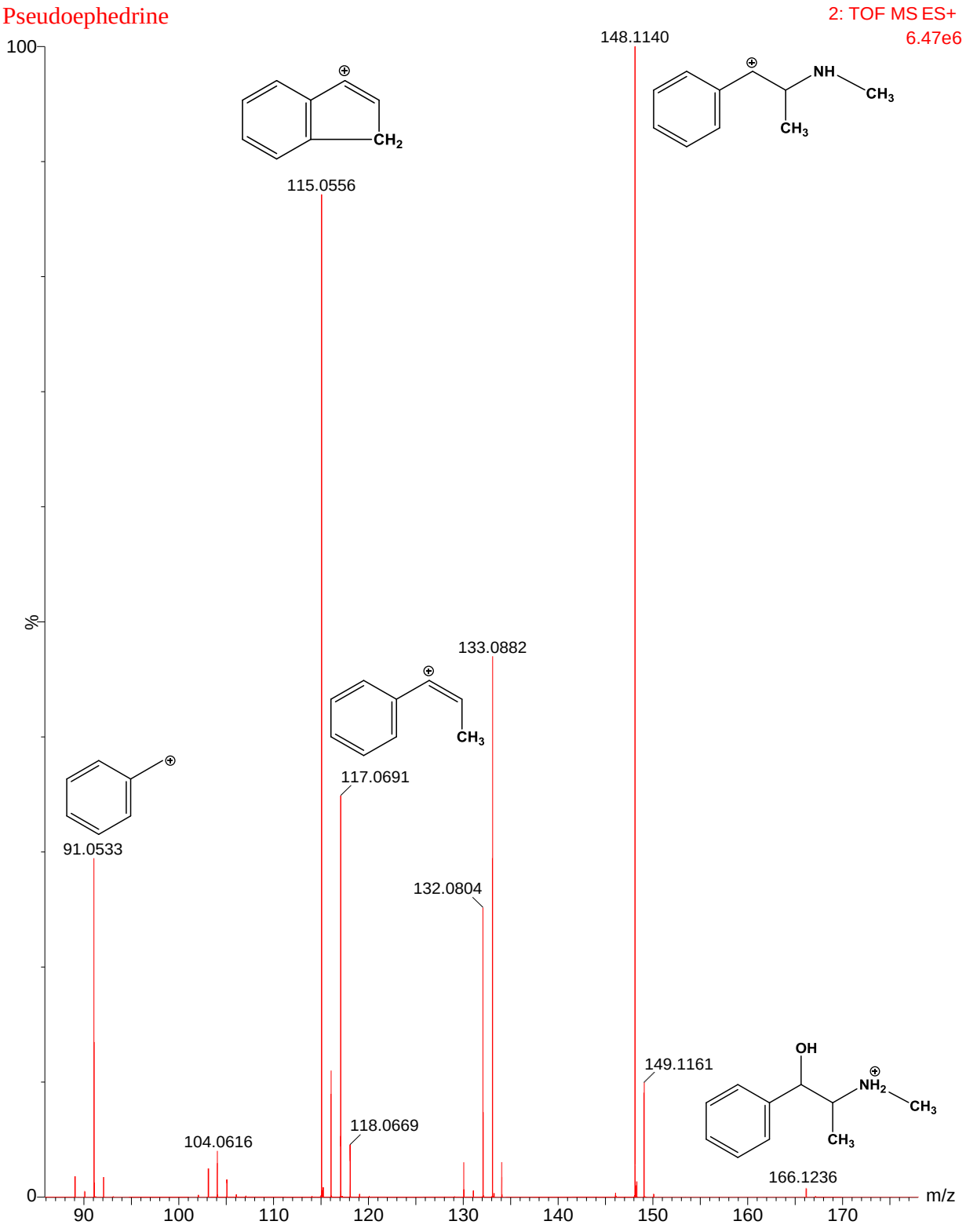

Figure 10: MS^E (HE) spectra of pseudoephedrine

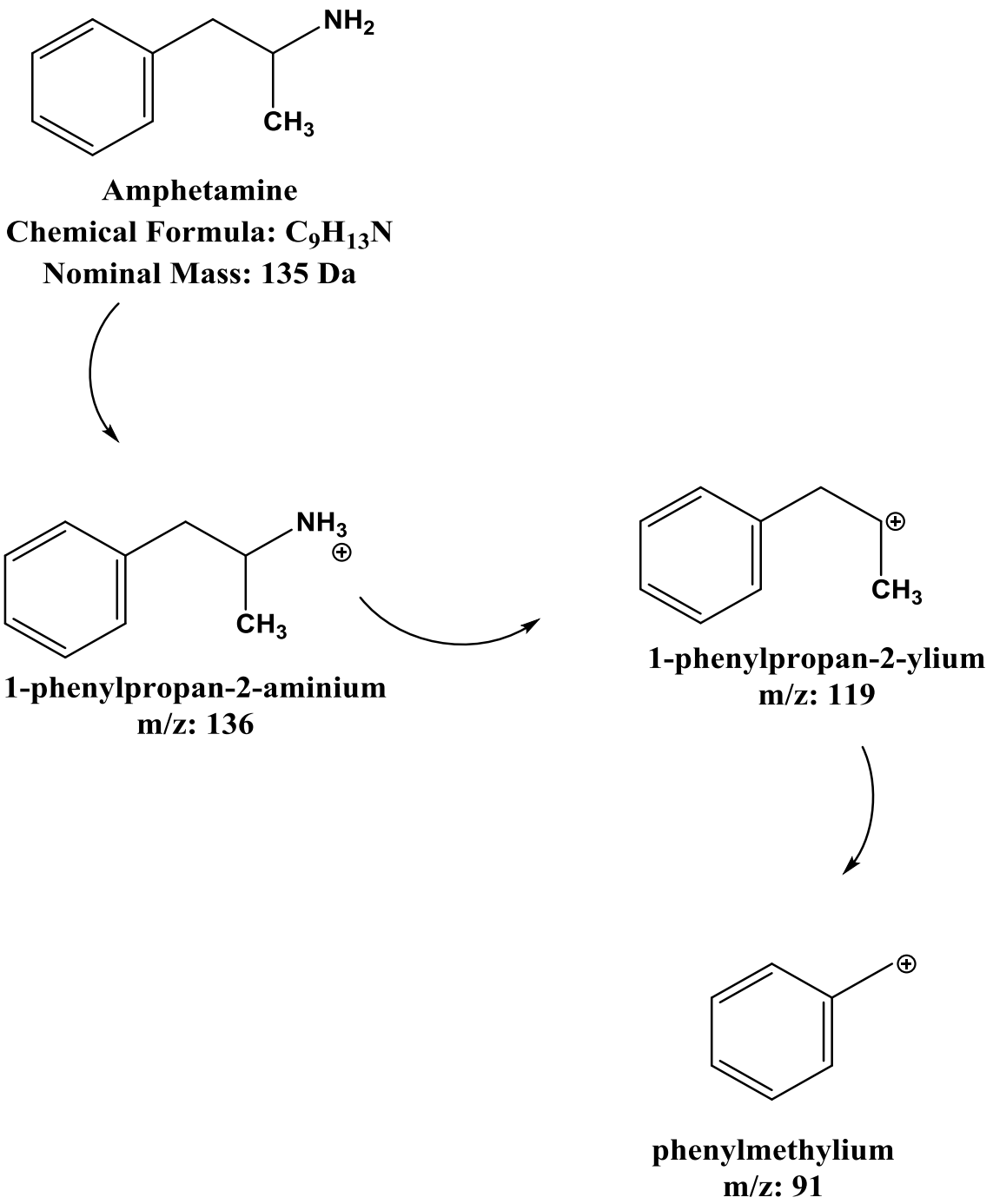

Figure 11: Structure proposals of the molecular ion and some of the fragment ions in the product ion mass spectra of amphetamine

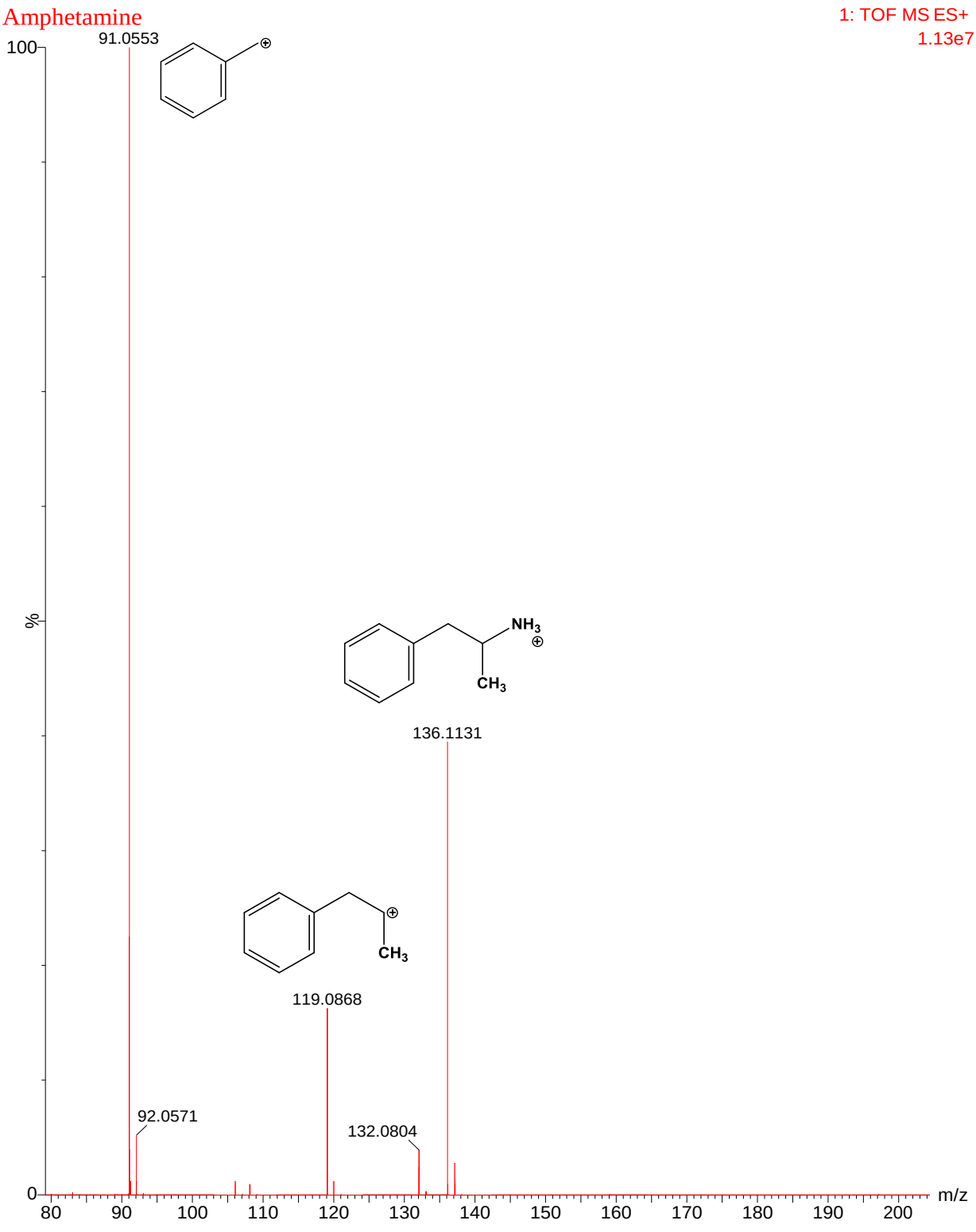

Figure 12: MS^E (HE) spectra of amphetamine

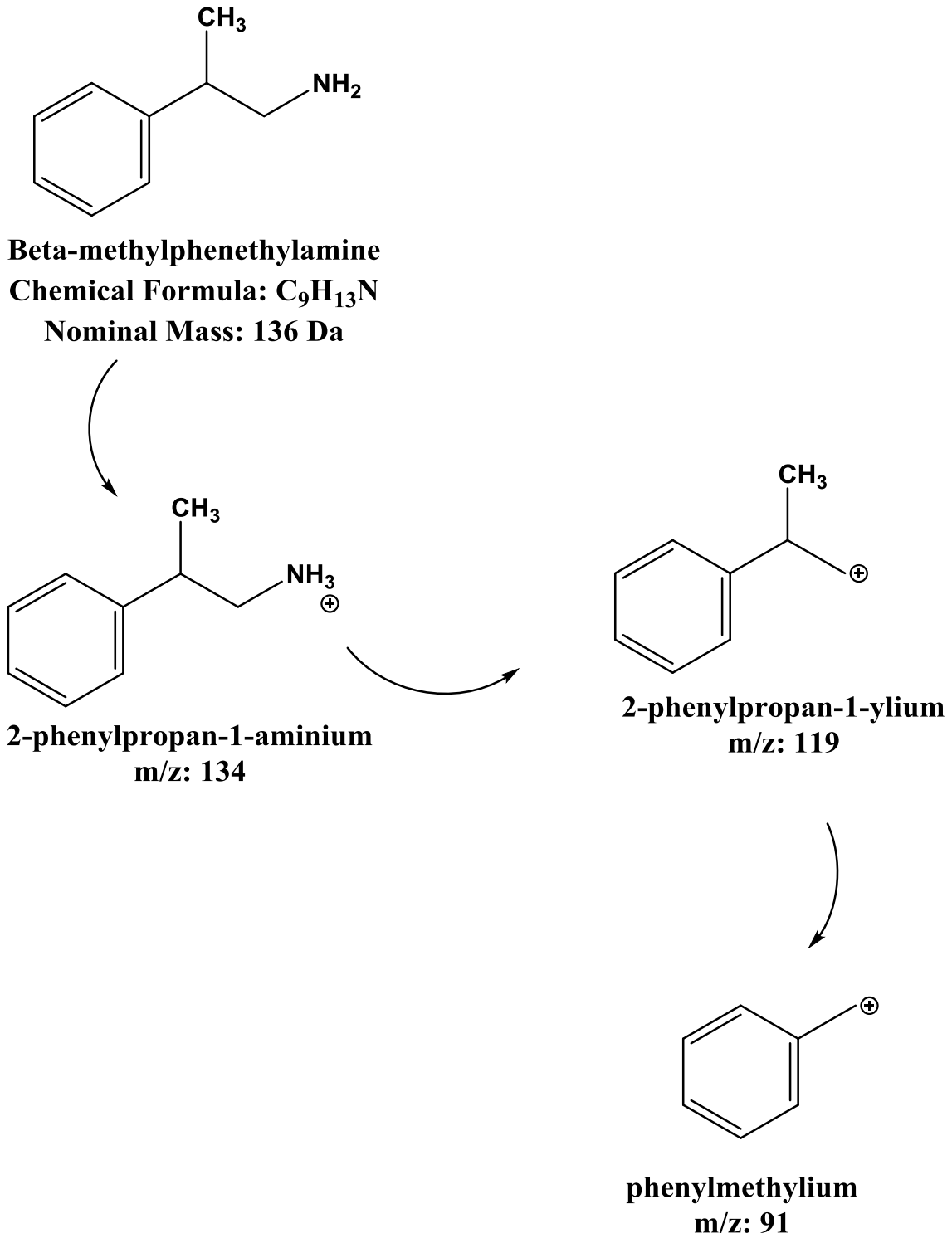

Figure 13: Structure proposals of the molecular ion and some of the fragment ions in the product ion mass spectra of βetamethylphenethylamie

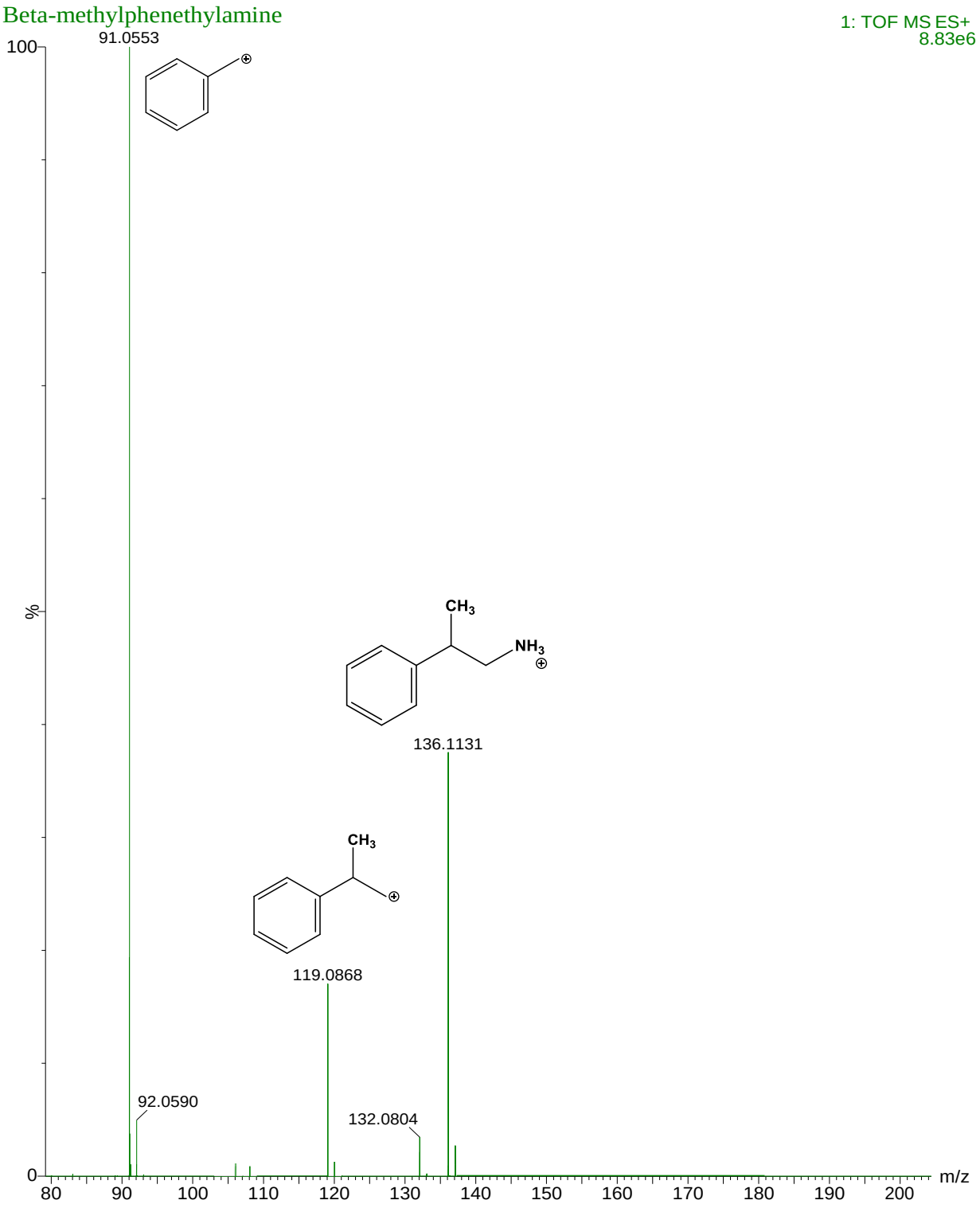

Figure 14: MS^E (HE) spectra of β-methylphenethylamine

References

1. Hodgson, E. (2015) A textbook of modern toxicology. Wiley, Hoboken, New Jersey.

2. White, P. (2004) Crime Scene to Court: The Essentials of Forensic Science. 2nd ed., The Royal Society of Chemistry, Norfolk.

3. Gjerde, H., Øiestad, E. and Christophersen, A. (2011) Using biological samples in epidemiological research on drugs of abuse. *Norsk Epidemiologi*, 21.

4. Skopp, G. (2004) Preanalytic aspects in postmortem toxicology. *Forensic Science International*, 142, 75-100.

5. Birkler, R., Telving, R., Ingemann-Hansen, O., Charles, A., Johannsen, M. and Andreasen, M. (2012) Screening analysis for medicinal drugs and drugs of abuse in whole blood using ultra-performance liquid chromatography time-of-flight mass spectrometry (UPLC–TOF-MS)—Toxicological findings in cases of alleged sexual assault. *Forensic Science International*, 222, 154-161.

6. Waugh, A., Grant, A., Chambers, G., Ross, J. and Wilson, K. (2014) Ross and Wilson anatomy and physiology in health and illness. 12th ed., Elsevier, China.

7. Thompson, G. (2015) Understanding anatomy & physiology. 2nd ed., F. A. Davis Company, Philadelphia.

8. Stanfield, C. (2013) Principles of human physiology. Pearson Education, Boston.

9. Manzone, T., Dam, H., Soltis, D. and Sagar, V. (2007) Blood Volume Analysis: A New Technique and New Clinical Interest Reinvigorate a Classic Study. *Journal of Nuclear Medicine Technology*, 35, 55-63.

10. Panuwet, P., Hunter, R., D'Souza, P., Chen, X., Radford, S. and Cohen, J. *et al*. (2015) Biological Matrix Effects in Quantitative Tandem Mass Spectrometry-Based Analytical Methods: Advancing Biomonitoring. *Critical Reviews in Analytical Chemistry*, 46, 93-105.

11. Wu, S., Schoener, D. and Jemal, M. (2008) Plasma phospholipids implicated in the matrix effect observed in liquid chromatography/tandem mass spectrometry bioanalysis: evaluation of the use of colloidal silica in combination with divalent or trivalent cations for the selective removal of phospholipids from plasma. *Rapid Communications in Mass Spectrometry*, 22, 2873-2881.

12. Nicolò, A., Cantù, M. and D'Avolio, A. (2017) Matrix effect management in liquid chromatography mass spectrometry: the internal standard normalized matrix effect. *Bioanalysis*, 9, 1093-1105.

13. Cooper, G. and Negrusz, A. (2013) Clarke's Analytical Forensic Toxicology. Pharmaceutical Press, London and Chicago.

14. Preedy, V. (2016) Neuropathology of drug addictions and substance misuse. 2nd ed., Elsevier, London.

15. Xu, Q. and Madden, T. (2012) LC-MS in drug bioanalysis. Springer, New York.

16. Telepchak, M. (2010) Forensic and clinical applications of solid phase extraction. Humana, Totowa, N.J.

17. Brusius, M. (2016) Navigating the Vast Array of Sample Preparation Techniques for Biological Samples – Whole Blood. *Chromatography Today*, 9, 40-47.

18. Polson, C., Sarkar, P., Incledon, B., Raguvaran, V. and Grant, R. (2003) Optimization of protein precipitation based upon effectiveness of protein removal and ionization effect in liquid chromatography–tandem mass spectrometry. *Journal of Chromatography B*, 785, 263-275.

19. Chakravorty, D., Parameswaran, S., Dubey, V. and Patra, S. (2012) Unraveling the Rationale Behind Organic Solvent Stability of Lipases. *Applied Biochemistry and Biotechnology*, 167, 439-461.

20. Gekko, K., Ohmae, E., Kameyama, K. and Takagi, T. (1998) Acetonitrile-protein interactions: amino acid solubility and preferential solvation. *Biochimica et Biophysica Acta (BBA) - Protein Structure and Molecular Enzymology*, 1387, 195-205.

21. Chamberlain, J. (1995) The analysis of drugs in biological fluids. 2nd ed., CRC Press, Boca Raton.

22. Bylda, C., Thiele, R., Kobold, U. and Volmer, D. (2014) Recent advances in sample preparation techniques to overcome difficulties encountered during quantitative analysis of small molecules from biofluids using LC-MS/MS. *The Analyst*, 139, 2265.

23. Pucci, V., Di Palma, S., Alfieri, A., Bonelli, F. and Monteagudo, E. (2009) A novel strategy for reducing phospholipids-based matrix effect in LC–ESI-MS bioanalysis by means of HybridSPE. *Journal of Pharmaceutical and Biomedical Analysis*, 50, 867-871.

24. Ferreiro-Vera, C., Priego-Capote, F. and Luque de Castro, M. (2012) Comparison of sample preparation approaches for phospholipids profiling in human serum by liquid chromatography–tandem mass spectrometry. *Journal of Chromatography A*, 1240, 21-28.

25. Moriarty, M., Lee, A., O'Connell, B., Lehane, M., Keeley, H. and Furey, A. (2012) The Application and Validation of HybridSPE-Precipitation Cartridge Technology for the Rapid Clean-up of Serum Matrices (from Phospholipids) for the Clinical Analysis of Serotonin, Dopamine and Melatonin. *Chromatographia*, 75, 1257-1269.

26. Jiang, H., Zhang, Y., Ida, M., LaFayette, A. and Fast, D. (2011) Determination of carboplatin in human plasma using HybridSPE-precipitation along with liquid chromatography–tandem mass spectrometry. *Journal of Chromatography B*, 879, 2162-2170.

27. Tanaka, S., Uchida, S., Inui, N., Takeuchi, K., Watanabe, H. and Namiki, N. (2014) Simultaneous LC-MS/MS Analysis of the Plasma Concentrations of a Cocktail of 5 Cytochrome P450 Substrate Drugs and Their Metabolites. *Biological and Pharmaceutical Bulletin*, 37, 18-25.

28. Nilsson, K., Andersson, M. and Beck, O. (2014) Phospholipid removal combined with a semi-automated 96-well SPE application for determination of budesonide in human plasma with LC–MS/MS. *Journal of Chromatography B*, 970, 31-35.

29. Cvan Trobec, K., Trontelj, J., Springer, J., Lainscak, M. and Kerec Kos, M. (2014) Liquid chromatography–tandem mass spectrometry method for simultaneous quantification of bisoprolol, ramiprilat, propranolol and midazolam in rat dried blood spots. *Journal of Chromatography B*, 958, 29-35.

30. Salihovic, S., Kärrman, A., Lindström, G., Lind, P., Lind, L. and van Bavel, B. (2013) A rapid method for the determination of perfluoroalkyl substances including structural isomers of perfluorooctane sulfonic acid in human serum using 96-well plates and column-switching ultra-high-performance liquid chromatography tandem mass spectrometry. *Journal of Chromatography A*, 1305, 164-170.

31. Mazzola, P., Lopes, A., Hasmann, F., Jozala, A., Penna, T. and Magalhaes, P. *et al*. (2008) Liquid–liquid extraction of biomolecules: an overview and update of the main techniques. *Journal of Chemical Technology & Biotechnology*, 83, 143-157.

32. Hendriks, G., Uges, D. and Franke, J. (2007) Reconsideration of sample pH adjustment in bioanalytical liquid–liquid extraction of ionisable compounds. *Journal of Chromatography B*, 853, 234-241.

33. Arsenault, J. (2012) Beginner's guide to SPE. Waters Corporation, Milford, Mass.

34. MITRA, S. (2003) Sample preparation techniques in analytical chemistry. John Wiley & Sons, Hoboken, New Jersey.

35. Solid Phase Extraction Products-SPE Tubes and Sample Preparation Products from Phenomenex (2017) *Phenomenex.com*, 2017. http://www.phenomenex.com/sample-preparation/solid-phase-extraction (13 September 2017).

36. Christophersen, A. and Mørland, J. (1994) Drug Analysis for Control Purposes in Forensic Toxicology, Workplace Testing, Sports Medicine and Related Areas. *Pharmacology & Toxicology*, 74, 202-210.

37. De Hoffmann, E. and Stroobant, V. (2013) Mass Spectrometry. 3rd ed., Wiley, Somerset.

38. Chauhan, A. (2014) GC-MS Technique and its Analytical Applications in Science and Technology. *Journal of Analytical & Bioanalytical Techniques*, 5.

39. Mbughuni, M., Jannetto, P. and Langman, L. (2016) Mass spectrometry applications for toxicology. *International Federation of Clinical Chemistry and Laboratory Medicine*, 27, 278-287. http://www.ifcc.org/ (14 September 2017).

40. Xinghua, G. (2014) Advances in gas chromatography. INTECH, Rijeka, Croatia.

41. Wen, B. and Zhu, M. (2015) Applications of mass spectrometry in drug metabolism: 50 years of progress. *Drug Metabolism Reviews*, 47, 71-87.

42. Lynch, K., Breaud, A., Vandenberghe, H., Wu, A. and Clarke, W. (2010) Performance evaluation of three liquid chromatography mass spectrometry methods for broad spectrum drug screening. *Clinica Chimica Acta*, 411, 1474-1481.

43. Köppel, C. and Tenczer, J. (1995) Scope and limitations of a general unknown screening by gas chromatography—mass spectrometry in acute poisoning. *Journal of the American Society for Mass Spectrometry*, 6, 995-1003.

44. Yuan, C., Chen, D. and Wang, S. (2015) Drug confirmation by mass spectrometry: Identification criteria and complicating factors. *Clinica Chimica Acta*, 438, 119-125.

45. Holčapek, M., Jirásko, R. and Lísa, M. (2012) Recent developments in liquid chromatography–mass spectrometry and related techniques. *Journal of Chromatography A*, 1259, 3-15.

46. Gelpí, E. (2002) Interfaces for coupled liquid-phase separation/mass spectrometry techniques. An update on recent developments. *Journal of Mass Spectrometry*, 37, 241-253.

47. Dong, M. (2006) Modern HPLC for practicing scientists. Wiley-Interscience, Hoboken, New Jersey.

48. Snyder, L., Kirkland, J. and Dolan, J. (2010) Introduction to modern liquid chromatography. Wiley, Hoboken, N.J.

49. J. Fountain, K. (2017) UPLC versus UHPLC: Comparison of Loading and Peak Capacity for Small Molecule Drugs. Waters Corporation. http://www.waters.com/webassets/cms/library/docs/720003869en.pdf (19 September 2017).

50. Peters, F. (2011) Recent advances of liquid chromatography–(tandem) mass spectrometry in clinical and forensic toxicology. *Clinical Biochemistry*, 44, 54-65.

51. Eichhorst, J., Etter, M., Rousseaux, N. and Lehotay, D. (2009) Drugs of abuse testing by tandem mass spectrometry: A rapid, simple method to replace immunoassays. *Clinical Biochemistry*, 42, 1531-1542.

52. Swartz, M. (2005) UPLC™: An Introduction and Review. *Journal of Liquid Chromatography & Related Technologies*, 28, 1253-1263.

53. Dettmer-Wilde, K. and Engewald, W. (2014) Practical Gas Chromatography. Springer Berlin Heidelberg, Berlin, Heidelberg.

54. Meyer, V. (2008) Practical high-performance liquid chromatography. 4th ed., Wiley, Chichester [u.a.].

55. Fauvelle, V., Mazzella, N., Morin, S., Moreira, S., Delest, B. and Budzinski, H. (2014) Hydrophilic interaction liquid chromatography coupled with tandem mass spectrometry for acidic herbicides and metabolites analysis in fresh water. *Environmental Science and Pollution Research*, 22, 3988-3996.

56. Chołbiński, P., Wicka, M., Kowalczyk, K., Jarek, A., Kaliszewski, P. and Pokrywka, A. *et al*. (2014) Detection of β-methylphenethylamine, a novel doping substance, by means of UPLC/MS/MS. *Analytical and Bioanalytical Chemistry*, 406, 3681-3688.

57. Hamilton, R. (2013) Introduction to high performance liquid chromatography. Springer, London.

58. Gaskell, S. (1997) Electrospray: Principles and Practice. *Journal of Mass Spectrometry*, 32, 677-688.

59. Start (2017) *Visualize your Science*, 2017. http://visualizeyourscience.com (22 September 2017).

60. XS Collision Cell White Paper (2017) Waters. http://www.waters.com/webassets/cms/library/docs/720005071en.pdf (22 September 2017).

61. Drummer, O. and Gerostamoulos, D. Forensic drug analysis. Future Science Ltd, London.

62. Depressant Drug Abuse and Side Effects (2017) *Treatment4addiction.com*, 2017. http://www.treatment4addiction.com/drugs/depressants/ (24 September 2017).

63. Ciccarone, D. (2011) Stimulant Abuse: Pharmacology, Cocaine, Methamphetamine, Treatment, Attempts at Pharmacotherapy. *Primary Care: Clinics in Office Practice*, 38, 41-58.

64. Di Chiara, G. and Imperato, A. (1988) Drugs abused by humans preferentially increase synaptic dopamine concentrations in the mesolimbic system of freely moving rats. *Proceedings of the National Academy of Sciences*, 85, 5274-5278.

65. Sitte, H. and Freissmuth, M. (2015) Amphetamines, new psychoactive drugs and the monoamine transporter cycle. *Trends in Pharmacological Sciences*, 36, 41-50.

66. Fleckenstein, A., Volz, T., Riddle, E., Gibb, J. and Hanson, G. (2007) New Insights into the Mechanism of Action of Amphetamines. *Annual Review of Pharmacology and Toxicology*, 47, 681-698.

67. Sulzer, D., Sonders, M., Poulsen, N. and Galli, A. (2005) Mechanisms of neurotransmitter release by amphetamines: A review. *Progress in Neurobiology*, 75, 406-433.

68. Pizarro, N., Ortuño, J., Segura, J., Farré, M., Mas, M. and Camí, J. *et al*. (1999) Quantification of amphetamine plasma concentrations by gas chromatography coupled to mass spectrometry. *Journal of Pharmaceutical and Biomedical Analysis*, 21, 739-747.

69. Heal, D., Smith, S., Gosden, J. and Nutt, D. (2013) Amphetamine, past and present – a pharmacological and clinical perspective. *Journal of Psychopharmacology*, 27, 479-496.

70. Calipari, E. and Ferris, M. (2013) Amphetamine Mechanisms and Actions at the Dopamine Terminal Revisited. *Journal of Neuroscience*, 33, 8923-8925.

71. Daberkow, D., Brown, H., Bunner, K., Kraniotis, S., Doellman, M. and Ragozzino, M. *et al*. (2013) Amphetamine Paradoxically Augments Exocytotic Dopamine Release and Phasic Dopamine Signals. *Journal of Neuroscience*, 33, 452-463.

72. JAMES, R., SHARP, W., BASTAIN, T., LEE, P., WALTER, J. and CZARNOLEWSKI, M. *et al*. (2001) Double-Blind, Placebo-Controlled Study of Single-Dose Amphetamine Formulations in ADHD. *Journal of the American Academy of Child & Adolescent Psychiatry*, 40, 1268-1276.

73. R, M. (2002) Double-blind, placebo-controlled study of single-dose amphetamine formulations in ADHD. *Journal of Developmental & Behavioral Pediatrics*, 23, 120-121.

74. McElroy, S., Hudson, J., Mitchell, J., Wilfley, D., Ferreira-Cornwell, M. and Gao, J. *et al*. (2015) Efficacy and Safety of Lisdexamfetamine for Treatment of Adults With Moderate to Severe Binge-Eating Disorder. *JAMA Psychiatry*, 72, 235.

75. Adler, L., Goodman, D., Kollins, S., Weisler, R., Krishnan, S. and Zhang, Y. *et al*. (2008) Double-Blind, Placebo-Controlled Study of the Efficacy and Safety of Lisdexamfetamine Dimesylate in Adults With Attention-Deficit/Hyperactivity Disorder. *The Journal of Clinical Psychiatry*, 69, 1364-1373.

76. Biederman, J., Boellner, S., Childress, A., Lopez, F., Krishnan, S. and Zhang, Y. (2007) Lisdexamfetamine Dimesylate and Mixed Amphetamine Salts Extended-Release in Children with ADHD: A Double-Blind, Placebo-Controlled, Crossover Analog Classroom Study. *Biological Psychiatry*, 62, 970-976.

77. Goodman, D., Ginsberg, L., Weisler, R., Cutler, A. and Hodgkins, P. (2005) An Interim Analysis of the Quality of Life, Effectiveness, Safety, and Tolerability (QU.E.S.T.) Evaluation of Mixed Amphetamine Salts Extended Release in Adults With ADHD. *CNS Spectrums*, 10, 26-34.

78. Hall, W., Hando, J., Darke, S. and Ross, J. (1996) Psychological morbidity and route of administration among amphetamine users in Sydney, Australia. *Addiction*, 91, 81-88.

79. Hall, W. and Hando, J. (1994) Route of administration and adverse effects of amphetamine use among young adults in Syndney, Australia. *Drug and Alcohol Review*, 13, 277-284.

80. Hall, W. and Hando, J. (1994) Route of administration and adverse effects of amphetamine use among young adults in Syndney, Australia. *Drug and Alcohol Review*, 13, 277-284.

81. Carvalho, M., Carmo, H., Costa, V., Capela, J., Pontes, H. and Remião, F. *et al*. (2012) Toxicity of amphetamines: an update. *Archives of Toxicology*, 86, 1167-1231.

82. de la Torre, R., Farre, M., Navarro, M., Pacifici, R., Zuccaro, P. and Pichini, S. (2004) Clinical Pharmacokinetics of Amfetamine and Related Substances. *Clinical Pharmacokinetics*, 43, 157-185.

83. Kraemer, T. and Maurer, H. (2002) Toxicokinetics of Amphetamines: Metabolism and Toxicokinetic Data of Designer Drugs, Amphetamine, Methamphetamine, and Their N-Alkyl Derivatives. *Therapeutic Drug Monitoring*, 24, 277-289.

84. Busto, U., Bendayan, R. and Sellers, E. (1989) Clinical Pharmacokinetics of Non-Opiate Abused Drugs. *Clinical Pharmacokinetics*, 16, 1-26.

85. Carvalho, F., Remião, F., Amado, F., Domingues, P., Correia, A. and Bastos, M. (1996) d-Amphetamine Interaction with Glutathione in Freshly Isolated Rat Hepatocytes. *Chemical Research in Toxicology*, 9, 1031-1036.

86. YAMADA, H., SHIIYAMA, S., SOEJIMAOHKUMA, T., HONDA, S., KUMAGAI, Y. and CHO, A. *et al.* (1997) Deamination of amphetamines by cytochromes P450: studies on substrate specificity and regioselectivity with microsomes and purified CYP2C subfamily isozymes. *The Journal of Toxicological Sciences*, 22, 65-73.

87. BACH, M., COUTTS, R. and BAKER, G. (1999) Involvement of CYP2D6 in the in vitro metabolism of amphetamine, two N-alkylamphetamines and their 4-methoxylated derivatives. *Xenobiotica*, 29, 719-732.

88. Quinn, D., Wodak, A. and Day, R. (1997) Pharmacokinetic and Pharmacodynamic Principles of Illicit Drug Use and Treatment of Illicit Drug Users. *Clinical Pharmacokinetics*, 33, 344-400.

89. Angrist, B., Corwin, J., Bartlik, B. and Cooper, T. (1987) Early pharmacokinetics and clinical effects of oral d-amphetamine in normal subjects. *Biological Psychiatry*, 22, 1357-1368.

90. Perez-Reyes, M., White, W., McDonald, S. and Hicks, R. (1992) Interaction between Ethanol and Dextroamphetamine: Effects on Psychomotor Performance. *Alcoholism: Clinical and Experimental Research*, 16, 75-81.

91. Wan, S., Matin, S. and Azarnoff, D. (1978) Kinetics, salivary excretion of amphetamine isomers, and effect of urinary pH. *Clinical Pharmacology & Therapeutics*, 23, 585-590.

92. Poklis, A., Still, J., Slattum, P., Edinboro, L., Saady, J. and Costantino, A. (1998) Urinary Excretion of d-Amphetamine Following Oral Doses in Humans: Implications for Urine Drug Testing. *Journal of Analytical Toxicology*, 22, 481-486.

93. Druid, H., Holmgren, P. and Ahlner, J. (1999) Interpretation of post mortem femoral blood levels of amphetamine- a compilation of intoxication and control cases. *Presented at the annual meeting of the American Academy of Forensic Sciences, Orlando, Florida*, 1999.

94. Baselt, R. (2004) Disposition of toxic drugs and chemicals in man. Biomedical publicationsl, Foster City, California.

95. Hartung, W. and Munch, J. (1931) AMINO ALCOHOLS. VI. THE PREPARATION AND PHARMACODYNAMIC ACTIVITY OF FOUR ISOMERIC PHENYLPROPYLAMINES. *Journal of the American Chemical Society*, 53, 1875-1879.

96. Cohen, P., Bloszies, C., Yee, C. and Gerona, R. (2015) An amphetamine isomer whose efficacy and safety in humans has never been studied, β-methylphenylethylamine (BMPEA), is found in multiple dietary supplements. *Drug Testing and Analysis*, 8, 328-333.

97. Graham, B., Cartland, G. and Woodruff, E. (1945) Phenyl Propyl and Phenyl Isopropyl Amines. *Industrial & Engineering Chemistry*, 37, 149-151.

98. Tainter, M. (1933) Comparative actions of sympathomimetic compounds: phenyl and substituted phenyl derivatives. Non-phenylic ring compounds and aliphatic amines. *Arch. Intern. Pharmaco. Ther.*, 46.

99. Graham, B. and Cartland, G. (1944) Some comparative pharmacological actions of beta-hydroxy and methoxy phenyl-n-propylamines. *J. Pharm. Exp. Ther*, 81, 360-367.

100. Warren, M., Marsh, D., Thompson, C., Shelton, R. and Becker, T. (1943) Pharmacological studies on dl-β-phenyl-n-propylmethylamine, a volatile amine. *J. Pharm. Exp. Ther*, 79, 187.

101. Winder, C., Anderson, M. and Parke, H. (1948) Comparative properties of six phenethylamines, with observations on the nature of tachyphylaxis. *J. Pharm. Exp. Ther*, 93, 63.

102. Marsh, D. (1948) The comparative pharmacology of the cyclohexylalkylamines. *J. Pharm. Exp. Ther*, 93, 338.

103. Mosnaim, A., Callaghan, O., Hudzik, T. and Wolf, M. (2013) Rat Brain-Uptake Index for Phenylethylamine and Various Monomethylated Derivatives. *Neurochemical Research*, 38, 842-846.

104. Schulte, J., Reif, E., Bacher, ,., Lawrence, W. and Painter, M. (1948) Further study of central stimulation from sympathomimetic amines. *J. Pharm. Exp. Ther.*, 71, 62.

105. Laccourreye, O., Werner, A., Giroud, J., Couloigner, V., Bonfils, P. and Bondon-Guitton, E. (2015) Benefits, limits and danger of ephedrine and pseudoephedrine as nasal decongestants. *European Annals of Otorhinolaryngology, Head and Neck Diseases*, 132, 31-34.

106. Clark, C., Dikötter, F., Laamann, L. and Xun, Z. (2005) Narcotic Culture: A History of Drugs in China. *Health and History*, 7, 112.

107. Vansal, S. and Feller, D. (1999) Direct effects of ephedrine isomers on human β-adrenergic receptor subtypes. *Biochemical Pharmacology*, 58, 807-810.

108. Young, R. (1998) Discriminative Stimulus Properties of (−)Ephedrine. *Pharmacology Biochemistry and Behavior*, 60, 771-775.

109. Kobayashi, S., Endou, M., Sakuraya, F., Matsuda, N., Zhang, X. and Azuma, M. *et al*. (2003) The Sympathomimetic Actions of l-Ephedrine and d-Pseudoephedrine: Direct Receptor Activation or Norepinephrine Release?. *Anesthesia & Analgesia*, 2003: 10.1213/01.ane.0000092917.96558.3c.

110. Ma, G., Bavadekar, S., Davis, Y., Lalchandani, S., Nagmani, R. and Schaneberg, B. *et al*. (2007) Pharmacological Effects of Ephedrine Alkaloids on Human 1- and 2-Adrenergic Receptor Subtypes. *Journal of Pharmacology and Experimental Therapeutics*, 322, 214-221.

111. Munhall, A. and Johnson, S. (2006) Dopamine-mediated actions of ephedrine in the rat substantia nigra. *Brain Research*, 1069, 96-103.

112. Miller, S. (2004) Safety Concerns Regarding Ephedrine-Type Alkaloid-Containing Dietary Supplements. *Military Medicine*, 169, 87-93.

113. Wahl, M., Grant, C. and Jesperson, R. (2000) Acute psychosis from a dietary weight control supplement. *J Toxicol-Clin Toxicol*, 38, 522-523.

114. Haller, C., Jacob, P. and Benowitz, N. (2002) Pharmacology of ephedra alkaloids and caffeine after single-dose dietary supplement use*. *Clinical Pharmacology & Therapeutics*, 71, 421-432.

115. Gurley, B., Gardner, S., White, L. and Wang, P. (1998) Ephedrine Pharmacokinetics After the Ingestion of Nutritional Supplements Containing Ephedra sinica (ma huang). *Therapeutic Drug Monitoring*, 20, 439-445.

116. Pickup, M., May, C., Ssendagire, R. and Paterson, J. (1976) The pharmacokinetics of ephedrine after oral dosage in asthmatics receiving acute and chronic treatment. *British Journal of Clinical Pharmacology*, 3, 123-134.

117. Ryall, J. (1984) Caffeine and ephedrine fatality. Bulletin. *The International Academy of Forensic Toxicologists*, 17: 3.

118. Garriott, J., Simmons, L., Poklis, A. and Mackell, M. (1985) Five Cases of Fatal Overdose from Caffeine-Containing "Look-Alike" Drugs. *Journal of Analytical Toxicology*, 9, 141-143.

119. Backer, R., Tautman, D., Lowry, S., Harvey, C. and Poklis, A. (1997) Fatal Ephedrine Intoxication. *Journal of Forensic Sciences*, 42, 14089J.

120. Dalpe-Scott, M., Degouffe, M., Garbutt, D. and Drost, M. (1995) A Comparison of Drug Concentrations in Postmortem Cardiac and Peripheral Blood in 320 Cases. *Canadian Society of Forensic Science Journal*, 28, 113-121.

121. Kubo, S., Waters, B., Hara, K., Fukunaga, T. and Ikematsu, K. (2017) A report of novel psychoactive substances in forensic autopsy cases and a review of fatal cases in the literature. Legal Medicine, 26, 79-85.

122. Neffati, M., Najjaa, H. and Máthé, A. (2017) Medicinal and aromatic plants of the world. Springer.

123. Abourashed, E., El-Alfy, A., Khan, I. and Walker, L. (2003) Ephedra in perspective - a current review. *Phytotherapy Research*, 17, 703-712.

124. Drew, C., Knight, G., Hughes, D. and Bush, M. (1978) Comparison of the effects of D-(-)-ephedrine and L-(+)-pseudoephedrine on the cardiovascular and respiratory systems in man. *British Journal of Clinical Pharmacology*, 6, 221-225.

125. Kumarnsit, E., Harnyuttanakorn, P., Meksuriyen, D., Govitrapong, P., Baldwin, B. and Kotchabhakdi, N. *et al*. (1999) Pseudoephedrine, a sympathomimetic agent, induces Fos-like immunoreactivity in rat nucleus accumbens and striatum. *Neuropharmacology*, 38, 1381-1387.

126. Kanfer, l., Dowse, R. and Vuma, V. (2017) Pharmacokinetics of oral decongestants. Pharmacotherapy. *Pharmacotherapy: The Journal of Human Pharmacology and Drug Therapy*, 13, 116S-128S.

127. Craig Brater, D., Kaojarern, S., Benet, L., Lin, E., Lockwood, T. and Curtis Morris, R. *et al*. (1980) Renal excretion of pseudoephedrine. *Clinical Pharmacology and Therapeutics*, 28, 690-694.

128. Dickerson, J., Perrier, D., Mayersohn, M. and Bressler, R. (1978) Dose tolerance and pharmacokinetic studies of L (+) pseudoephedrine capsules in man. *European Journal of Clinical Pharmacology*, 14, 253-259.

129. Bye, C., Hill, H., Hughes, D. and Peck, A. (1975) A comparison of plasma levels of L(+) pseudoephedrine following different formulations, and their relation to cardiovascular and subjective effects in man. *European Journal of Clinical Pharmacology*, 8, 47-53.

130. Litovitz, T., Schmitz, B. and Bailey, K. (1990) 1989 Annual report of the American Association of Poison Control Centers National Data Collection System. *The American Journal of Emergency Medicine*, 8, 394-442.

131. Hanzlick, R. (1995) National Association of Medical Examiners Pediatric Toxicology (PedTox) Registry Report 3. *The American Journal of Forensic Medicine and Pathology*, 16, 270-277.

132. Reynolds, P. (1983) Institute of Forensic Sciences, Oakland, CA. Personal Communication. 1983.

133. Registry of Human Toxicology. American Academy of Forensic Sciences (1978) *Clinical Toxicology*, 14, 211-212.

134. Krizevski, R., Bar, E., Dudai, N., Levy, A., Lewinsohn, E. and Sitrit, Y. *et al*. (2012) Naturally Occurring Norephedrine Oxazolidine Derivatives in Khat (Catha edulis). *Planta Medica*, 78, 838-842.

135. Kalix, P. (1996) Catha edulis, a plant that has amphetamine effects. *Pharmacy World and Science*, 18, 69-73.

136. Rothman, R. (2003) In Vitro Characterization of Ephedrine-Related Stereoisomers at Biogenic Amine Transporters and the Receptorome Reveals Selective Actions as Norepinephrine Transporter Substrates. *Journal of Pharmacology and Experimental Therapeutics*, 307, 138-145.

137. Goodman, L., Gilman, A., Brunton, L., Chabner, B. and Knollmann, B. (2011) Goodman & Gilman's the pharmacological basis of therapeutics. McGraw Hill Medical, New York.

138. Toennes, S., Harder, S., Schramm, M., Niess, C. and Kauert, G. (2003) Pharmacokinetics of cathinone, cathine and norephedrine after the chewing of khat leaves. *British Journal of Clinical Pharmacology*, 56, 125-130.

139. Heimlich, K., MacDonnell, D., Flanagan, T. and O'Brien, P. (1961) Evaluation of a Sustained Release Form of Phenylpropanolamine Hydrochloride by Urinary Excretion Studies. *Journal of Pharmaceutical Sciences*, 50, 232-237.

140. Zimmerman, C. (1988) The Effect of Urinary pH Modification on the Disposition of Phenylpropanolamine. *Pharmaceutical Research*, 5, 120-122.

141. Chester, N., Mottram, D., Reilly, T. and Powell, M. (2003) Elimination of ephedrines in urine following multiple dosing: the consequences for athletes, in relation to doping control. *British Journal of Clinical Pharmacology*, 57, 62-67.

142. Cravey, R. (1981) Orange County Sheriff-Coroner's Office, Santa Ana, CA. Personal Communication. 1981.

143. Augenstein, W., Bakerman, P. and Radetsky, M. (1988) Phenylpropanolamine (PPA) overdose resulting in pulmonary edema and death. *Vet Hum Tox*, 30, 365.

144. Launiainen, T. and Ojanperä, I. (2013) Drug concentrations in post-mortem femoral blood compared with therapeutic concentrations in plasma. Drug Testing and Analysis, 6, 308-316.

145. Musshoff, F., Padosch, S., Steinborn, S. and Madea, B. (2004) Fatal blood and tissue concentrations of more than 200 drugs. *Forensic Science International*, 142, 161-210.

146. Hoffman, R. and Al'Absi, M. (2010) Khat use and neurobehavioral functions: Suggestions for future studies. *Journal of Ethnopharmacology*, 132, 554-563.

147. Kalix, P. (1992) Cathinone, a Natural Amphetamine. *Pharmacology & Toxicology*, 70, 77-86.

148. Cox, G. (2003) Adverse effects of khat: a review. *Advances in Psychiatric Treatment*, 9, 456-463.

149. Cathine - DrugBank (2017) *Drugbank.ca*, 2017. https://www.drugbank.ca/drugs/DB01486 (6 October 2017).

150. Wolff, K., White, J. and Karch, S. (2016) The SAGE Handbook of Drug and Alcohol Studies. SAGE Publications, Limited, London.

151. (R)-(+)-Beta-Methylphenethylamine 95+% (2017) *Activate Scientific*, 2017. https://shop.activate-scientific.com/code/as33136 (6 October 2017).

152. Dasgupta, A. (2010) Beating drug tests and defending positive results. Humana Press, New York.

153. Dobos, A., Hidvegi, E. and Somogyi, G. (2012) Comparison of Five Derivatizing Agents for the Determination of Amphetamine-Type Stimulants in Human Urine by Extractive Acylation and Gas Chromatography-Mass Spectrometry. *Journal of Analytical Toxicology*, 36, 340-344.

154. Klette, K., Jamerson, M., Morris-Kukoski, C., Kettle, A. and Snyder, J. (2005) Rapid Simultaneous Determination of Amphetamine, Methamphetamine, 3,4-Methylenedioxyamphetamine, 3,4-Methylenedioxymethamphetamine, and 3,4-Methylenedioxyethylamphetamine in Urine by Fast Gas chromatography-mass Spectrometry. *Journal of Analytical Toxicology*, 29, 669-674.

155. Kudo, K., Ishida, T., Hara, K., Kashimura, S., Tsuji, A. and Ikeda, N. (2007) Simultaneous determination of 13 amphetamine related drugs in human whole blood using an enhanced polymer column and gas chromatography–mass spectrometry. *Journal of Chromatography B*, 855, 115-120.

156. KANKAANPAA, A., GUNNAR, T., ARINIEMI, K., LILLSUNDE, P., MYKKANEN, S. and SEPPALA, T. (2004) Single-step procedure for gas chromatography–mass spectrometry screening and quantitative determination of amphetamine-type stimulants and related drugs in blood, serum, oral fluid and urine samples. *Journal of Chromatography B*, 810, 57-68.

157. Pujadas, M., Pichini, S., Civit, E., Santamariña, E., Perez, K. and de la Torre, R. (2007) A simple and reliable procedure for the determination of psychoactive drugs in oral fluid by gas chromatography–mass spectrometry. *Journal of Pharmaceutical and Biomedical Analysis*, 44, 594-601.

158. del Mar Ramirez Fernandez, M. and Samyn, N. (2011) Ultra-Performance Liquid Chromatography-Tandem Mass Spectrometry Method for the Analysis of Amphetamines in Plasma. *Journal of Analytical Toxicology*, 35, 577-582.

159. PW, D., AJ, R., BS, R., MK, B., DI, P. and KA, M. *et al*. (2013) Quantitative Analysis of 30 Drugs in Whole Blood by SPE and UHPLC-TOF-MS. *JOURNAL OF FORENSIC SCIENCE & CRIMINOLOGY*, 1.

160. Sørensen, L. (2011) Determination of cathinones and related ephedrines in forensic whole-blood samples by liquid-chromatography–electrospray tandem mass spectrometry. *Journal of Chromatography B*, 879, 727-736.

161. Apollonio, L., Pianca, D., Whittall, I., Mahera, W. and Kyd, J. (2011) A demonstration of the use of ultra-performance liquid chromatography–mass spectrometry [UPLC/MS] in the determination of amphetamine-type substances and ketamine for forensic and toxicological analysis. *Journal of Chromatography B*, 836, 111–115.

162. Lambert, W., Meyer, E. and De Leenheer, A. (1995) Systematic Toxicological Analysis of Basic Drugs by Gradient Elution of an Alumina-Based HPLC Packing Material under Alkaline Conditions. *Journal of Analytical Toxicology*, 19, 73-78.

163. Bowyer, J., Clausing, P. and Newport, G. (1995) Determination of d-amphetamine in biological samples using high-performance liquid chromatography after precolumn derivatization with o-phthaldialdehyde and 3-mercaptopropionic acid. *Journal of Chromatography B: Biomedical Sciences and Applications*, 666, 241-250.

164. Kraemer, T. and Maurer, H. (1998) Determination of amphetamine, methamphetamine and amphetamine-derived designer drugs or medicaments in blood and urine. *Journal of Chromatography B: Biomedical Sciences and Applications*, 713, 163-187.

165. Logan, B. (2001) Amphetamines: An Update on Forensic Issues. *Journal of Analytical Toxicology*, 25, 400-404.

166. Moffat, A., Osselton, M., Widdop, B. and Watts, J. (2011) Clarke's Analysis of Drugs and Poisons. Pharmaceutical Press, London and Chicago.

167. Änggård, E., Gunne, L. and Niklasson, F. (1970) Gas Chromatographic Determination of Amphetamine in Blood, Tissue, and Urine. *Scandinavian Journal of Clinical and Laboratory Investigation*, 26, 137-143.

168. Baselt, R. and Cravey, R. (1977) A Compendium of Therapeutic and Toxic Concentrations of Toxicologically Significant Drugs in Human Biofluids. *Journal of Analytical Toxicology*, 1, 81-103.

169. Snook, C., Otten, M. and Hassan, M. (1992) Massive ephedrine overdose. *Veterinary and Human Toxicology*, 34, 335.

170. Dowse, R., Haigh, J. and Kanfer, I. (1987) Pharmacokinetics of phenylpropanolamine in humans after a single-dose study. *International Journal of Pharmaceutics*, 39, 141-148.

171. Allan, A. and Roberts, I. (2009) Post-mortem toxicology of commonly-abused drugs. *Diagnostic Histopathology*, 15, 33-41.

172. Yarema, M. and Becker, C. (2005) Key Concepts in Postmortem Drug Redistribution. *Clinical Toxicology*, 43, 235-241.

173. Barceloux, D. and Palmer, R. (2012) Medical toxicology of drug abuse. John Wiley & Sons, Hoboken, N.J.

174. Vasapollo, G., Sole, R., Mergola, L., Lazzoi, M., Scardino, A. and Scorrano, S. *et al*. (2011) Molecularly Imprinted Polymers: Present and Future Prospective. *International Journal of Molecular Sciences*, 12, 5908-5945.

175. Haupt, K. (2003) Peer Reviewed: Molecularly Imprinted Polymers: The Next Generation. *Analytical Chemistry*, 75, 376 A-383 A.

176. Scientific Working Group for Forensic Toxicology (SWGTOX) Standard Practices for Method Validation in Forensic Toxicology (2013) *Journal of Analytical Toxicology*, 37, 452-474.

177. Hernández, F., Bijlsma, L., Sancho, J., Díaz, R. and Ibáñez, M. (2011) Rapid wide-scope screening of drugs of abuse, prescription drugs with potential for abuse and their metabolites in influent and effluent urban wastewater by ultrahigh pressure liquid chromatography–quadrupole-time-of-flight-mass spectrometry. *Analytica Chimica Acta*, 684, 96-106.

178. Bijlsma, L., Sancho, J., Hernández, F. and Niessen, W. (2011) Fragmentation pathways of drugs of abuse and their metabolites based on QTOF MS/MS and MSE accurate-mass spectra. *Journal of Mass Spectrometry*, 46, 865-875.

179. McIntyre, I., Nelson, C., Schaber, B. and Hamm, C. (2013) Antemortem and Postmortem Methamphetamine Blood Concentrations: Three Case Reports. *Journal of Analytical Toxicology*, 37, 386-389.